Texture and Hydration of Expanded Rice

Clive Norton

September 1998

Thesis submitted for the degree of Doctor of Philosophy at the University of Nottingham, UK

Acknowledgements

To Mike Chapman, who was usually willing to help with something, spent many hours helping with extrusion, or just to be used as a sounding board while I was trying to figure things out.

To John Mitchell, who gave up his weekends to guide me while writing this thesis.

To Mark Alston for proof reading things I wrote.

This research was supported by grants from the BBSRC and generously from Nestec York Ltd.

This thesis was edited by Nestec York Ltd to protect confidentiality.

1 Contents

1.1 Table of Contents

1.2 Table of Figures

1.3 Table of Tables

1.4 Table of Equations

2 Abstract

The differences between conventionally processed and extruded puffed rice were examined, with a view to determining the reasons for their different storage behaviour in confectionery.

Differences between the two forms of puffed rice have been identified, both in their performance and their properties.

Under certain viewing conditions, the starch granules in conventionally processed and extruded rice appear to be different. The starch granules in conventionally puffed Rice remain intact, but with no crystalline structure (i.e. no Maltese crosses are visible, though starch ghosts are abundant.). Cell walls of conventionally processed rice appear to be a layer of these gelatinised intact granules. The ghostlike granules have not undergone notable swelling, remaining slightly greater than 10μm in diameter, similar to the size of unprocessed granules

In contrast, the starch granules in extruded puffed rice are rarely visible, in either their birefringent Maltese cross form, or as gelatinised but intact ghosts.

By altering the extrusion conditions, the microscopic appearance of the product and its behaviour in water or water vapour becomes similar to that of conventionally processed rice. The extrusion parameters required for this similarity to conventionally processed rice fall within a window that is relatively narrow when compared to the ranges of variables available. Under more severe processing conditions the granules lose their integrity because shear and heat disrupt them. Under less severe conditions, the granules form clusters that do not gelatinise. The conditions at which this product is made cannot be interpolated or extrapolated from samples made under other conditions.

However, at these extrusion parameters, the extrudate does not expand. It is necessary to expand the extrudate separately from the extrusion process. A novel method for the analysis of multi-peak force responses from compression of low moisture puffed cereal products was developed. This enabled crisp and crackly to be distinguished instrumentally. The results correlated well with sensory evaluation.

3 Introduction

Extruded puffed rice did not perform as well as conventionally puffed rice when used in confectionery bars. It was found the texture of the extruded krispies deteriorated after only a week, whereas the conventionally processed product was able to maintain its crispiness for three or four months.

The original hypothesis was that at any given storage humidity, the extruded samples equilibrate to a higher moisture content than their conventionally processed counterparts. The work in this thesis examined this hypothesis and investigated structural differences between the two types of product with the aim of developing knowledge that would improve the properties of extruded rice.

During the work, a new approach to analysing the texture of these expanded foods was developed.

4 Literature review

4.1 Rice

4.1.1 Rice origin

Rice (*Oryza sativa Linn* and *Oryza glaberrima Steud*), along with wheat and maize, is one of the three major cereal crops produced in the world. Although traditionally a staple food in Asia, rice has become increasingly significant in the west (Bray, 1986). Although 90% of the world rice crop is produced in Asia where 54% percent of the world population live (IRRI, 1988), only 4% of the world rice crop was traded on international markets during 1987 (FAO, 1989). These facts imply that in general either national rice consumption dictates national rice production, or vice-versa. Rice may be consumed as boiled, puffed, flaked, compressed, or glutinous rice products. Milled rice (rice flour) may also be used as a food ingredient.

4.1.2 Rice structure

The genetic relationships in Table 4-1 and the microscopic structures of different cereals in Table 4-2 indicate rice has closer similarities to oats than to other cereals. Sub-species of *Oryza sativa* also exist, but are not displayed on the chart. The most notable sub-species are *japonica* grown in Japan, Korea, and China, and *indica* grown in India, China, and the West. Additionally there is *javanica*, which mainly embraces the Indonesian rices (Chang, 1976; Bray, 1986).

When harvested, rice grains are encased in a husk that forms 20% of the whole grain (Figure 4-1). The husk is a tough siliceous layer comprising of the palea and lemma, and protects the grain from insectal, fungal, or mechanical damage (Ong, 1994). Beneath the husk is a bran layer that forms 5% of the whole grain, and consists of pericarp, seed coat, and nucellus. The bran layer contains lipid and protein, and is rich in oil. (Ong, 1994). Beneath the nucellus and forming 2% of the whole grain is the outer layer of the endosperm tissue, the aleurone layer, which is rich in lipid and protein. The germ or embryo section accounts for only 2% of, and is found near the

base of the whole grain. The inner aleurone layer (subaleurone layer) and the starchy endosperm form the remaining 73% of the whole grain. (Ong, 1994).

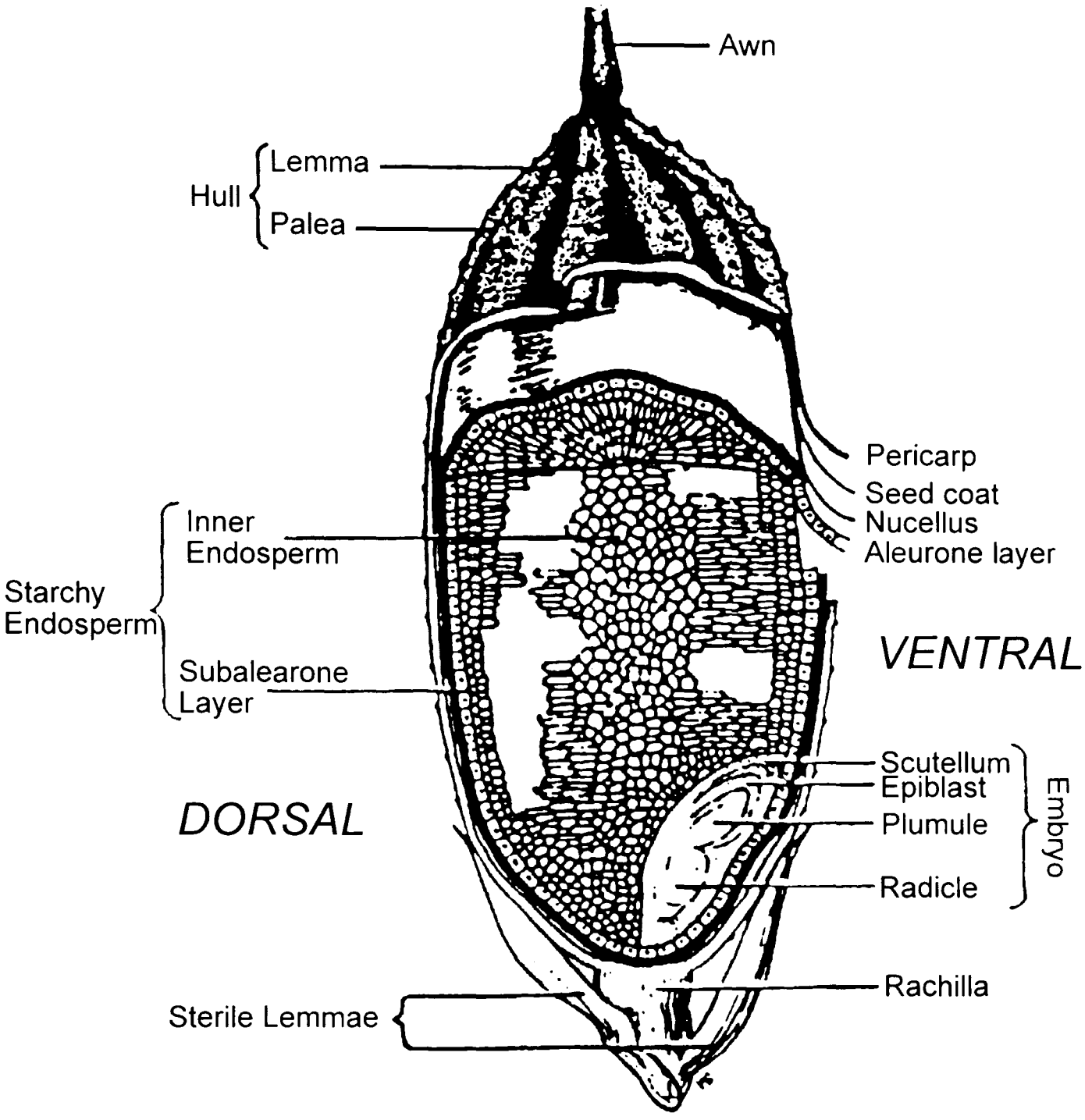

Figure 4-1 Longitudinal section of a rice grain (Juliano 1985)

Family	Gramineae								
Subfamily	Festudcoideae					Panicoideae			
Tribe	Triticeae			Aveneae	Oryzeae	Andropogoneae			Paniceae
Subtribe	Triticineae		Hordineae			Tripsacineae		Arthraxon-ineae	
Genus	Triticum	Secale	Hordeum	Avena	Oryza	Zea	Tripsacum	Sorghum	Pennisetum
Common Name	Wheat	Rye	Barley	Oat	Rice	Maize		Sorghum	Millet

Table 4-1 Genetic Relationships among Common Cereal Grains (From Bietz, 1982)

Cereal	Rice Oats Barley	Wheat Rye Maize Sorghum
Caryopsis	Covered	Naked
Aleurone Layer	Multiple Cell	Single Cell
Starch Granule	Compound	Individual
Protein Bodies	Yes	No

Table 4-2 Microscopic Structure of Rice and Other Cereal Grains (from Rooney et al., 1982)

4.1.3 Chemical composition of Rice

About 90% of rice (without husk) composition is carbohydrate, which is primarily starch, detailed in Section 4.2. Table 4-3 and Table 4-4 display the composition of rice and its products as reported in Brockington and Kelly (1972).

4.2 Starch

4.2.1 Starch Structure

4.2.1.1 Chemical Structure of Starch

Starch primarily consists of amylose and amylopectin. The amylose content varies from one variety to another. Other chemicals are also present in small quantities such as protein, lipid, and phosphorus (Table 4-3 and 4-4). Amylose (α-(1,4)-D-glucopyranosyl) is a primarily linear polymer of α-D-glucan units (α-D-glucose prior to polymerisation) linked by α-1-4 bonds (Figure 4-2). Galliard and Bowler (1987) report the extent of polymerisation of amylose as 500-5000 glucan units. Amylopectin is a highly branched polymer of glucose (Colonna *et al.*, 1989); the branches of length 15 – 45 glucan units are linked by α-(1→6)-D-glucosidic bonds (MacGregor and Greenwood, 1980) (Figure 4-3). Amylopectin is conventionally believed to be one of the highest molecular weight natural polymers with a degree of polymerisation of 10^4

– 10^5 glucan units. However, Ramesh *et al.* has shown that amylopectin can also exist as much smaller molecules. Amylose chains can be shortened by the enzyme α-amylase, and amylopectin can be debranched by isoamylase.

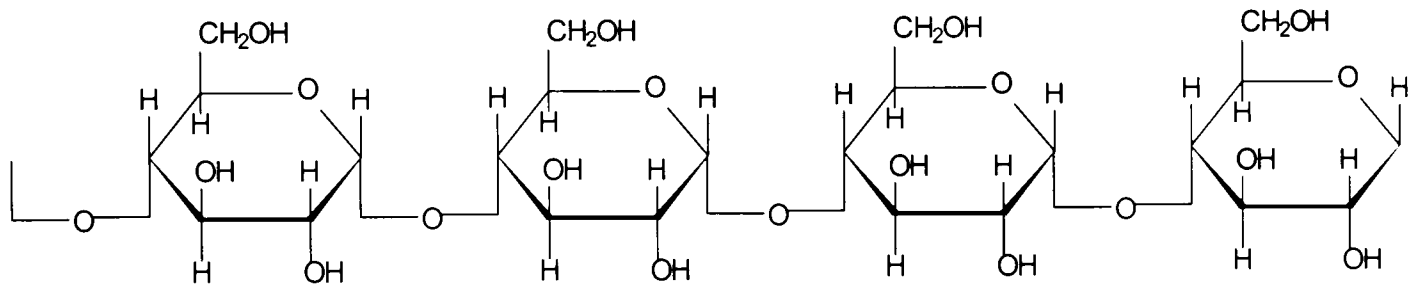

Figure 4-2 Amylose schematic. The inter-unit links are α(1→4) bonds.

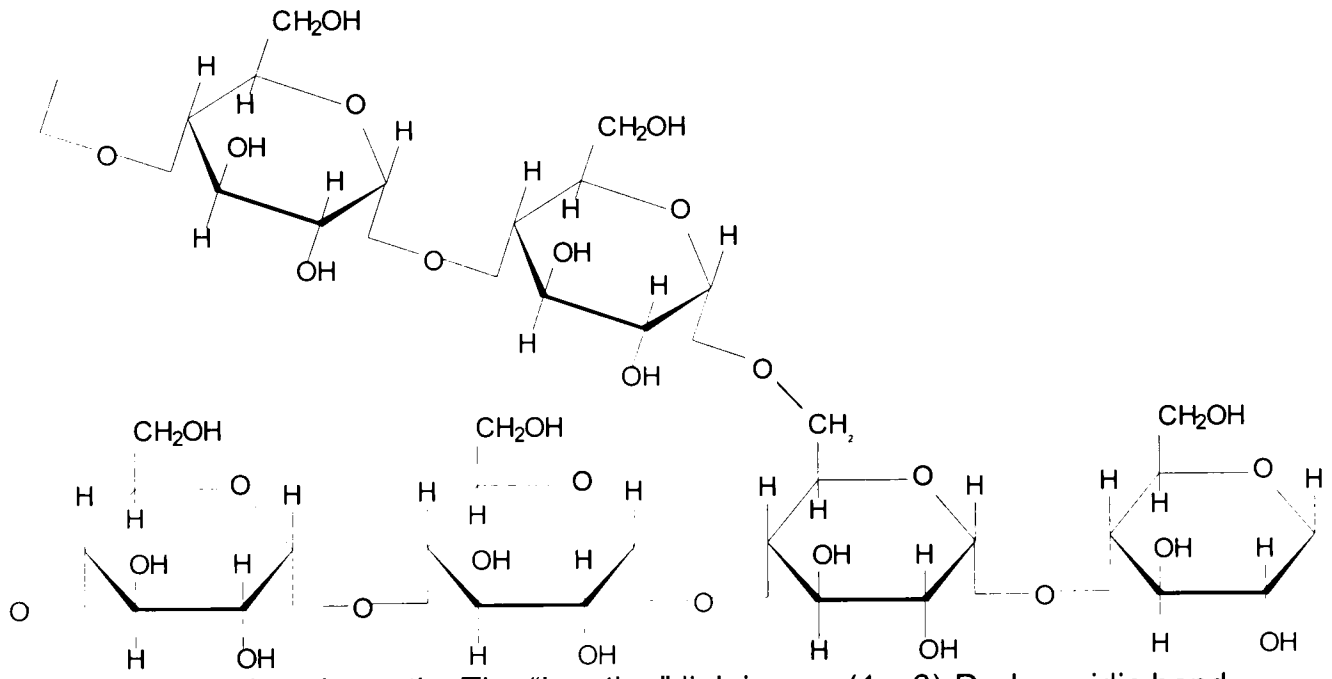

Figure 4-3 Amylopectin schematic. The "junction" link is an α(1→6)-D-glucosidic bond.

	Milled Rice	Gran. Rice	Rice Flakes[a]	Puffed Rice[a]	Rice Cereal[b]	Shredded Rice[a]	"Instant" Rice
	%	%	%	%	%	%	%
Moisture	12.0	7.4	3.2	3.7	1.8	3.0	9.6
Protein	6.7	6.0	5.9	6.0	4.2	5.2	7.5
Fat	0.4	0.3	0.3	0.4	0.7	0.3	0.2
Fibre	0.3	0.2	0.6	0.6	0.2	0.3	0.4
Ash	0.5	0.4	2.9	0.4	2.7	2.7	0.2
	mg $100g^{-1}$	mg $100g^{-1}$	mg $100g^{-1}$	mg $100g^{-1}$	mg $100g^{-1}$	mg $100g^{-1}$	mg $100g^{-1}$
Calcium	24	9	29	20	46	14	5
Phosphorus	94	96	132	90	74	95	65
Iron	2.9	5.4	1.6	1.8	0.9	1.8	2.9
Sodium	5	---	987	2	706	846	1.0
Thiamine	0.07	0.42	0.35	0.44	0.33	0.39	0.44
Riboflavin	0.03	0.11	0.04	0.04	---	---	---
Niacin	1.6	5.8	5.4	4.4	4.6	7.0	3.5

[a] Contains added nutrients

[b] Contains added nutrients and is pre-sweetened.

Table 4-3 Composition of rice cereals adapted from Watt and Merrill (1963) by Brockington and Kelly (1972)

	Brown Rice mg $100g^{-1}$	Milled Rice mg $100g^{-1}$	Rice Bran mg $100g^{-1}$	Rice Polish mg $100g^{-1}$	Rice Germ mg $100g^{-1}$
Thiamine	0.34	0.07	2.26	1.84	6.5
Riboflavin	0.05	.003	0.25	0.18	0.5
Niacin	4.7	1.6	29.8	28.2	3.3
Pyridoxine	1.03	0.45	2.5	2.0	1.6
Pantothenic acid	1.5	0.75	2.8	3.3	3.0
Folic acid	0.02	0.016	0.15	0.19	0.43
Inositol	119	10	463	454	373
Choline	112	59	170	102	300
Biotin	0.012	0.005	0.06	0.057	0.058

Table 4-4 Vitamin contents of rice and its by-products (Brockington and Kelly, 1972)

A number of possible structural models have been presented for amylopectin, and the currently accepted model is the Racemose model in Figure 4-4 proposed by Robin *et al.* (1974). Chains are categorised as B or A, depending on whether or not they carry other branches respectively. A chains are connected to the rest of the molecule at only one point, and typically have DP 15-20. B chains are similar to A-chains, but also carry one or more A or B chains, and typically have DP 45. There is a single C chain that carries the only reducing end group. This simple picture has been questioned for rice, and possibly for all starches, by Ramesh *et al.* (1998) who conducted further work into debranching and chromatography of rice starches following work by Chinnaswamy and Bhattacharya (1986), Takeda *et al.* (1987, 1989), Hizukuri *et al.* (1989), Radhika Reddy *et al.* (1993, 1994), Sandhya Rani and Battacharya (1995a, 1995b) and Ong and Blanshard (1995). Although chromatography studies separated rice starch into a high molecular and low molecular weight, on enzymic debranching the distribution of chain lengths was similar to that obtained with the high molecular weight component. This would suggest that the low molecular weight fraction was much more highly branched than normally believed for amylose. Ong and Blanshard (1995) examined the chain distribution of the debranched material using GPC/MALLS. They found a residual moderately high molecular fraction in rice

starch that was regarded as amylose. The exact proportion of this material is not clear, as it was not quantified by Ong and Blanshard (1995).

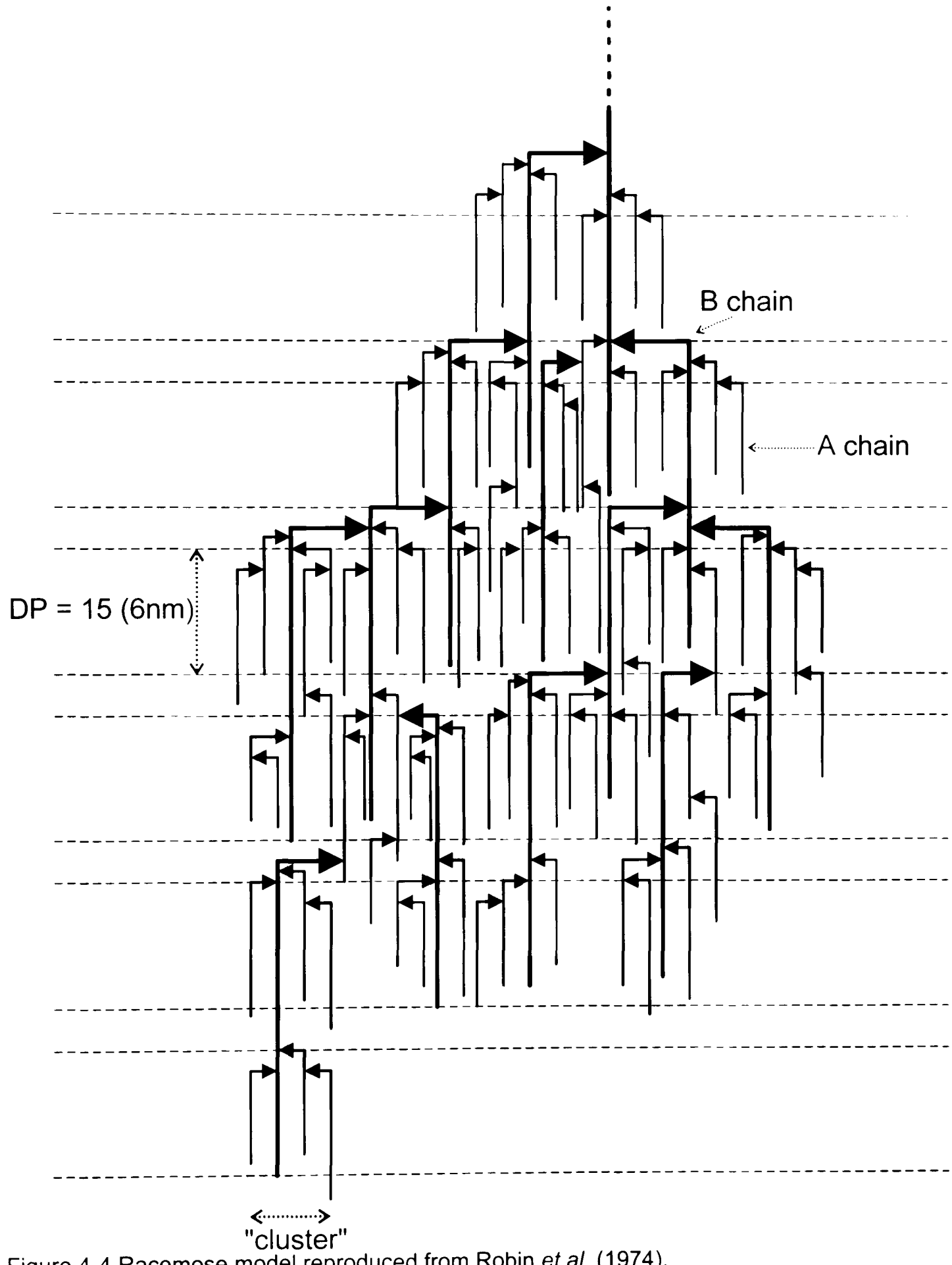

Figure 4-4 Racemose model reproduced from Robin *et al.* (1974).

For many years iodine-binding methods have been used to quantify amylose content. In a cold aqueous solution of sample, amylose complexes with iodine upon the addition of KI_3. Wooton (1971) found that the intensity of the blue-black complex

was proportional to the amount of gelatinised starch. However, Radhika Reddy *et al.* (1993) found that long B chains of amylopectin reacted equally well with iodine.

Although there is no doubt that progress has been made in correlating the fine structure of the rice polysaccharide with texture of cooked rice (Ong, 1994; Ong and Blanshard, 1995; Ramesh *et al.*, 1998), there is still further work to be undertaken.

4.2.1.2 Organisation of Polysaccharide within the Granule

The two starch polymers are arranged in semi-crystalline layers in granules that are insoluble at room temperature (Figure 4-5). The size of these varies according to the source. Rice is one of the smaller with diameters 3-8μm.

From the available information, Blanshard (1987) presented the model Figure 4-6 proposing radial arrangement of the starch polymers within the crystalline region of the granule, along with possible amylose-lipid complexes. This can be incorporated into the broader picture elegantly described by Cameron and Donald (1992).

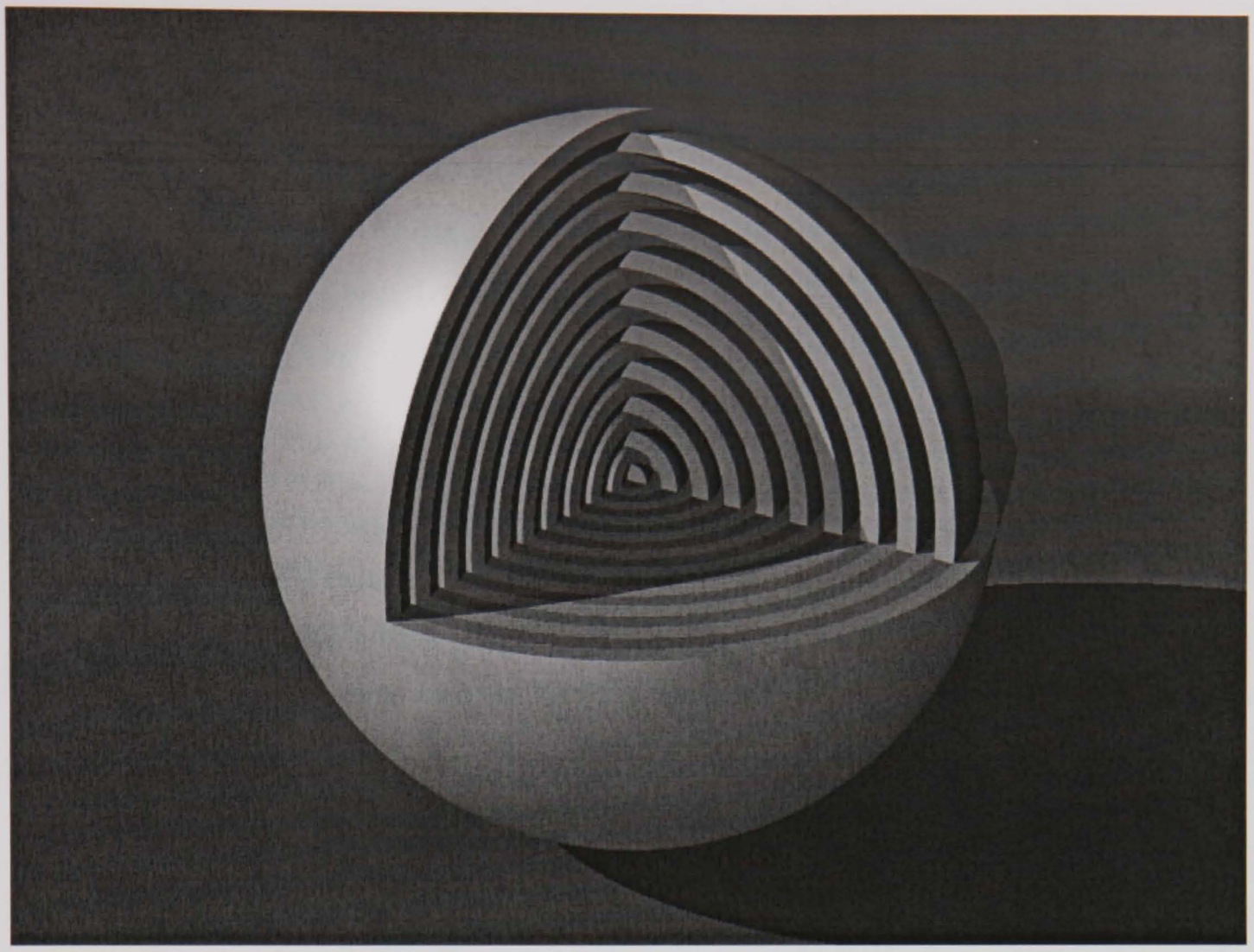

Figure 4-5 Schematic representation of concentric crystalline and amorphous layer structure in starch granules. Based on findings of French (1984) and Hollinger and Marschessault (1975).

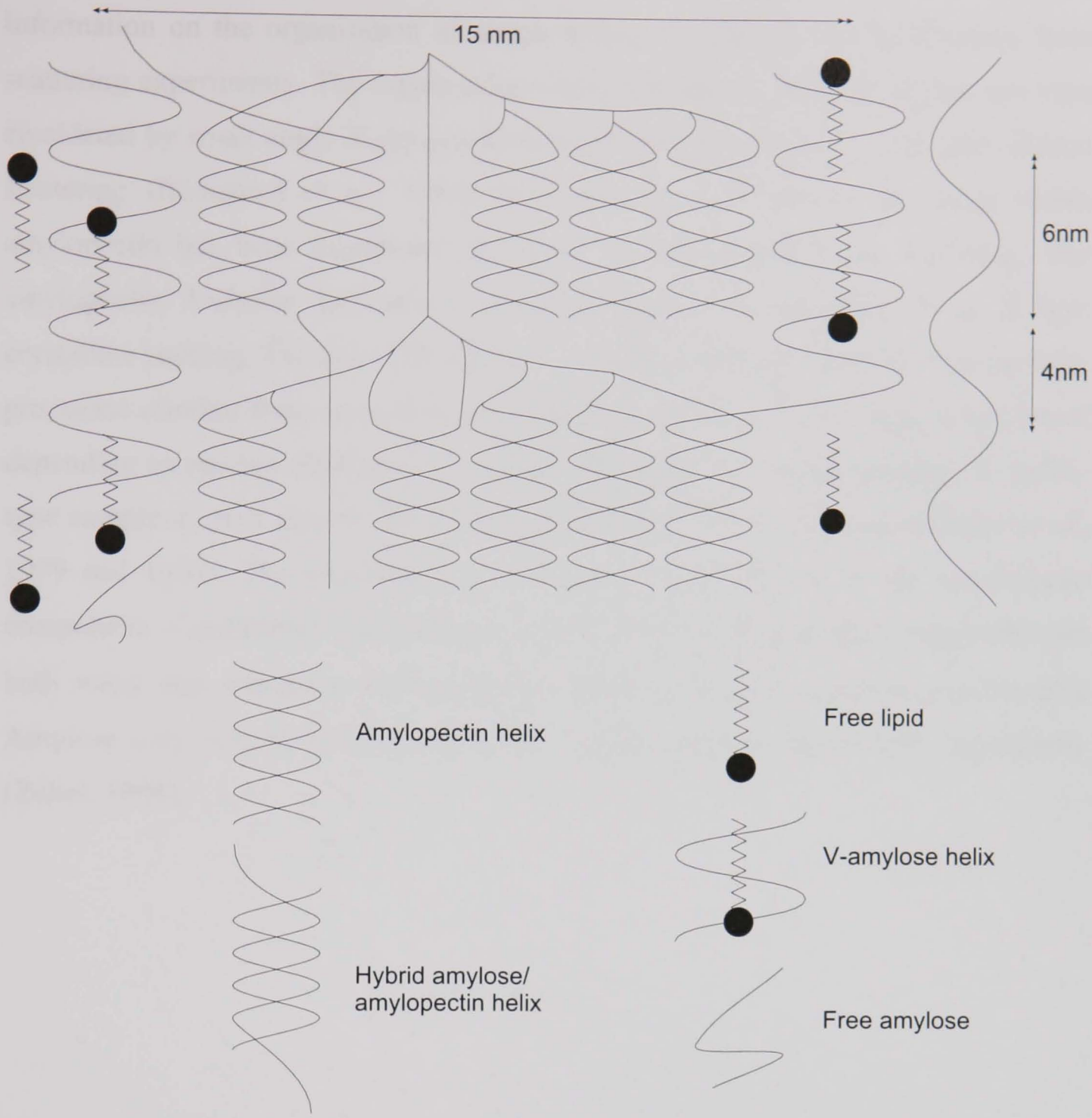

Figure 4-6 Model of order in crystalline region proposed by Blanshard (1987).

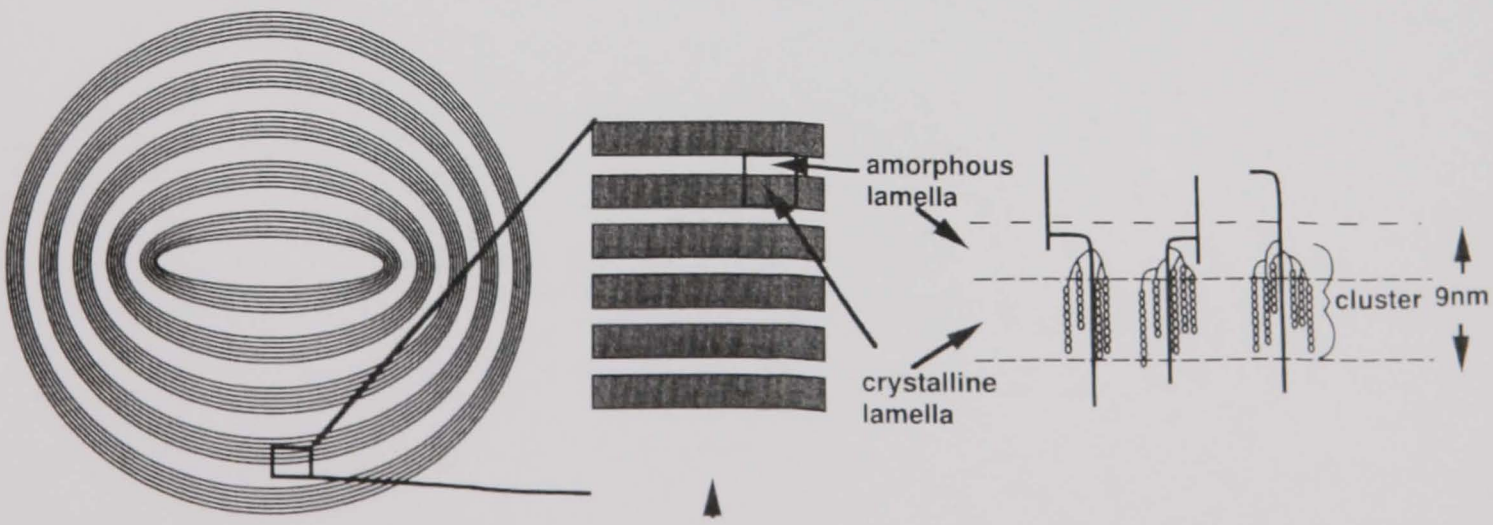

Figure 4-7 Model of starch granule developed by Donald and co-workers (Cameron and Donald, 1992; Jenkins *et al.*, 1994; Donald *et al.*, 1997).

Information on the organisation of starch within the granule can be obtained from scattering experiments. The organisation within the semi-crystalline region has been elucidated by small angle X-ray scattering (Cameron and Donald, 1992) and neutron scattering (Blanshard *et al.*, 1984). The ordering and packing of chains within amylopectin has been determined primarily by wide angle X-ray scattering. The amylopectin A-chains associate as double helices with generally A or B type crystalline packing. The unit cells are shown in Figure 4-8 and Figure 4-9. In contrast, processed starches form amylose-lipid complexes of either V- or E-type arrangement depending on process conditions. As with A and B type crystalline packing, V- and E-type complexes may also be identified by wide angle X-ray scattering (Mercier *et al.*, 1979 and 1980). The crystallinity of the starch is mainly due to the amylopectin component. Crystallinity measured by wide angle X-ray diffraction is comparable for both waxy and non-waxy maize starches (≈0% and ≈28% amylose respectively). Amylose may also be leached out of the granule without altering the crystallinity (Zobel, 1988).

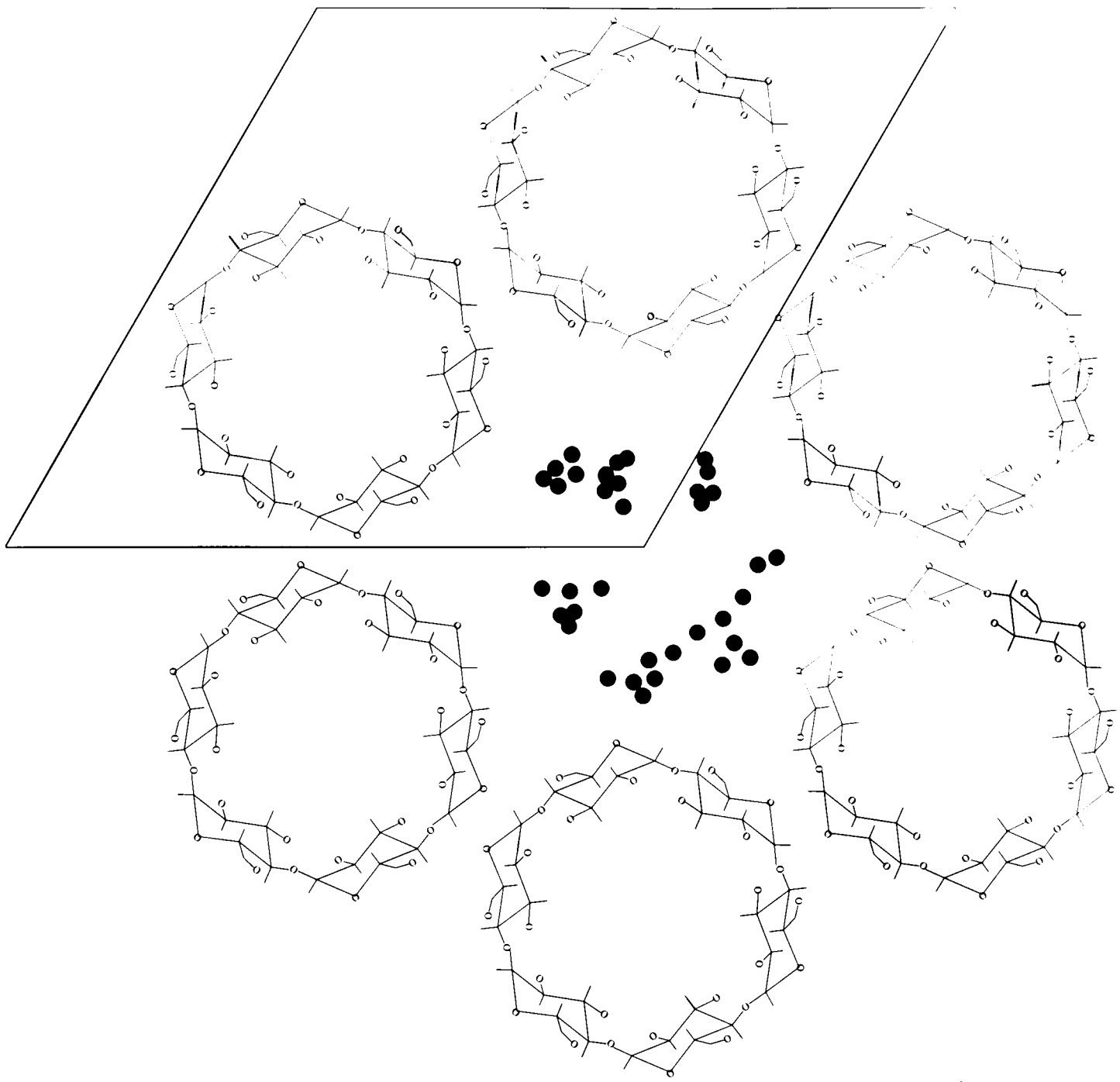

Figure 4-8 Unit cell and helix packing of A-amylose (Kassenbeck, 1975). The ring structures represent the end view of starch helices. The black dots represent water molecules. The trapezoid represents the unit cell.

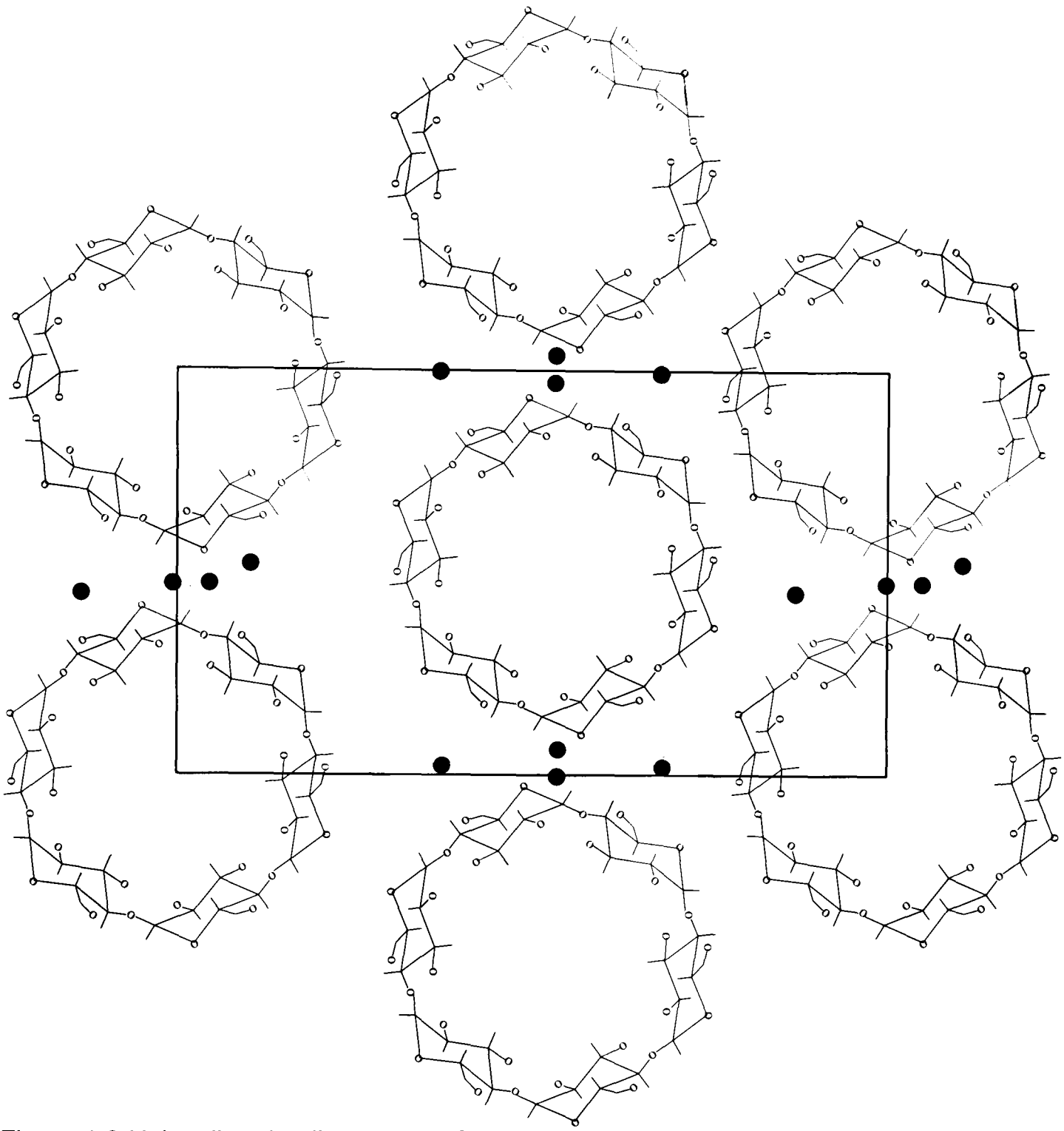

Figure 4-9 Unit cell and helix packing of B-amylose (Kassenbeck, 1975). The ring structures represent the end view of starch helices. The black dots represent water molecules. The rectangle represents the unit cell.

4.2.2 Starch modification by processing

Starch is not normally consumed raw but is modified, usually by a heat process. Native starch is insoluble in cold water, does not swell, and will absorb only about 30% moisture. On heating in excess water starch undergoes the process known as gelatinisation. This is a complex phenomenon involving the loss of the ordered amylopectin regions, swelling of the granule and release of polysaccharide, particularly amylose from the granule matrix. Blanshard (1987) described gelatinisation as the breaking of hydrogen bonds between poly-α-1,4-glucan chains,

leading to loss of crystallinity. A range of different techniques can monitor the extent of gelatinisation.

Starch can be easily identified by optical microscopy when native starch is in aqueous suspension at ambient temperature, and two polarising filters are placed below and above the sample, rotated axially through 90° to one another. Starch granules transmit a white disc with a black cross, usually referred to as a Maltese Cross, due to birefringence. A photograph of this phenomenon is reproduced in Figure 4-10. The birefringence of the starch granules suggests a radial arrangement of the starch polymers within the granule French (1972). This was supported by small-angle light scattering studies (Borch *et al.*, 1972).

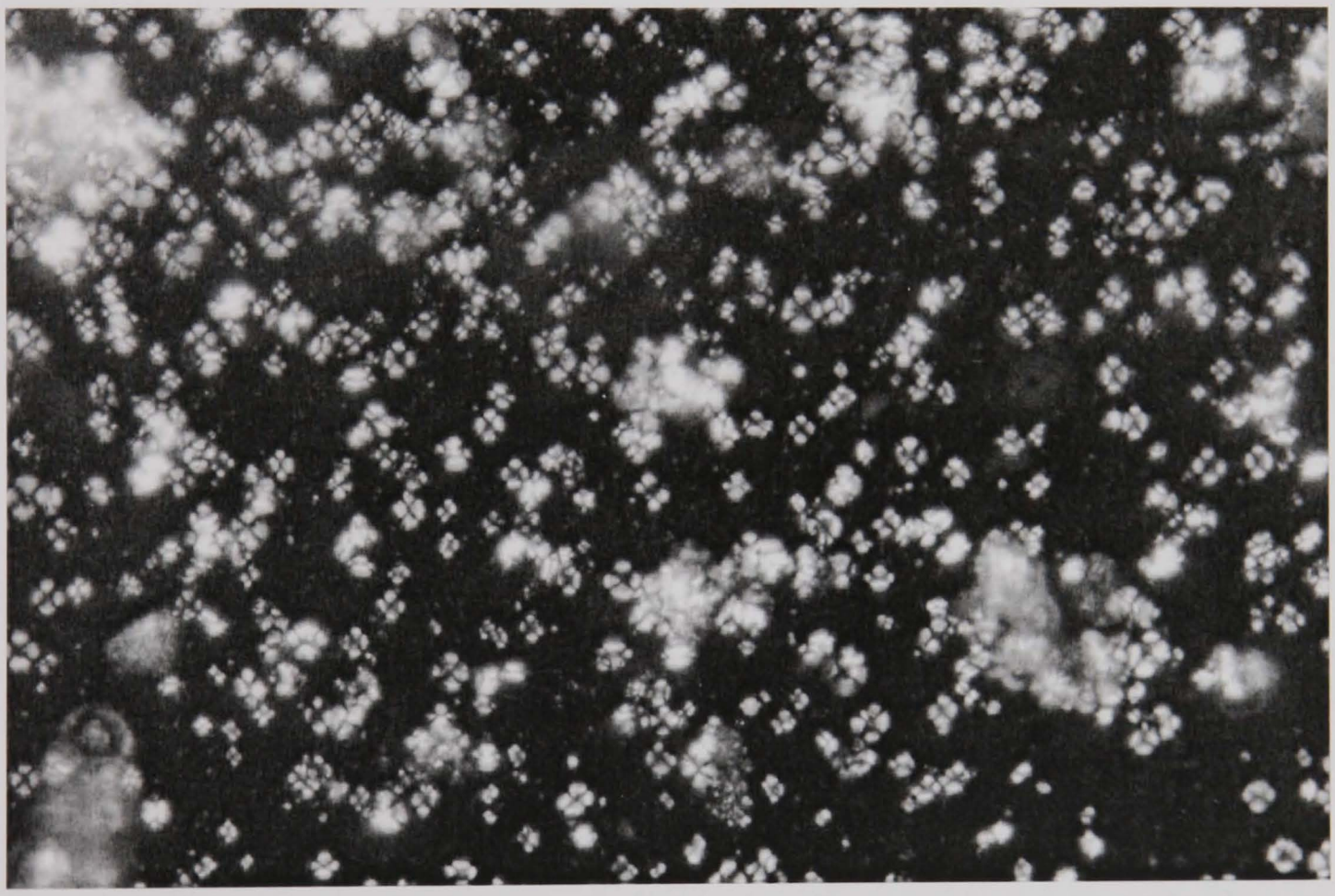

Figure 4-10 Maltese Crosses transmitted by rice flour starch granules. Viewed in aqueous suspension with crossed polarising filters.

Loss of order as a result of gelatinisation can be followed by observing the disappearance of birefringence using a polarising microscope equipped with a hot stage.

Table 4-5 shows the initial, mid-point, and final temperatures over which this loss is observed for a range of starches.

Starch	Type	Granule size (microns)	Gelatinisation Range (Kofler hotstage method) (°C) Initiation	Midpoint	Completion
Maize	Cereal	5-25	62	67	72
High amylose maize (55%)	Cereal	-	67	80	>100
Waxy maize	Cereal	10-25	63	68	72
Sorghum	Cereal	5-25	68	73.5	78
Waxy Sorghum	Cereal	6-30	67.5	70.5	74
Barley	Cereal	5-40	51.5	57	59.5
Rye	Cereal	5-50	57	61	70
Wheat	Cereal	2-45	58	61	64
Oat	Cereal	5-12	-	-	-
Rice	Cereal	3-8	68	74.5	78
Potato	Tuber	15-100	59	63	68
Tapioca, Brazilian	Root	5-35	49	57	64.5
Tapioca, Dominican	Root	5-35	58.5	64.5	70
Sago	Pith	15-70	-	66.2	70
Arrowroot	Root	15-50	66.2	66.2	70

Table 4-5 Temperatures over which starches gelatinise

X-ray diffraction and differential scanning calorimetry can also observe loss of order. When starch is heated in a DSC in excess water an endothermic event is observed corresponding to the initial stages of the gelatinisation event. DSC is useful in quantifying the fraction of ungelatinised starch present in a processed product.

Changes will occur to starch after the loss in birefringence and the disappearance of the DSC endotherm. These changes can be followed by the measurement of viscosity through a heat cycle. The industry standard instrument for determining this is the Brabender Amylograph. A dispersion is heated with rapid stirring through a

temperature cycle that generally involves heating to 95°C, holding at this temperature, then subsequently cooling. Figure 4-11 gives examples of the traces that are obtained. The initial viscosity rise is associated with granule swelling, and the decrease in viscosity on holding at 95°C with disruption of the swollen granules.

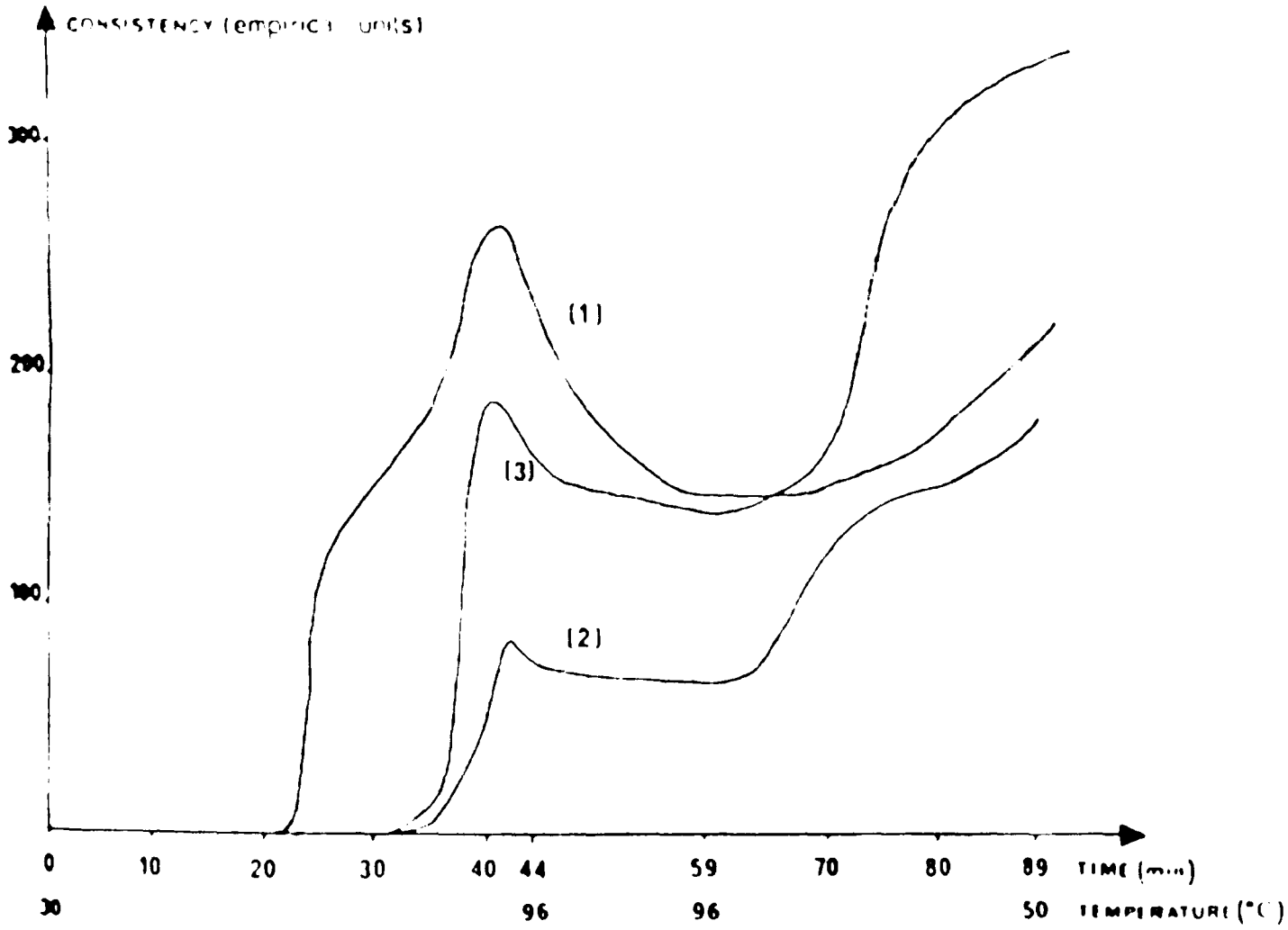

Figure 4-11 Typical Brabender Amylograph traces of potato starch (1, 3.3%); wheat starch (2, 7.2%); and maize starch (3, 6%) (Doublier, unpublished).

Information about the amount of polysaccharide leaving the swollen granule and the degree of swelling can be obtained by centrifuging a suspension and measuring the pellet volume and the supernatant concentration. The parameters WAI and WSI are defined in Section 5.3.5

As the water is decreased the temperature required to gelatinise the starch increases (Lelièvre, 1973). Clearly the rate of thermal gelatinisation at any temperature will decrease with decreasing moisture content.

4.2.2.1 *The Influence of Mechanical Energy*

There has been an increasing interest in the extrusion process for converting starch. The process relies partly on the input of mechanical energy into the material. As the moisture content decreases thermal conversion becomes more difficult as outlined above. The "viscosity" of the material will increase with decreasing moisture content and therefore the mechanical energy input in a screw extrusion process will increase.

In a cooking extrusion process materials are forced through a barrel by a single or twin screw conveying system. The barrel is jacketed and heated by steam, electrical or hot oil systems. Residue times within the extruder are of the order of one minute and pressure can be as high as 300 bar. Twin screw food extruders are generally co-rotating and are more versatile in terms of product type than single screw extruders.

The relative importance of mechanical energy and thermal energy can be compared by calculating the expected amount of thermal conversion from knowledge of time and temperature through a process and the rate constant. Under conditions where maximum temperatures are not greatly in excess of the peak gelatinisation temperature it is found that the mechanical component of conversion dominates. Extrusion cooking processes "convert" starch very efficiently. Often the specific mechanical energy (SME) which is defined as the mechanical energy per unit mass imparted to the extrudate is used as a measure of the severity of the process, the temperature being less important. For most commercial processes this is in the range 100-1000 kJ kg^{-1}, though may be as high as 6000 kJ kg^{-1} (Table 4-6, Colonna *et al.* 1989).

Product	SME (kJ kg^{-1})	Extruder
Corn Grits	360-600	Single screw
	400-600	Single screw
	1500-6000	Single screw
Pregelatinised corn flour	45-120	Single screw
Diamylopectine phosphate	500-700	Single screw
High-moisture dough	32-64	Single screw
Corn-gluten mix	150-950	Single screw
Corn-soy mix	360-400	Single screw
Flat-bread mix	800-1100	Twin screw
	200-350	Twin screw
	1200-2100	Twin screw
Wheat starch	300-750	Twin screw
Potato starch	200-500	Twin screw
Wheat flour	200-1000	Twin screw

Table 4-6 Specific mechanical energy (SME) input for varous products (Colonna *et al.*, 1989)

Products produced by extrusion often have a different character to those produced simply by thermal processing of starch. This may in part be due to the greater degradation of the starch polysaccharides in the extrusion process. This has been quantified and related to mechanical energy by several investigators.

4.3 The Role of the Glass-Rubber Transition

Central to the understanding of the low moisture content processes is the glass to rubber transition. At ambient temperature the glass transition of amylopectin occurs at about 20% moisture (wwb) (Kalichevsky *et al.* 1993c). This moisture content is not much lower than that encountered in extrusion and conventional cereal processes. In this low water region the viscosity changes very rapidly with both moisture and temperature. Viscosity has a major influence on mechanical energy input in an

extruder and on subsequent expansion and shrinkage processes. In contrast, viscosity has almost no effect on the energy input in conventional processes.

4.3.1 Glass Transition Overview

The glass transition temperature (T_g) is the point at which materials pass from a glass to a rubber structure; a material can form a glass if crystallisation is inhibited by steric hindrance, kinetics, etc (Farhat 1996). Slade and Levine (1991) defined a glass as an amorphous supercooled liquid of extremely high viscosity (between 10^{10} and 10^{13} Pa.s.).

4.3.2 Molecular Mobility in the Glassy and Rubbery States

Traditionally, T_g has been found by studying the discontinuity in the changes in the thermal and rheological properties of a system, either as a function of sample temperature or composition (Farhat 1996). However, similar discontinuities have been reported in NMR proton relaxation (Kalichevsky *et al.* 1992; Ablett *et al.* 1993), rotational correlation times (Sandrecski and Brown 1988; Roozen and Hemminga 1990, 1991; Le Meste *et al.* 1991) and translational diffusion (Karel and Langer 1988; Karel and Saguy 1991; Ablett *et al.* 1993).

The situation in terms of the molecular mobility in the glassy and rubbery states can be summarised as follows:

~ The molecular mobility of the matrix molecules in a system is very reduced in the glassy state as compared to the rubbery state.

~ The mobility of small molecules can be observed in glassy biomolecular systems.

~ The majority of the workers in the field attribute the enhanced stability of food systems in the glassy state to the reduced mobility below T_g (Farhat 1996).

4.3.2.1 Main Glass-Transition Theories

This is a brief summary of concepts; more detailed explanations can be found in Slade and Levine (1991), Mansfield (1993) and Kalichevsky (1993a).

4.3.2.1.1 Thermodynamic or Entropy Theories

The glass transition is a second order phase transition with discontinuities in the thermal and calorific values. These theories were devised by Gibbs *et al.* (1956, 1958) based on the work of Flory (1953). It was suggested the glass transition occurs when the relaxation time of the system exceeds the measurement time scale. However, this approached is criticised for several reasons, the most important being that thermodynamic theories assume the system is at equilibrium although it is now accepted the glass transition is determined kinetically (Farhat 1996).

4.3.2.1.2 Free Volume Theory

If individual molecules are considered to be spheres in the glassy state, the unoccupied or free volume is reduced. For molecules to change their location or motional state, they must be able to move into the free volume. Increasing the temperature to higher than T_g (i.e. into the rubbery state) provides an increase in the free volume, allowing an increase in both rotational and translational molecular mobility Diagrams. However, kinetically dependent processes such as viscosity or volume expansion (Farhat 1996) determine the free volume.

4.3.2.1.3 Kinetic Theories

It is widely accepted the measured value of T_g depends on the experimental frequency and heating rate and sample history. This approach does not attempt a molecular understanding, but is based on the observed rate dependent behaviour in terms of several relaxation times (Farhat 1996).

4.3.3 The Glass Transition and Expanded Cereal Products

Expanded cereal products are dependent on the glass-rubber transition in two main ways. Firstly, the unexpanded material must be in the rubbery state before it can expand during production (Fan *et al.*, 1994) and secondly, the material must be in the glassy state when eaten to be perceived as crunchy, crackly, or crispy. This change in states is achieved by utilising high temperatures and moisture contents during production, then drying or toasting and cooling before consumption.

Extruded samples do not expand at die temperatures below 100°C or 373K. Above this temperature, moisture within the extrudate vaporises as it leaves the extruder die, expanding the product due to internal vapour pressure. Rupture of the cell walls or cooling may lead to a drop in vapour pressure in the cells. If a drop in pressure occurs before the cell walls have cooled sufficiently, then the cell may shrink or collapse. Mitchell *et al.* (1994) reported domains in which materials exhibit bubble growth and shrinkage, shown in Figure 4-12. Both expansion and collapse are only noted while the temperature of the material is greater than T_g+30. Expansion can only occur above the critical temperature T_c, at which internal and external vapour pressures are equal (P_a and P_b). Similarly, collapse of unruptured cells can only occur below T_c. For example, extrudate at the moisture content and temperature represented by point A will expand. The extrudate will cool and dry, following the curve to point B, where expansion and rapid moisture loss will cease. Further cooling will cause the extrudate to collapse, until point C is reached (T_g+30). Further cooling or drying will not lead to expansion or collapse as the extrudate is too inelastic. It is interesting to note that the T_g+30 curve and the T_c curve cross at point O. At lower moisture contents than this, collapse cannot occur.

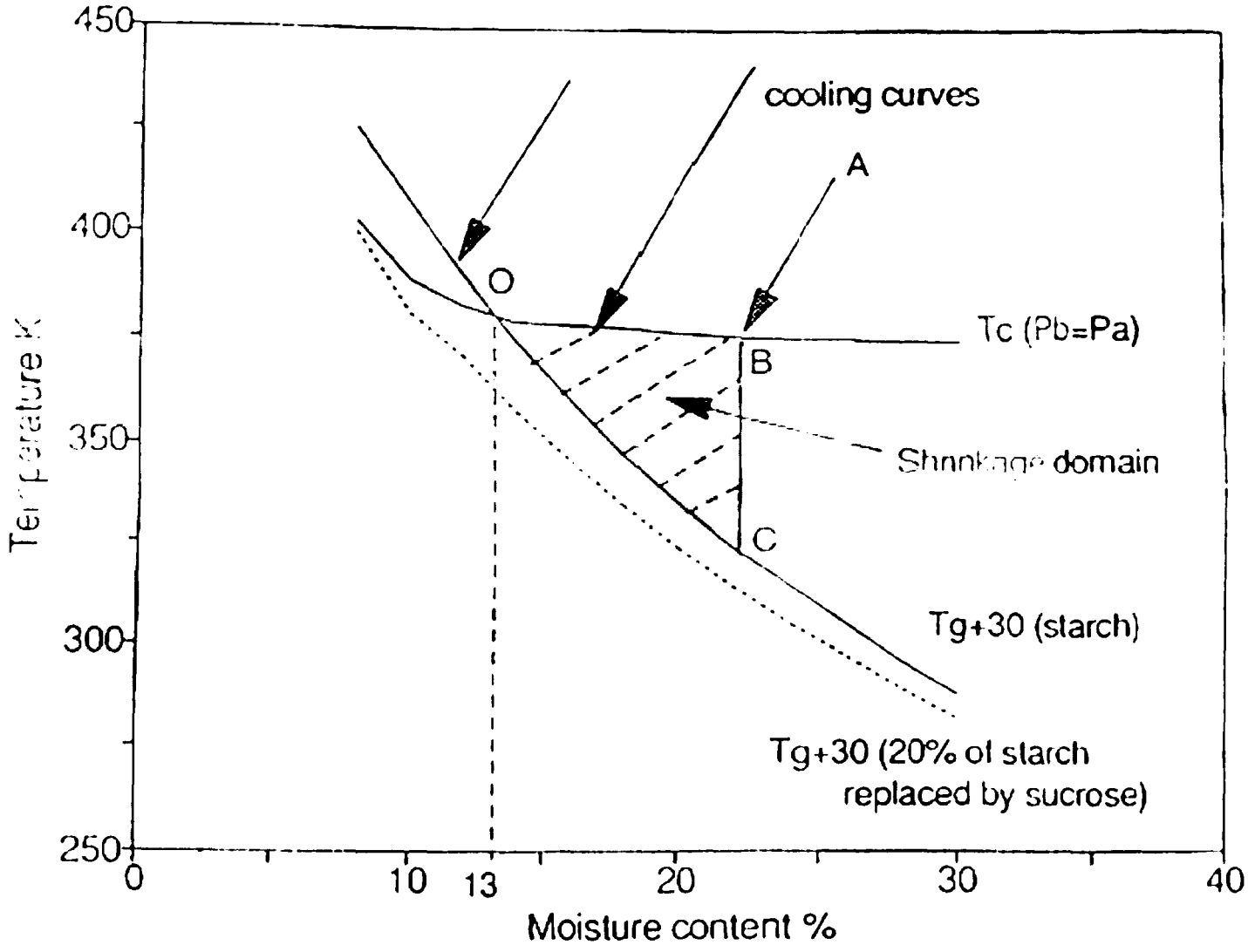

Figure 4-12 Growth and shrinkage domains during bubble growth (Mitchell *et al.*, 1994; Fan *et al.*, 1996a). Points A, B, C, O are to aid commentary in Section 4.3.3. T_c is the critical temperature at which forces promoting expansion and collapse are equal (i.e. $P_a=P_b$). T_g is the glass transition temperature

4.3.4 Retrogradation and the Glass Transition

The term retrogradation is frequently given to the process by which gelatinised starch may recrystallise, giving the impression of staling. Due to the commercial importance of retrogradation, there have been many studies over the past eighty years since a review by Katz (1928) of his work between 1912 and 1916. Indeed, published studies began in 1852 when Boussingault showed bread could be "refreshened" by heating to 60°C.

Farhat (1996) explains that the rate of retrogradation has a maximum due to opposing effects. Between the glass transition point (T_g) and the melting point (T_m), the rate of crystal nucleation decreases to zero with increasing temperature. However, between the same two points, the rate of crystal propagation increases from zero with increasing temperature. Due to these effects, the maximum rate of propagation lies

between T_g and T_m, see Figure 4-13. As the amount of sugars, water, or other plasticisers in the starch mixture reduces both the T_g and the T_m of the mixture, then the rate of retrogradation is also affected. Retrogradation leads to A-type starch crystallinity at high temperatures or low moisture contents, and to B-type crystallinity at low temperatures or high water contents.

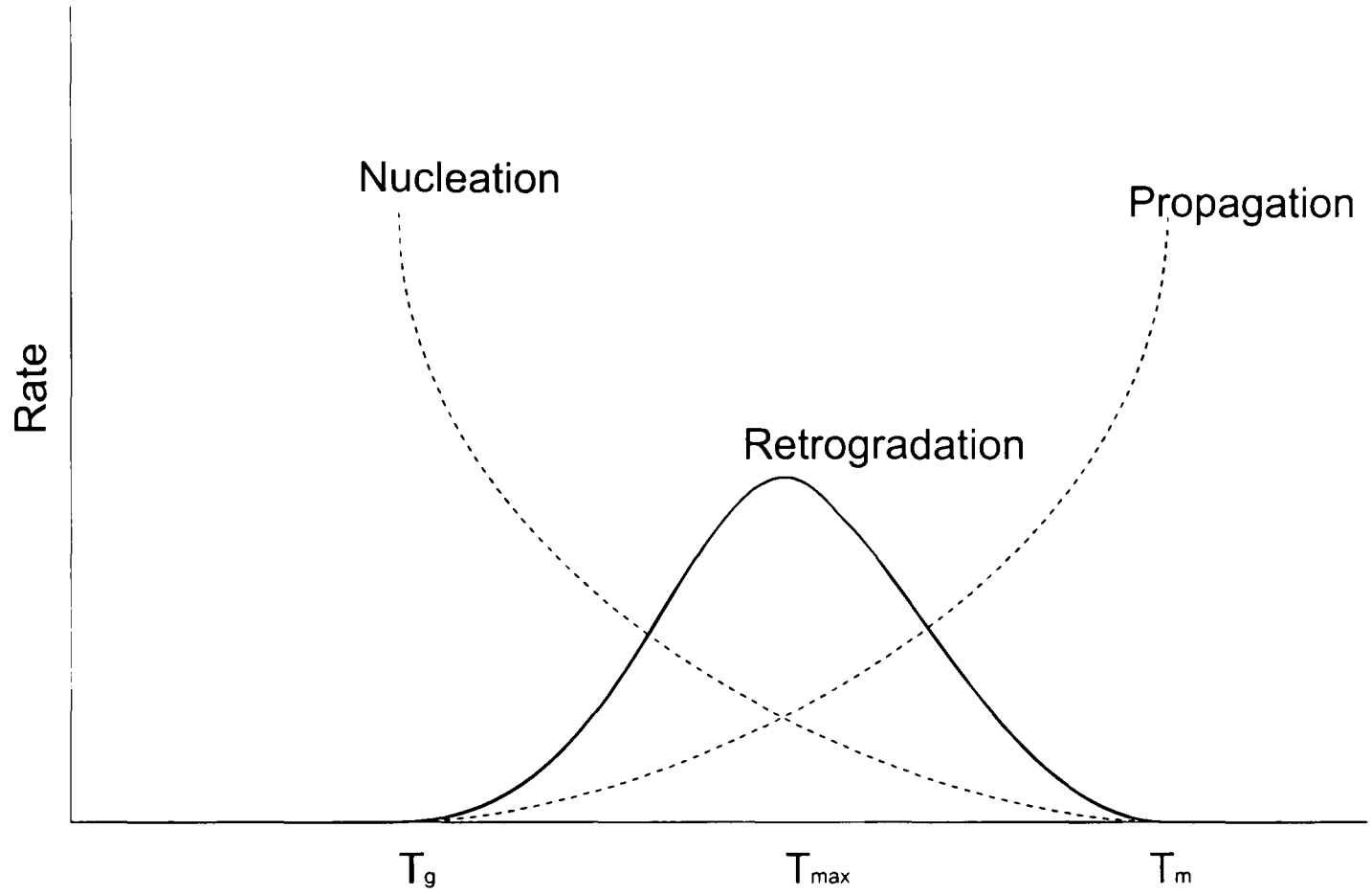

Figure 4-13 Diagram representing the effect of temperature on the crystallisation kinetics of partially-crystalline polymers (Farhat, 1996)

4.4 Plasticisers

Small molecule plasticisers such as water or sugars will lower the glass transition temperature T_g (Section 4.3), in an amount estimable by the Couchman-Karatz Equation, given for two and for n component systems.

$$T_g = \frac{W_1 \Delta C_{p1} T_{g1} + W_2 \Delta C_{p2} T_{g2}}{W_1 \Delta C_{p1} + W_2 \Delta C_{p2}}$$

Equation 4-1 Couchman-Karatz equation for a two component system (Blanshard, 1995)

$$T_g = \frac{\sum_1^n \left[W_n \Delta C_{pn} T_{gn} \right]}{\sum_1^n \left[W_n \Delta C_{pn} \right]}$$

Equation 4-2 Couchman-Karatz equation for an n component system (ten Brinke *et al.* (1983), developed from Couchman and Karatz (1978)).

Where T_g is the glass transition temperature of the system; W_1, W_2, W_n are the weight fractions of the components; ΔC_{p1}, ΔC_{p2}, ΔC_{pn} are the changes in heat capacity of the components; T_{g1}, T_{g2}, T_{gn} are the glass transition temperatures of the components. Some useful values are recorded in Table 4-7.

	T_g /K	ΔC_p /JK^{-1}kg^{-1}
Water	134[d]	1.94[d]
Amylopectin	502[a,b]	0.41[a], 0.425[b]
Sucrose	343[c]	0.76[c]

[a] Kalichevsky and Blanshard (1993b)

[b] Kalichevsky *et al.* (1993a)

[c] Orford *et al.* (1990)

[d] Sugisaki and Suga (1968)

Table 4-7 Glass transition temperatures and changes in heat capacity for water, amylopectin, and sucrose

Figure 4-14 shows the influence of sucrose and water on the glass transition temperature of starch calculated using Equation 4-1 and Equation 4-2.

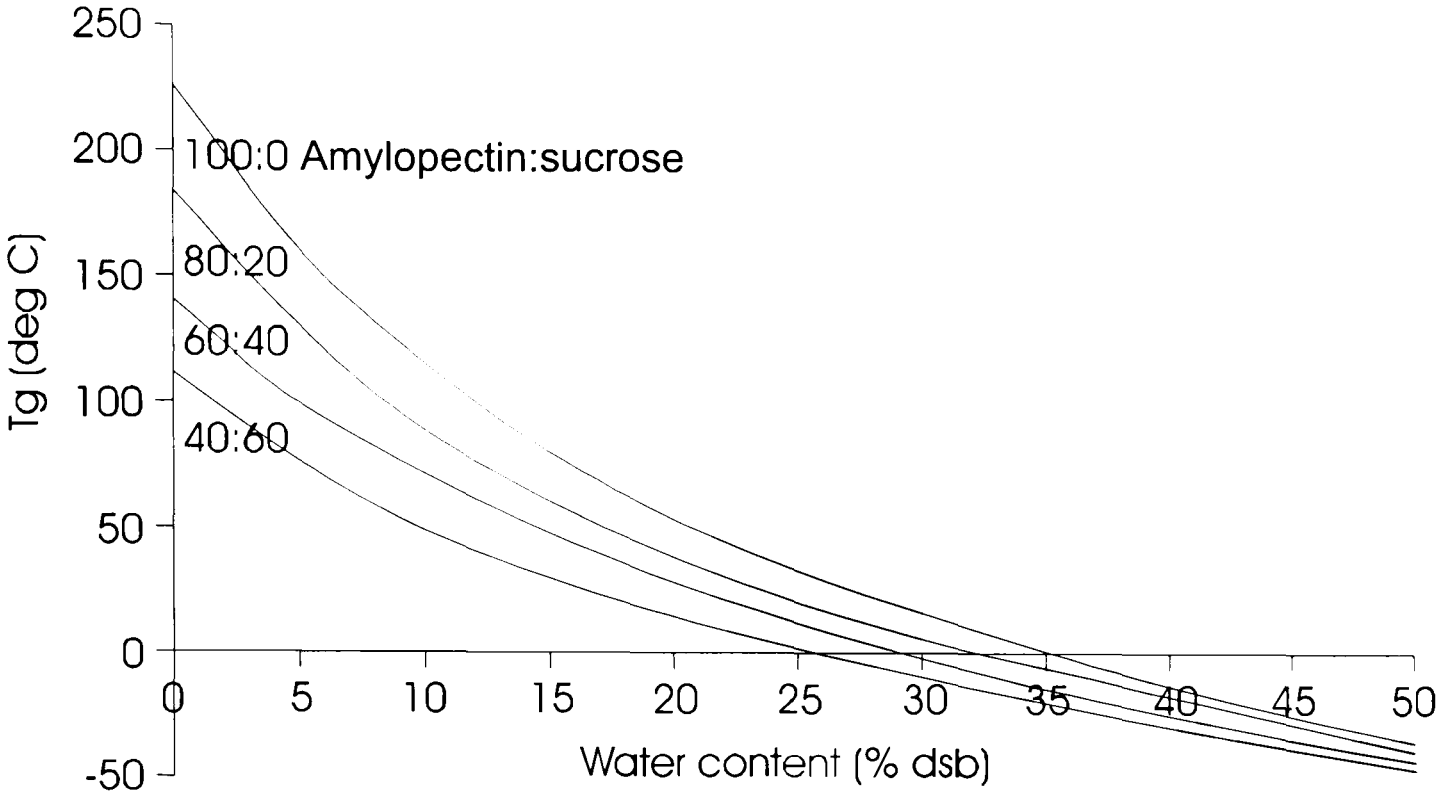

Figure 4-14 Effect of moisture and sucrose on the Tg of amylopectin

Since the replacement of starch by sucrose at constant moisture content will lower T_g, it will also lower viscosity and hence the SME in an extrusion process. Fan *et al.* (1996b) demonstrated how sucrose addition reduces the degree of maize starch conversion during extrusion. Addition of sucrose also reduces expansion at the extruder die as a result of collapse due to the decreased T_g and therefore lower T_g+30 at which extrudate viscosity is low enough for expansion or collapse to occur (Section 4.3.3).

4.5 Water Uptake by Rubbery and Glassy Polymers

An important property of processed cereal products is the rate of water uptake. Penetrant transport in both rubbery and glassy polymers may be classified as Fickian (Case I), non-Fickian (anomalous), Case II, or super Case II transport. The type of transport depends on the thermodynamic activity and temperature of the system, structural parameters such as molecular weight, degrees of crosslinking and branching, and thermal and expansion coefficients of the polymer (Peppas and Brannon-Peppas, 1994). Identification of which transport mechanism is in effect may be found by gravimetric methods; the amount of water absorbed by the polymer is plotted versus time, and fitted to the equation

$$\frac{M_t}{M_\infty} = kt^n$$

Equation 4-3 Generic diffusion equation

Where M_t and M_∞ are the masses at time t and ∞, and k is a constant. If the exponent n is 0.5 then the diffusion is Fickian. Non-Fickian behaviour is observed for $0.5<n<1$, and Case II diffusion is the limiting behaviour when n is equal to 1. Non-Fickian and Case II transports indicate relaxational mechanisms may be affecting the transport mechanism (Peppas and Brannon-Peppas, 1994).

However, though the above mechanisms of diffusion apply to the solid phase of expanded rice, the effect of large-scale structure must also be considered. Intuition demands that a sponge like sample (i.e. continuous solid and gaseous phases) will adsorb moisture vapour more quickly than a continuous solid sample; indeed, observations show this to be true. The effect of a foam (i.e. continuous solid and discontinuous gaseous phases) is less clear; the gaseous phases may accelerate diffusion, or may act as insulation against diffusion. Simple observations show foams adsorb water vapour more quickly than solid phases. However, in these comparisons, it should be noted the starch in the three structures cannot be identical.

4.5.1 Fickian (Case I) Diffusion

In a one dimensional system, Fick's Law states that the flux of molecular diffusion, Q, is dependent upon the coefficient of diffusion, D, and the concentration gradient of the diffusing molecules, $\frac{\partial c}{\partial x}$.

$$Q = -D\frac{\partial c}{\partial x}$$

Equation 4-4 Fick's Law for a one-dimensional diffusion

Fick's Law can be adapted to three dimensions by

$$\underline{Q} = -\underline{D}.\underline{\nabla}c$$

Equation 4-5 Fick's Law for a three dimensional diffusion

4.5.2 Case II Diffusion

Whereas Fickian (Case I) transport was characterised by a single coefficient of diffusion, Case II can be characterised by a relaxation constant, k_0. For a sample of thickness l and cross-sectional area A, the Case II diffusion in the region $0 < x < \frac{l}{2}$, where x is the position of the advancing front, is given by Equation 4-6 (Peppas and Brannon-Peppas, 1994).

$$Q = k_0 A$$

Equation 4-6 Case II diffusion in a plane

4.5.3 Non-Fickian (anomalous) Diffusion

Non-Fickian diffusion is a combination of Fickian (Case I) and Case II diffusion mechanisms, requiring two or more parameters to describe the interaction between diffusion and relaxation effects. Mathematical analyses of these interactions are not well understood (Peppas and Brannon-Peppas, 1994).

4.5.4 Extension to Expanded Biopolymers ~ the Effects of Sponge or Foam Structures

The expanded form of the polymers studied in this project render the mechanics of diffusion through solids largely irrelevant. The solid polymers are interspersed with gas pockets in the case of a foam. Such air pockets interrupt advancing waterfronts, altering the diffusion of water through the product. In the case of a sponge, air and the solid polymer each form one of two continuous phases. Water molecules are able to diffuse through either phase, air currents may cause water vapour to flow through the gaseous phase, and liquid water is able to fill the air phase due to capillary action.

Other workers have acknowledged the importance of open and closed structures (sponge and foam respectively) (Launay and Lisch, 1983; Donald *et al.*, 1993; Mitchell *et al.*, 1994; Fan *et al.*, 1996). Launay and Lisch (1983) used a pycnometer to show the specific gravities of several expanded starch-based products were close to that of the same products when ground. These findings indicated most of the cells

were open, forming a sponge. However, Donald *et al.* (1993) used microscopy to show that expanded maize samples contained closed cells, forming a foam. These findings supported a proposal by Mitchell *et al.* (1994) that it is possible for ruptured cells to "heal" under suitable conditions. A "healing" theory helps explain how water can be lost so rapidly during expansion of extrudate at the die when diffusion through cell walls is a relatively slow mechanism. Fan *et al.* (1996) concluded that the reduction in extrudate viscosity caused by addition of plasticisers (Section 4.4) can reduce starch conversion and consequently promote cell rupture at smaller degrees of expansion.

4.6 Manufacture of Breakfast Cereals

Breakfast foods made from cereal grains are of two main types, those requiring cooking and those that are ready to eat (Brockington and Kelly, 1972), such as porridge and corn flakes respectively. The ready to eat genre were invented at the start of the 20th century with the development of corn flakes by Kellogg and puffed rice by Anderson in 1904 (Brockington, 1950; Brockington and Kelly, 1972). Breakfast cereals may be made from whole cereal grains, or from flour milled from those cereals (Brockington and Kelly, 1972).

4.6.1 Puffed Rice Based Breakfast Cereals

The most common rice cereals are puffed rice, most notably Kellogg's® Rice Krispies®. Variations on this are sugarcoated and cocoa-flavoured puffed rice (Kellogg's® Ricicles® and Coco-Pops® respectively). Expanded rice products are usually made from short to medium grain rice (Ong, 1994, Brockington and Kelly, 1972).

A method for preparation of conventionally puffed rice is given in Fast and Caldwell (1990):

4.6.1.1 Production of Puffed Rice

"Oven-puffed cereals are almost exclusively made from rice or corn or mixtures of these two grains. These two grains inherently puff in the presence of high heat when the moisture content is correct, whereas wheat and oats do not. [Of course, puffed wheat or oats must not be discounted completely - Quaker's® Sugar Puffs® are sugar-coated puffed wheat]

4.6.1.2 Formulation and cooking

"Usually medium grain rice is the starting material for oven puffed rice. It is pressure cooked with sugar, salt, and malt flavouring for about an hour at 15-18 psi. A typical formula is as follows: medium grain white rice, 100 lb; sugar, 6-10 lb; salt, 2 lb; malt extract, 2 lb; and water sufficient to yield cooked rice at 28% moisture.

After cooking, the rice is conveyed through a cooling and sizing operation, which removes the heat of cooking and returns the rice to ambient temperature. It also breaks agglomerates into individual kernels.

4.6.1.3 Drying and Bumping

"Drying is an additional process, with additional steps between the first and second drying. First, the rice is dried to reduce the moisture content from 28% to about 17%. Then it is tempered 4-8 hr, or long enough for good moisture equilibrium. After tempering, it is bumped, that is, run through flaking rolls to slightly flatten the kernels but not to make thin flakes out of them. Bumping presumably creates fissures in the kernel structure, which promote expansion at high oven temperatures. The thinner dimension also allows for faster heat penetration. Bumping is essential for proper puffing in the heat of the oven.

After bumping, the rice is dried a second time, to reduce the moisture content from 17% to 9-11%. This second drying is needed for good oven puffing, an operation that requires a proper balance between the grain moisture content and the oven temperature.

4.6.1.4 Oven Puffing

"Generally, oven puffing is characterised by extremely high oven temperatures (550-650°F, or 288-343°C) in the latter half of the oven cycle. Final toasting and puffing are accomplished in about 90 sec in rotary flake-toasting ovens or other fluid-bed ovens. After oven puffing, the cereal is cooled, fortified with vitamins if used, and frequently treated with antioxidants to preserve freshness," (Fast and Caldwell, 1990).

4.6.2 Flaked Rice Based Breakfast Cereals

Flaked rice cereals, such as ReadyBrek®, are also available and often served with hot instead of cold milk. Flaked rice products usually use short grain rice (Brockington and Kelly, 1972). The preparation method for flaked rice is given in Brockington and Kelly (1972) as follows: *"Rice is cooked in a rotary cooker at 18-19 lb pressure. After 20 minutes, the steam pressure is bled off to remove steam and gases. Cooking is continued for 1-2 hours. The completeness of cooking is determined by the presence of uncooked centres in individual grains. An anti-coagulant is often used to prevent the agglomeration of large clusters of rice grains. Finely ground wheat bran is often added to the recipe in quantities up to 5%. Post-cooking moisture content should be about 33%. The surfaces of the rice grains are dried to aid handling in later stages. After being further dried to about 17% moisture, the rice is tempered for several hours to allow equilibration of moisture. After tempering the rice is flaked between rollers, then toasted. The final moisture content should be about 3%, and the colour a light tan,"* (Brockington and Kelly, 1972).

4.6.3 Extruded Rice

The extrusion of rice leads to a hard non-expanded product or to an expanded product of foam or sponge construction depending on extrusion parameters. The extruded expanded rice was used as a filling in a popular confectionery bar.

4.6.4 Effect of Extrusion Process Variables on Properties of Expanded Rice Products

It is recognised that there are strong interactions between extrusion process variables. Because of these interactions, it is important to have some understanding or hypothesis before designing experiments. In this section, each process variable will be discussed in terms of how it affects processing, how it affects other variables, and as a consequence how it may affect product properties. One of the objectives of the subsequent discussion is to consider the effects of extrusion process variables. An important process parameter that will be influenced by all three variables is the specific mechanical energy (SME). The three variables to be considered are-

a) Barrel temperature

b) Water addition

c) Screw speed

4.6.4.1 Barrel Temperature

The four heating zones of the extruder used during this project are controllable (Figure 4-15). Each zone is equipped with a thermocouple and water coolant system, and the last three zones also have 800W heaters. The coolant and heating systems are switched on and off automatically to try to maintain a fixed temperature, typically 40-160°C, which is set by the operator. By controlling the temperature of the barrel wall, some control over the temperature of the extrusion melt is gained.

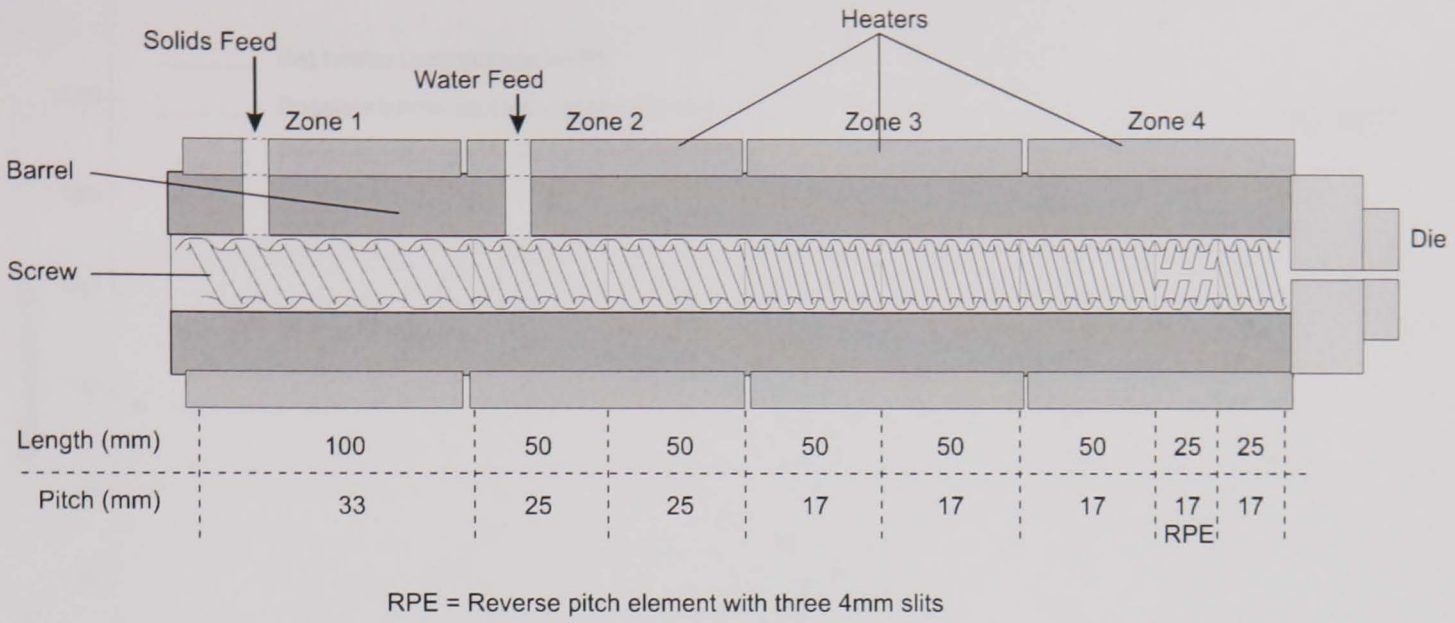

Figure 4-15 Clextral BC-21 Twin screw extruder in cross section.

It is important to appreciate that the heater temperature is not normally the same as the melt temperature for any given distance along the barrel. The thermocouples are inside the bulk of the extruder barrel, not on the interior surface. This error cannot be overcome with an offset to the measured versus recorded temperatures as the extrusion melt may be of a higher or cooler temperature than the extruder barrel. Figure 4-16 schematically shows the possible differences between heater temperature, barrel wall temperature, and melt or extrudate temperature. The die has neither heating nor cooling capabilities, so the only effects the die may have are heating through mechanical resistance, or merely insulating. The temperature at the centre of the extrusion melt is unlikely to be identical to that of the extrusion melt in contact with the extruder barrel, also suggested in Figure 4-16. Additionally, the extrudate may be at a higher temperature than the barrel, due to mechanical heating; the example in Figure 4-16 shows this effect in heating zone 4. Even if the barrel temperature did follow the set profile exactly, the temperature of the extrusion melt would not change between the two zone temperatures immediately that the melt crosses the zone boundaries as this would require an infinitely large heat flux through the melt, or for the melt to have no heat capacity. Figure 4-16 also shows the sudden heat loss due to expansion shortly after the melt exits the die.

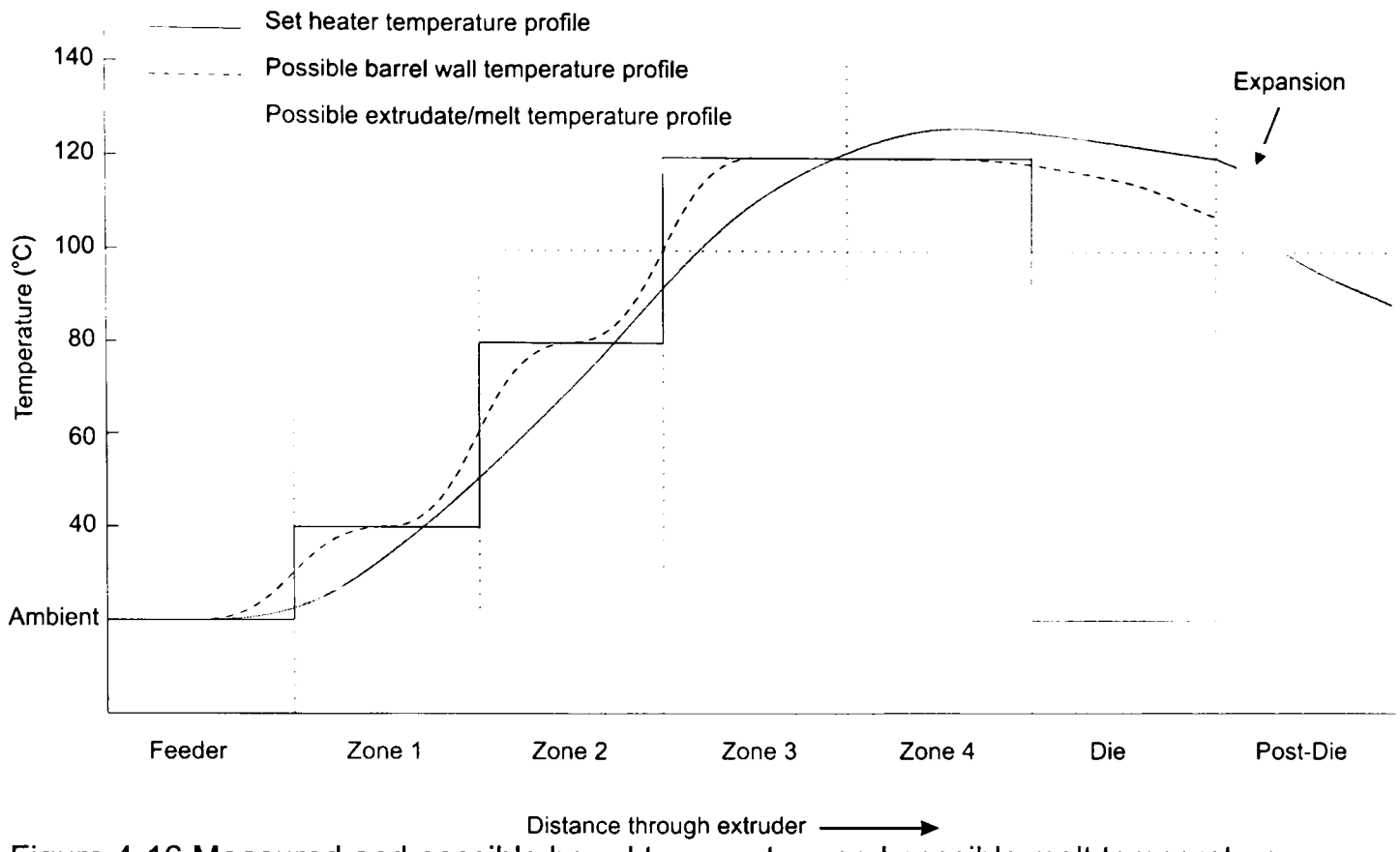

Figure 4-16 Measured and possible barrel temperature and possible melt temperature

4.6.4.1.1 Effect of Temperature on Processing

Increased temperature will increase thermal gelatinisation and/or melting of the starch granules. For expansion after the die, the extrudate must be greater than 100° C to develop internal steam pressure, and must also be hotter than Tg+30 K for the extrudate to be sufficiently flexible to expand (Fan *et al.*, 1994). Extreme temperatures and/or low moisture contents cause the extrudate to expand violently after leaving the die.

An increase in temperature will reduce the viscosity of the extrusion melt, thus reducing backpressure and torque, and therefore reducing specific mechanical energy.

4.6.4.2 Extrusion Moisture Content

Many food processes require water, and the extrusion of expanded rice is no exception as water is needed for a number of reasons; notably gelatinisation, expansion, and reduction in viscosity. Water is typically added to an extruder by two routes. Firstly, rice flour has an inherent moisture content (unless dried further) of around 13-14% on a dry weight basis. Secondly, additional water is usually added; during this project water was inserted at the second heating zone (Figure 4-16). This added water was in the range 0-43% of the mass of the original undried rice flour.

4.6.4.2.1 Effect of Moisture Content on Processing

During this project, though the lightest textured samples were made with no added water, the samples perceived as most crisp and most crackly by a sensory panel were those samples with 8% and 12% added water respectively. Microscopic examination showed that samples made at 120° C with less than 3% added water created sponges, whereas samples with more than 3% added water created foams, or did not expand. Examination by optical microscopy showed that when little water was present, the granules could not gelatinise aqueously and so remained intact or became broken into fragments due to shear. Alternatively, thermal gelatinisation (melting) occurred if the temperature was sufficiently high. Granules that melted did not allow amylose to leach from the granule, though the granule probably became mixed into others due to high shear and mixing. As the starch molecules did not mix and had very little molecular mobility, they could not recombine or retrograde to form E- or V-type complexes. This was seen in both X-ray diffraction spectra and in microscopy where the samples appeared opaque instead of translucent and refracting.

Extruded samples with higher moisture contents (above 15% dwb) although still below the glass transition temperature of amylopectin at ambient room temperature (Kalichevsky *et al.*, 1992) were perceived as soft, rubbery, or leathery. This is consistent with Nichols *et al.* (1991) and Roudaut *et al.* (1998) who have shown loss of crispness at moisture contents of the order of 9% wwb.

Although moisture is required for expansion, a range of samples produced at a fixed temperature and screw speed generally had a negative co-relationship between added water and extent of expansion because the SME is decreased with increased water.

4.6.4.2.2 Effects of Moisture Content on other Variables

The addition of water will decrease the viscosity of the extrusion melt, reducing the backpressure, torque, and SME. In addition, as the total feed rate increases as the fluids feed rate increases, the SME will also be reduced as it is defined as an inverse function of the feed rate. The change in SME is noticeable by the behaviour of the temperature controllers during extrusion as with very little added water, the heating zones generally cool the extrudate, whereas with more added water, the heating zones

generally heat the sample. The addition of water will increase the heat capacity of the extrusion melt, increasing the demands on the heating zones, and reducing the ability of the extruder to raise or lower the temperature of the extrusion melt to the four zone temperatures.

4.6.4.3 Screw Speed

The rate of rotation of the extruder screws (Figure 4-15) can be controlled. As the screw speed increases, the rate of mixing and propagation of the extrusion melt increases.

4.6.4.3.1 Effect of Screw Speed on Processing

An increase in screw speed typically increases the extent of expansion. Mechanical degradation of the starch granules also increases, as can be seen microscopically.

As the screw speed increases, the ratio of mechanical to thermal energies imparted to the melt within the extruder is increased dramatically. Low screw speeds do not provide enough mechanical energy to gelatinise starch granules, so all starch processing must be provided by thermal energy. However, at high screw speeds, the energy imparted to the extrusion melt by the screws is so great that the heating zones actually try to cool the extrudate to maintain a temperature set-point. Thus thermal energy is removed from, not imparted to, the extrudate. Therefore at high screw speeds, all starch processing is due to mechanical energy. Naturally, there is a smooth transition between these extreme ratios of screw speed as it is increased.

4.6.4.3.2 Effects of Screw Speed on other Variables

Increasing the screw speed will generally increase the torque required to turn the screw. As SME is a function of the product of these two parameters, SME will also increase. However, it has been noted torque decreases when attaining screw speeds above 400 rpm. This could be due to slip planes or alternatively reflect the dominating effect of shear thinning.

4.6.4.4 *Specific Mechanical Energy (SME)*

Like torque, SME is variable that is not operator definable. SME is the amount of mechanical energy imparted to each unit mass of extrudate. For extrusion of starch, typical values of SME vary from 50 to 1000 J g^{-1} (Colonna *et al.*, 1989), with expansion requiring about 200 J g^{-1} or more. SME may be calculated by either of the following methods.

$$SME = \frac{Power}{Feedrate} = \frac{P}{R \times \frac{1000}{60 \times 60}}$$

Equation 4-7 Calculation of SME from power measurements

$$SME = \frac{Torque \times screwspeed}{feedrate} = \frac{2\Gamma F \times \frac{2\pi}{60}}{R \times \frac{1000}{60 \times 60}}$$

Equation 4-8 Calculation of SME from torque measurements

Where P, R, Γ, and F are respectively the power (W), feedrate (kg hr^{-1}), torque (Nm), and screw speed (rpm) as recorded by the extruder. The constant 2 is because the extruder has two screws. The constants $\frac{1000}{60 \times 60}$, and $\frac{2\pi}{60}$ are to change the measured values into S.I. units: $\frac{1000}{60 \times 60}$ changes kg hr^{-1} to g sec^{-1}, and $\frac{2\pi}{60}$ changes rpm to rad sec^{-1}.

4.6.4.4.1 Effect of SME on Processing

SME is conventionally believed to be directly responsible for starch conversion

4.7 Influence of Moisture Content on the Properties of Breakfast Cereals.

4.7.1 The Differences between Water Activity and Relative Humidity

The terms water activity (A_w) and relative humidity (RH) are commonly (yet incorrectly) used in place of one another within literature. The confusion is often overlooked as for a closed system in equilibrium, $A_w \times 100\% = RH$.

4.7.1.1 Water Activity (A_w)

Water activity is a property of a solid or liquid material, and is a non-linear function of moisture content and temperature. Water activity is usually measured on a scale from zero to one, where zero corresponds to no activity (i.e. a completely dry material) and one corresponds to the activity of pure water. Materials placed in a closed system containing an atmosphere will transfer water to or from the atmosphere until equilibrium between the A_w of the sample and the RH of the atmosphere is reached. During the exchange of moisture, the A_w of the material will either change or stay constant depending on the nature of the material. In the case of a homogeneous material, the change in moisture content is likely to affect the A_w of the material. In the case of a saturated salt solution (Greenspan 1977), the mass of salt reserve fluctuates as water is lost or gained by the solution; hence the composition of the solution remains constant and the A_w does not change. Such saturated salt solutions are used to create a fixed RH.

4.7.1.2 Relative Humidity (RH)

Relative humidity is a property of a gaseous material or atmosphere. Relative humidity is usually measured from on a scale from 0% to 100%, where 0% corresponds to a completely dry atmosphere, and 100% corresponds to an atmosphere that is saturated with water vapour. As an atmosphere gains or loses water vapour or thermal energy, the RH of the atmosphere will change.

4.7.2 The Interrelationship between Moisture Content and Water Activity

Both moisture content and water activity are co-dependent, though as non-linear functions of one another. It is common to measure the equilibrium moisture content of samples as an isothermal function of relative humidity. The equilibrium moisture content rises quickly with increasing humidity at low humidities as water molecules are easily hydrogen bound to available suitable sites. When hydrogen binding sites are filled, the equilibrium moisture content remains fairly constant with increasing humidity until a much higher humidity is reached. At high humidities, water molecules condense onto the sample or bind through Van der Waals forces. As this

condensation occurs, equilibrium moisture content again rises rapidly with increasing relative humidity. Samples with quoted equilibrium moisture contents for humidities of 100% should inherently be regarded with scepticism, as to be in equilibrium with a humidity of 100% the sample must be pure water.

Figure 4-18 shows a typical sorption isotherm for processed starch, glucose, and sucrose. Such isotherms can be represented by semi-empirical relationships such as the GAB model (Equation 4-9), or more recently by the Flory-Friendlich model proposed by Benczedi *et al.* (1998a and 1998b)

$$\frac{w}{w_m} = \frac{GkA_w}{(1-kA_w)(1-kA_w+GkA_w)}$$

Equation 4-9 The GAB model for fitting isotherm data (Singh and Heldman, 1993).

Where w is the equilibrium moisture content (dsb); w_m is the monolayer moisture content (dsb); G is the Guggenheim constant; and k is a correction factor related to the properties of multilayer with respect to the bulk liquid.

$$\frac{N}{N^0}(p) = \int_0^\infty \frac{N^0(\varepsilon)d\varepsilon}{1+\frac{1}{a_1 q}\exp\left\{\frac{-\varepsilon}{kT}\right\}}$$

Equation 4-10 Flory-Freundlich model proposed by Benczedi *et al.* (1998).

Where N is the number of solvent molecules absorbed at pressure p and temperature T. ε is adsorption energy. $N^0(\varepsilon)d\varepsilon$ is the number of sites whose adsorption energy lies between ε and dε. k is the Boltzmann constant. q is the mean molecular partition function of the adsorbed molecules.

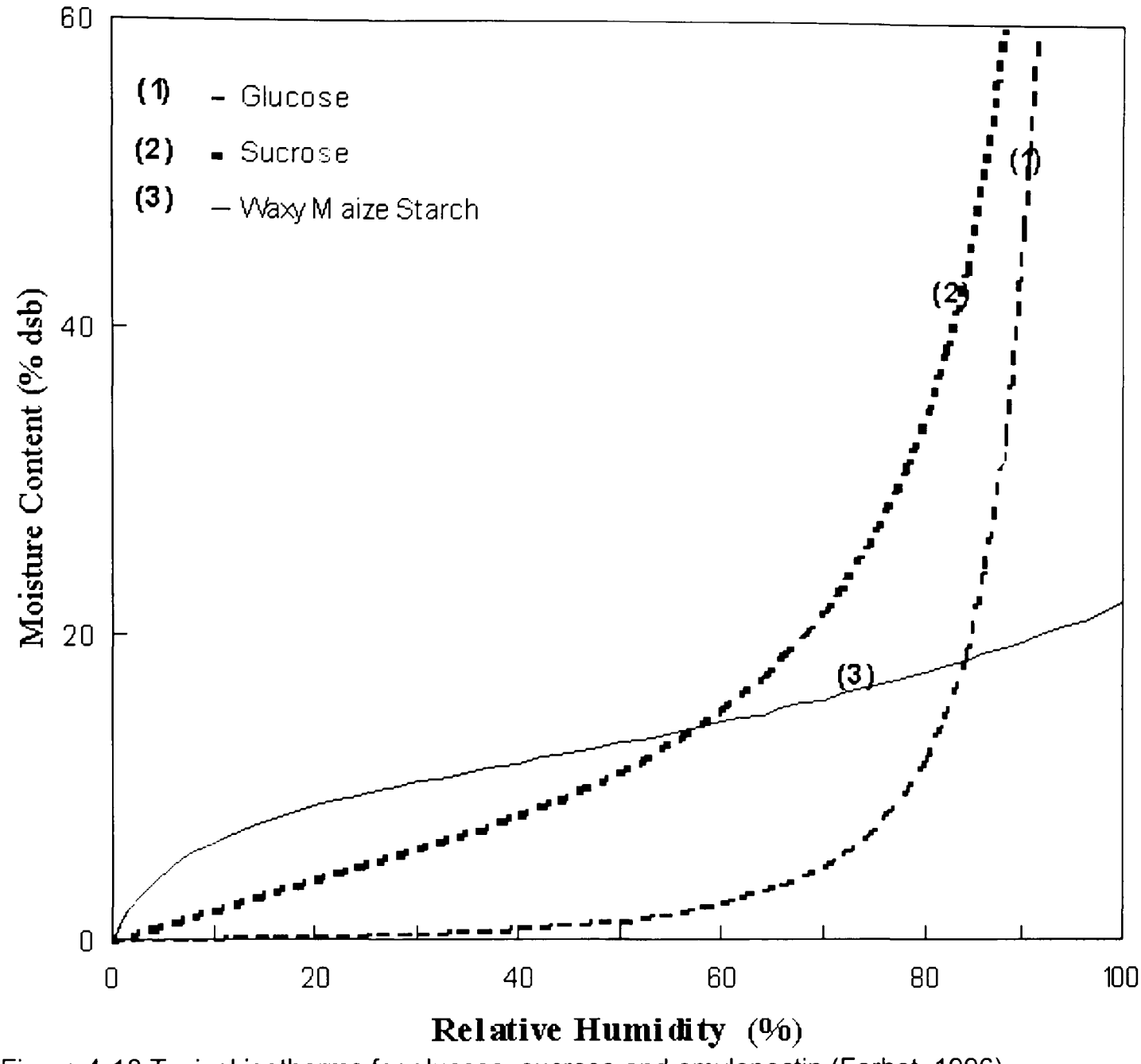

Figure 4-18 Typical isotherms for glucose, sucrose and amylopectin (Farhat, 1996)

4.7.3 Texture as a function of moisture content

Sauvageot and Blond (1991) showed that crispness of breakfast cereals as perceived by a taste panel followed a plateau type response to increased storage relative humidity. That is, crispness was perceived as relatively stable up to a relative humidity of around 50%; above that humidity, samples were perceived to have little crispness. Roudaut *et al.*, (1998) reported a substantial decrease in sensory crispness for bread at a moisture content of 9% wwb (Figure 4-19). It can be seen from the isotherm in Figure 4-18 that this corresponds to about 50% RH and is therefore consistent with the findings of Sauvageot and Blond (1991) who obtained similar responses as a function of relative humidity for various starchy products. The moisture content where the glass transition temperature is at ambient is around 28% dwb (Figure 4-14, page 4-44). Crispness for starch is lost well below T_g (Zeleznak and Hoseney, 1987; Sauvageot and Blond, 1991; Roudaut *et al.*, 1998) but for gluten

the moisture content where crispness is lost is closer to T_g (Nicholls *et al.* 1995). However, these systems are non-ideal due to the presence of proteins, lipids and multi-phase regions. Therefore it is possible these observations may not be as anomalous as they first seem.

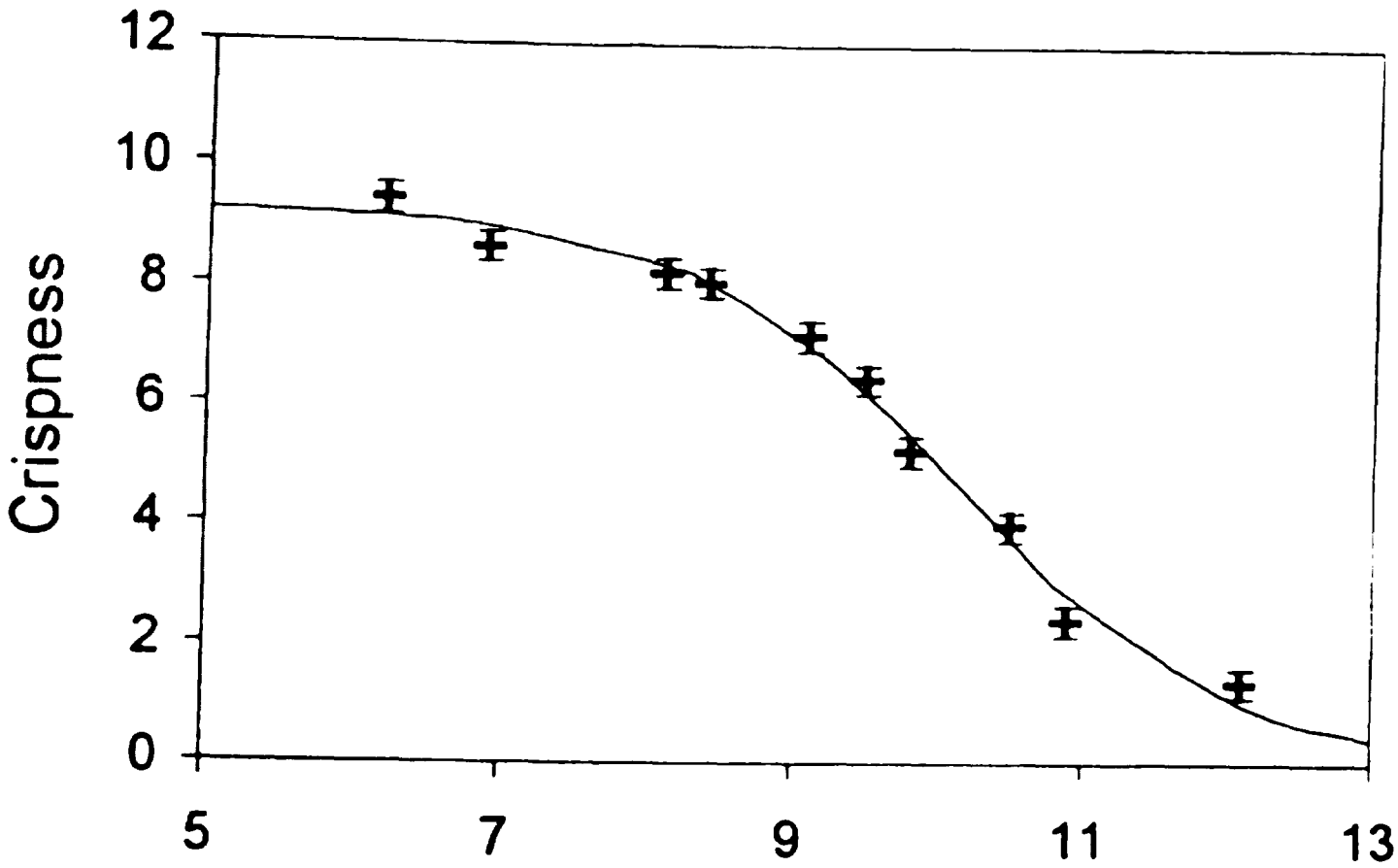

Figure 4-19 Crispness as function of water content (Roudaut *et al.*, 1998)

4.8 Texture

As foods are consumed, they are perceived to have an associated texture that forms part of the eating experience, whether that texture is the crunch of an apple, or the doughiness of fresh bread. Indeed, though many may find each of these two textures pleasant, few would want a doughy apple or crunchy fresh bread, so to improve or control the properties of products, it is useful to measure the texture of foods, which may be performed in several ways.

The evaluation of the texture of foods by compression testing is of substantial interest, and has recently progressed much further than earlier work such as stress relaxation curves of solid foods (Peleg, 1979). For foamed low moisture content foods (e.g. expanded cereals) a response consisting of a number of sharp force peaks is obtained,

such as those shown later in Figure 6-1. Such curves are inherently difficult to interpret as more traditional methods such as gradient, distance to fracture, maximum force, number of peaks, and total area are rendered meaningless as the order in which peaks occur and compound, which happens seemingly randomly from repetition to repetition, changes those measured values.

There are many approaches to analysing these types of multi-peak curves: for example, the determination of the power spectrum using Fourier transform analysis or the use of Richardson Plots to determine fractal dimension (Nuebel and Peleg 1993, 1994, Nixon and Peleg 1995). The determination of power spectra by Fast Fourier Transform (FFT) from data sets for texture analysis is not trivial (Ramirez 1985), and an external computer mathematical or statistical package is often used (Barrett *et al.* 1992).

Methods of analysis similar to those used for mechanical evaluation can be applied successfully to recorded sound during compression (Tesch *et al.*, 1994; Dacremont 1995; Roudaut *et al.*, 1998).

During the past five years, fractal techniques have become popular for analysing multi-peak textures from force-deformation curves (Nuebel and Peleg 1993, 1994, Nixon and Peleg 1995) or from sounds recorded during compression (Tesch *et al* 1994), and the algorithms themselves are well reported and widely accepted (Borges and Peleg, 1996).

Barrett *et al* (1992) normalised data by using normalised stress and strain curves for analysis. Strain is dimensionless by definition, so required no normalisation. The fitted stress σ_ε^* was calculated by fitting the measured data σ_ε to polynomials with three or four constants. To create a normalised dimensionless stress Y_ε, the differences between σ_ε and σ_ε^* were normalised to σ_ε^* for each data point by

$$Y_\varepsilon = \frac{\sigma_\varepsilon - \sigma_\varepsilon^*}{\sigma_\varepsilon^*}$$

Equation 4-11 Normalised dimensionless stress

Later works such as Nuebel and Peleg (1993) report the polynomial for fitting the measured data, taken from Swyngedau *et al.* (1991) as

$$\sigma = k_1 \varepsilon^{n_1} + k_2 \varepsilon^{n_2}$$

Equation 4-12 The fitting equation to obtain normalised dimensionless stress

Where the k's and n's are constants, $n_1<1<n_2$. The model of Swyngedau *et al.* (1991) was developed to describe the stress-strain characteristics of cellular solids under compression, following the compression curves as closely as possible with terms that can be interpreted as shape characteristics. The dimensionless stress is then a function of the difference between the measured and fitted stresses, not of the measured stress itself. Fractal analysis was then performed on the deviations from the model of Swyngedau *et al.* (1991). This principle was acceptable as only the relative, not absolute, fluctuations in stress are of interest.

The model of Swyngedau *et al.* (1991) closely describes the stress-strain curves of foams that do not fracture into separate pieces during compression, and with first inspection this model seems ideal to use to create Y_ε. In a true fractal, as the sampling resolution is decreased (or the step size increased) the measured length tends to a minimum (the exact value is dependent upon the method of analysis) and the Richardson plot (log resolution vs. log measured value) is linear. The fractal dimension D_f is obtained from the Richardson plot by D_f=|gradient| + 1, and $1 \leq D_f \leq 2$. For a straight line, $D_f = 1$. For a series of random numbers, $D_f = 2$. However, when force deformation curves are analysed by fractal algorithms, as the sampling resolution is decreased (or the step size increased), the measured length tends to a minimum value equal to the width of the curve (maximum strain, time or distance) (Barrett *et al.* 1992). Recently, many samples have been analysed and reported using the software supplied with Russ (1994) (Borges and Peleg, 1996). In all cases, the reports have used the Apple Macintosh version of the software. An IBM-PC version is also available.

4.9 Fractals

4.9.1 Introduction

For the reader wishing to learn or understand more about fractals and their potential applications, Kaye (1993) is highly recommended. Kaye gives lucid explanations and charming analogies throughout.

4.9.2 Background

Several fractal generating and/or exploration programs are available for the IBM-PC, some of which are commercially available, whereas others are freely distributable. There is little doubt that the most comprehensive, fastest, most featured, and most flexible package is Fractint (Stone Soup Group, 1996). Fractint is available in DOS, Windows, and Xwindows versions. The DOS version is fastest and contains most features.

Long adaptation from Stone Soup Group (1996). "*The ideas of fractal geometry can be traced to the late nineteenth century, when mathematicians created shapes—sets of points—that seemed to have no counterpart in nature. The mathematics descended from that work have now turned out to be* more *appropriate than any other for describing many natural shapes and processes.*

Beginning in the early 1870s, a 50-year crisis transformed mathematical thinking. Weierstrass described a function that was continuous but nondifferentiable as no tangent could be described at any point. Cantor showed how a simple, repeated procedure could turn a line into a dust of scattered points, and Peano generated a convoluted curve that eventually touched every point on a plane.

Other investigators trying to understand fluctuating, "noisy" phenomena such as the flooding of the Nile, price series in economics, or the paths of molecules in Brownian motion in fluids found that traditional models could not match the data. They had to introduce apparently arbitrary scaling features, with spikes in the data becoming rarer as they grew larger, but never disappearing. Like the pure mathematicians' curves and the chaotic orbital motions, the graphs of irregular time series often had

the property of self-similarity: a magnified small section looked very similar to a large one over a wide range of scales.

In an essay titled "How Long Is the Coast of Britain?" Mandelbrot noted that the answer depended on the scale at which measurements were made: it grows longer and longer as one takes into account every bay and inlet, every stone, every grain of sand. He codified the "self-similarity" characteristic of many fractal shapes; the reappearance of geometrically similar features at all scales.

First in isolated papers and lectures, then in two editions of his book, Mandelbrot argued that many traditional mathematical models were ill-suited to natural forms and processes, and that many of the "pathological" shapes mathematicians had discovered generations before were useful approximations of tree bark and lung tissue, clouds and galaxies." End of long adaptation (Stone Soup Group, 1996).

4.9.3 The Mandelbrot Set

The most complex geometric shape known is the Mandelbrot Set (Figure 4-20), a closed set bounded by an infinitely complex border. The set is described by the iterative equation

$$Z_{n+1} = Z_n^{\,2} + Z_0$$

Equation 4-13 The Mandelbrot Set

where Z_0 is the complex value of the point being plotted (e.g. a point which can be expressed as x=1.2 and y=2.6, or as (1.2, 2.6) relates to a complex value of Z_0=(1.2+2.6i) where $i = \sqrt{-1}$). If Z_n tends to zero, the point is inside the set; if Z_n tends to infinity, the point is outside the set. If the modulus of Z_n becomes greater than 2, then Z_n will tend to infinity. The test for tending to zero is complicated, and not valid for all points; it is therefore more convenient to repeat the iteration a fixed number of times (e.g. 100, 1,000, 10,000) then if Z_n has not tended to infinity, assume it will tend to zero. The number of repetitions is a compromise between time and accuracy. The Mandelbrot Set is self-similar under magnification, as are force-compression traces from tested foamed rice.

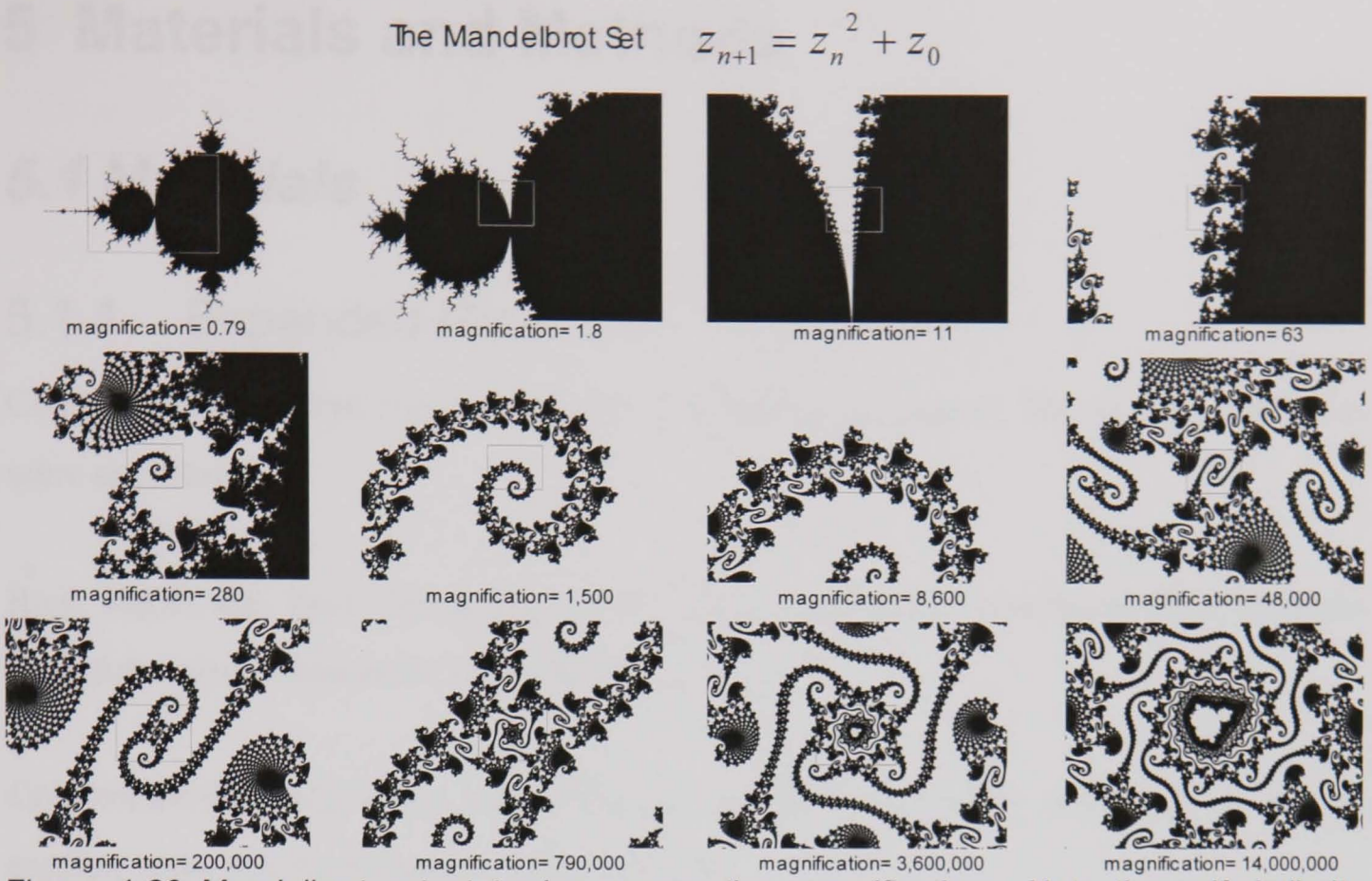

Figure 4-20 Mandelbrot set at twelve consecutive magnifications. Note the self-similarity between the first and final views. The first view displayed at the magnification of the final view would cover an area roughly 300 × 400 Km. The Mandelbrot set may be magnified an infinite number of times, yet will maintain self-similarity. Fractint 19.6 is capable of magnifications up to 10^{1600}, and for comparison quotes the ratio of the smallest quantum effects to the size of the visible universe as 10^{61}, continuing to say that that ratio to the power of 20 is the magnification possible.

5 Materials and Methods

5.1 Materials

5.1.1 Expanded Rice

Conventionally puffed rice was bought in a local supermarket. The stated ingredients were as follows;

Rice, sugar, salt, malt flavouring, niacin, iron, vitamin B_6, Riboflavin (B_2), Thiamin (B_1), folic acid, Vitamin D, Vitamin B_{12}.

Conventionally puffed rice and extruded expanded rice were provided by Nestlé, coming from different manufacturing sources.

5.1.2 Rice Flour

Milled white rice flour was obtained from Peacock, Anglo-Australian Rice Ltd., Liverpool.

5.1.3 Water

Water used during extrusion was obtained from a laboratory still.

Water used during tests other than extrusion was distilled and deionised.

5.1.4 Sucrose

Tate and Lyle natural cane sugar was purchased in a local supermarket.

Tate and Lyle natural cane icing sugar was also purchased in a local supermarket. The stated ingredients were 99.5% cane sugar, 0.5% anti-caking agent E554

5.1.5 Chitin

Poly-[1→4)-ß-d-N-acetyl-glucosamine (practical grade from crab shells, Figure 5-1) was purchased from Sigma Chemical Co., P.O. Box 14508 St. Louis. MO 63178, USA.

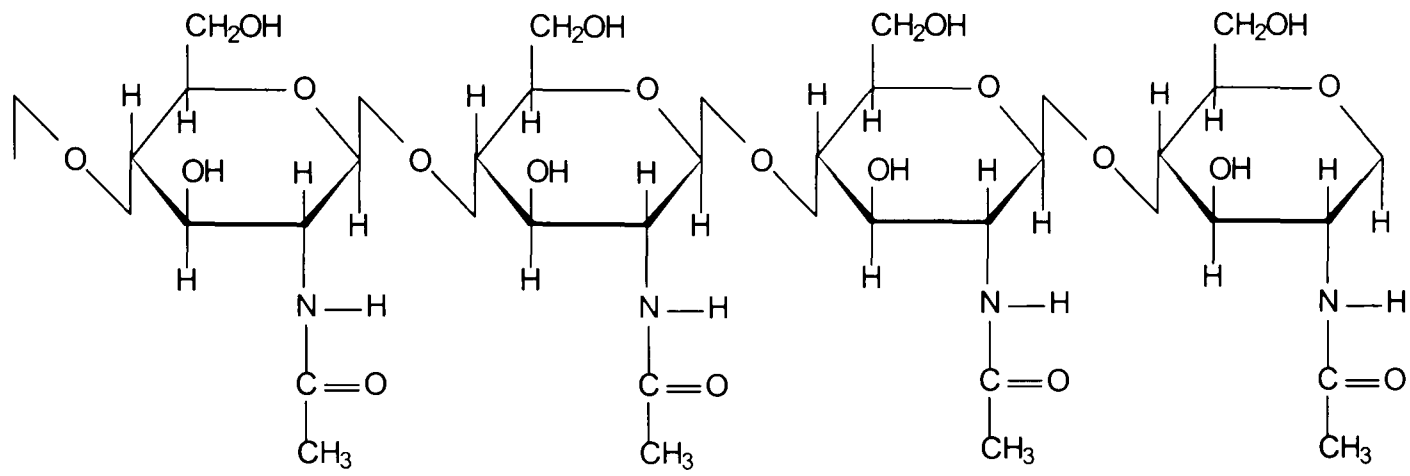

Figure 5-1 Structure of chitin

5.2 Methods

5.2.1 Extrusion

Samples were extruded on a Clextral BC-21 extruder (Figure 4-15). The BC-21 extruder has two intermeshing corotating screws, and four heating zones. The screws have a short reversing section to increase pressure and mixing. The screw profile is also shown in Figure 4-15. A 3mm diameter circular die was used throughout. Typical throughputs for material are 4 to 12 Kg hr^{-1}. Solids (i.e. the rice flour and any mixed in additives such as sucrose) are gravity fed at the first heating zone. Fluids (i.e. water) are injected into the extruder barrel at the second heating zone. The rate of feed for both the solids and liquids are controllable and were calibrated for each material used. If more than one solid were to be used (e.g. rice flour and sucrose) the solids were premixed in a Kenwood planetary mixer for thirty minutes before extrusion.

5.2.1.1 Calibration

As the solids were fed by a screw that was controllable by frequency only, it was necessary to calibrate the feeder screw speed to the flow rate of solids. This was achieved by collecting solids fed at 100, 200 and 400 rpm in a given time (usually 36

seconds for ease of multiplication to an hour). The solids feed rate was calibrated each time before use.

The water pump was graduated with an arbitrary scale, and needed to be calibrated to the water flow rate. This was not repeated each time before use.

The measurements of torque exerted on the screws were automatic, and supposedly correct. However, when used with no solids a torque registered. This torque may have been due to friction which may have been reduced when solids were present, or been an artefact of the equipment. The latter possibility would have led to a systematic error in results. However, as the torque that registered with no solids was actually higher than some experiments with low solids and high moisture, the former possibility seemed most likely.

5.2.1.2 *Extrusion Conditions*

Temperatures of 40°, 80°, 110-130° and 110-140°C were used in the four zones respectively. The solids feed rate was 4-12 Kg hr^{-1}. The liquids feed rate was 0-28% of the solids feed rate, entering the extruder barrel at heating zone 1. The screw speed was 30-440 rpm, and a 3mm circular die was used.

The cutter used when making expanded samples was double bladed, and typically used at 500 - 1000 rpm (1000 - 2000 cuts min^{-1}). The cutter was not used for non-expanded samples - these were cut by hand with scissors.

After collection, samples were allowed to cool on an aluminium table at ambient temperature for ten minutes. This was to prevent 'sticking' or 'sweating' during storage. The samples were then sealed in plastic bags.

5.3 Analysis of Samples

A large number of techniques were used to examine samples, including X-ray diffractometry, water absorption rates, water absorption equilibria, water activities, water absorption indices (WAI), water solubility indices (WSI), rheology of dry

samples, viscosity of dispersions, fractal analysis of texture, volumetric measurements, moisture contents, and sensorial perception.

5.3.1 Sample Preparation

Some procedures for evaluating processed rice involved no sample pre-preparation. These techniques were vacuum drying, water vapour absorption rates, colour analysis, water absorption equilibria, and texture measurement.

For methods of examination which may be dependent upon the sample size, such as X-ray diffraction, water absorption and solubility rates, and viscosity, the samples were ground using a pestle and mortar, then passed through a laboratory sieve with spacing 295μm. Material which did not pass through the sieve after grinding was reground. No material was discarded. Using liquid nitrogen to cool the sample during grinding was experimented with, in order to ensure the samples are far into the glassy region, and fracture cleanly. However, a preliminary investigation using X-rays did not detect any difference between cooled and uncooled samples. Because of this, and because of the danger of sample contamination by ice crystals, liquid nitrogen was not used when grinding only krispies, but was still used when grinding a mixture of krispies and cocoa wash taken from the centres of chocolate countline bars.

For examination by microscopy, samples were left whole, sectioned, crushed, or ground.

Trials grinding samples in a laboratory mill were made, and the flour collected. By altering the size of the mesh used in the mill, and dependent upon the sample, the flour produced could vary from 1.5 to 270μm. Although no difference could be detected between the different grades of flour using X-ray diffractometry, or water absorption indices, the mill is known to heat the samples, and to apply large shear forces, not dissimilar to the conditions found within an extruder (although to a lesser extent). This is known as some samples are found to develop a burnt aroma or colour during milling. These effects could alter the samples, and affect future results. Additionally, as different samples milled to produce different grades of flour, there

was an additional source of error when using techniques such as water absorption indices. For these reasons, mechanical milling was not used to prepare samples.

To monitor the ageing of krispies within chocolate countline bars, the bars were first chilled for a few minutes in a refrigerator to harden the chocolate and caramel. They were then bisected longitudinally along the horizontal plane. The krispies were then gently scraped from the inside of the bars, and collected. This left a 'shell' of toffee and chocolate, which was discarded. It was not possible to avoid collecting cocoa fat with the krispies, as cocoa fat was used to hold the krispies together.

5.3.2 Determination of Moisture Content

Moisture contents were determined by drying to constant mass in a vacuum oven at 75°C.

5.3.3 Determination of Water Sorption Isotherms

Approximately 1.5g of sample were placed into small open pots, which were in turn placed into desiccators at various relative humidities. The samples were left for three weeks to reach equilibrium, then the new masses were measured, and the samples were vacuum dried before being reweighed. The total moisture content was found as a function of the dried mass by

$$MC_{RH} = \frac{M_{equilibrium} - M_{dried}}{M_{dried}}$$

Equation 5-1 Equilibrium moisture content by mass

Where

MC_{RH} is the moisture content at equilibrium at the relative humidity RH

$M_{equilibrium}$ is the mass of the samples when they approach equilibrium in the dessicators

M_{dried} is the mass of the samples after drying in the vacuum oven

The results were plotted as isothermal moisture contents.

The dessicators were created using sealed containers containing saturated salt solutions of LiCl, KAc, $MgCl_2$, K_2CO_3, $Na_2Cr_2O_7$, NaBr, $CuCl_2$, NaCl, KCl and H_2O to produce relative humidities of 11, 22, 30, 44, 54, 59, 67, 75, 85 and 100%. The solutions were made at 60°C to ensure saturation.

5.3.4 Kinetics of Water Adsorption (WVAR)

Though sorption isotherms are a measure of equilibrium moisture content, there is no record of the rate at which the samples reach that equilibrium. A reasonable assumption is that the rate of water vapour adsorption (WVAR) of a material is dependent upon the form of the material, for example homogenous, foamed, or spongy. (Note; a foam has a continuous solid or liquid phase, and a discontinuous gaseous phase. A sponge has continuity in both phases.) It is also possible the state of the granules, molecules, or starch-lipid complexes may affect the rate of hydration.

Approximately 1.5g of sample were placed into small open pots of known mass, and the combined mass was found. The small pots were in turn placed into desiccators at various relative humidities. The samples were left to approach equilibrium, and the masses of the pots and krispies were monitored with time, typically for 48 hours. After this time there was little further change in mass. The total moisture content with time was found as a function of the dry mass by

$$MC_t = \frac{M_{time} - M_{dried}}{M_{dried}}$$

Equation 5-2 Moisture content at time t by mass

Where

MC_t is the moisture content of the sample at time t.

M_{time} is the mass of the sample at time t.

M_{dried} is the dry mass of the sample.

The results were plotted as percentage mass gain with respect to time for each A_w.

5.3.5 Water Solubility and Water Absorption Indices (WAI & WSI)

The amount of material soluble in cold water includes leached amylose, damaged gelatinised starch, undenatured globular proteins, inorganic ions, and small sugars. In systems with a high starch content which has been energetically processed, the protein, ionic, and sugar fraction of the soluble mass should remain small and constant. Variations in absolute starch gelatinisation, conversion, or granule damage are measurable by the amount of soluble material per gram of sample. More processing causes more damage to the starch granules, and leads to a greater solubility.

To measure the water absorption and solubility indices (WAI and WSI), 10.0ml distilled water was weighed into vials of known mass. 0.500g powdered sample were then added to the water, and shaken vigorously to disperse the mixture. The mixture was allowed to stand for one hour, then shaken again. The dispersions were allowed to stand overnight. The dispersions were then centrifuged at 1000rpm for 10 minutes, before decanting the supernatant into containers of known mass. The masses of the vials and gels were weighed to calculate the mass of gel. The mass of supernatant was weighed before being dried at 105°C in an oven at atmospheric pressure. The masses of solids in the dried supernatants were weighed.

WAI was calculated as

$$WAI = \frac{m_{gel}}{m_{sample}} \times 100\%$$

Equation 5-3 Water absorption index

and WSI was calculated as

$$WSI = \frac{m_{solutes}}{m_{sample}} \times 100\%$$

Equation 5-4 Water solubility index

where m_{gel}, m_{sample}, and $m_{solutes}$ are the mass of the gel formed, the mass of the sample used, and the mass of the dried supernatant respectively.

These tests were performed in quadruplicate.

5.3.6 Viscosity of Dispersions

10ml of distilled water was measured into vials using a Gilson pipette, and checked with a balance. 1g of powdered sample was added to each vial, then shaken vigorously to disperse the mixtures. A hydration period of 30 minutes was allowed for each dispersion, during which time the mixtures were shaken occasionally and the viscosities visibly increased. The viscosities of the hydrated samples were determined at 25°C using a Bohlin CS Rheometer in shear-stress mode. Cone and plate geometry was used with a 40mm diameter cone. A thin film of paraffin oil was applied around the extremes of the plates to prevent evaporation of moisture during the experiments. The viscosities of the hydrated samples were measured as the applied stress was scanned by increasing from 1 to 10Pa.

5.3.7 X-Ray Diffractometry

Wide angle X-ray diffraction is useful for studying polymers such as starch because of the ability of the technique to differentiate between amorphous and ordered states; even to distinguish between different types of ordered states and determine the extent of order. Whereas amorphous systems will yield a diffraction pattern consisting of a diffuse halo, a single crystal will yield an ordered diffraction pattern consisting of several sharp points. However, polymer samples such as starch are not a single crystal, but are many crystals of random orientation. Because of this, the pattern of points becomes a pattern of concentric rings, so only a radial cross section of the pattern need be measured. From the pattern of concentric circles, the type and extent of crystallisation may be determined. Although there is general agreement that the extent of crystallisation may be determined from the relative intensities of the sharp rings to the intensity of the diffuse halo, there is some discrepancy over how this should be conducted. The simplest technique is to plot the cross section of the diffraction pattern as intensity against angle, then to calculate the ratio of the areas of

the peaks to the total area. Imperfect crystals contribute to the amorphous region, thus simply finding the ratio of areas underestimates the absolute crystallinity, though the technique may still be used as a relative index.

The powdered specimens (Section 5.3) were placed in an aluminium holder, and levelled to present a flat surface of known height and rotation to the X-ray beam. The samples were analysed with a Phillips PW-1730 X-ray diffractometer fitted with a graphite crystal monochromator. The X-ray generator was operated at 40KV and 50mA. A copper target was used, producing CuKα radiation of wavelength 1.54Å. An integral computer collected results over the 2θ angular range of 4° to 38°, at a 2θ angular interval of 0.05°. The results were then transferred to BBC and IBM-PC microcomputers for analysis and printing.

Several samples were scanned in duplicate, and produced essentially identical spectra. Because of this consistency, duplicate scans were not made during experimentation unless there was doubt over their validity.

5.3.8 Measurement of Sample Crispness at Different A_w's by Compression

Samples were stored in a range of humidities (4.7.1) for two days to effect different water contents, but minimise retrogradation by using a short time-scale.

Individual krispies were placed between flat plates on a Stable Microsystems TA-XT2 Texture Analyser, in compression mode. The TA-XT2 version 3.6 software package was used on a 486SX IBM-PC to control the apparatus, and to collect the data. The probe speeds were 2, 0.1, and 10mms^{-1} for approach, compression, and withdraw respectively. The samples were compressed for 1.8mm. A sample rate of 400Hz was recorded. Ten repetitions were made for each sample at each water activity.

5.3.9 Microscopy

Naturally, the examination of samples by microscope may reveal details invisible to the naked eye, either due to the scale of the details, or because certain features are only visible when viewed through certain filters

Starchy samples may be stained with iodine vapour, highlighting fluctuations in the concentration or susceptibility of starch throughout the sample.

Native or gelatinised (but intact) starch granules may be identified using a microscope with crossed polarising filters. Granules are evident as specks of light or as Maltese Crosses (Figure 4-10), depending on conditions (magnification, medium (air, water, or amorphous starch), extent of granule swelling). The Maltese Crosses are formed due to birefringence of light within the starch granule. As the granule gelatinises, the cross disappears, leaving a slightly birefringent mass. Upon further gelatinisation, this birefringence also disappears. Also, swollen granules which have been stretched into cell walls or which form part of a sample that has been sectioned may be seen as glowing patches (Figure 5-2).

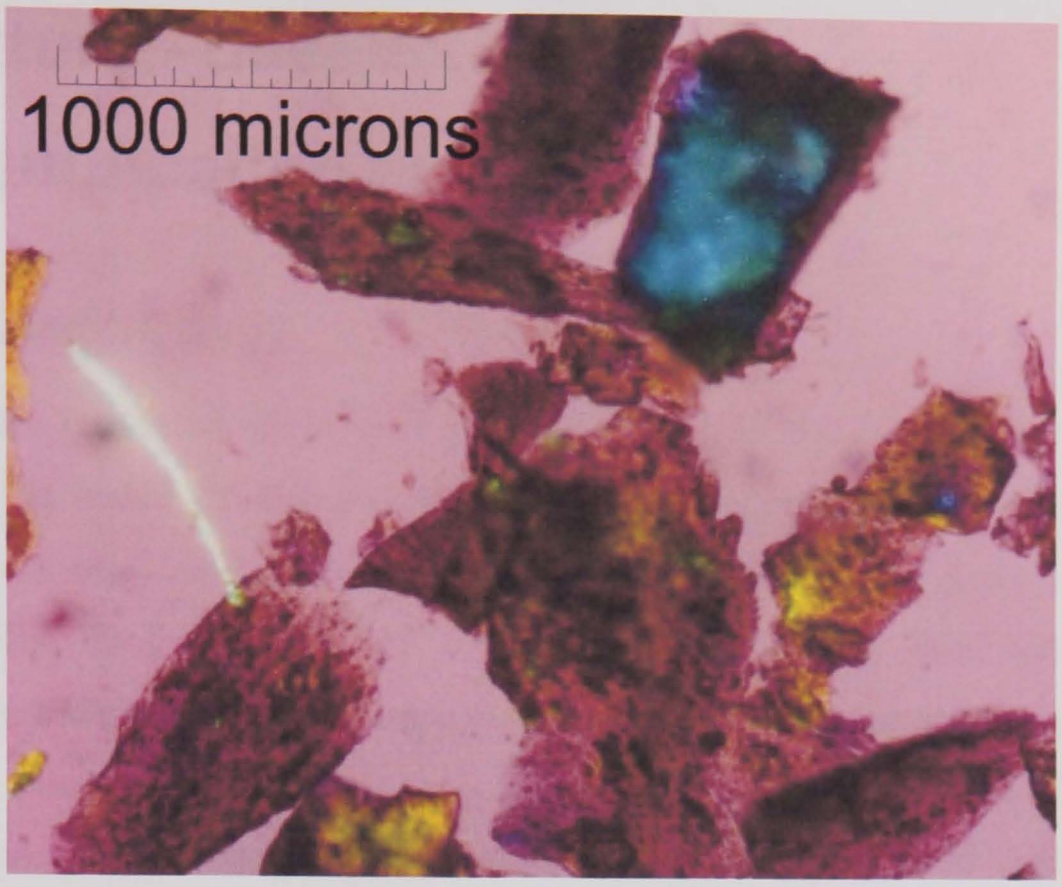

Figure 5-2 The small green glowing regions are partly gelatinised starch granules. Viewed in aqueous suspension with crossed polarising filters and a quarter wave plate. Sample made at 100rpm, temperatures of 45°, 80°, 90°, and 100°C for barrel zones 1-4 respectively, solids feed rate of 4kg hr^{-1}, and water addition rate of 1.8kg hr^{-1}. The solids consisted of white rice flour only.

Samples were examined with a Leitz Diaplan planar trinocular polarising phase contrast transmission optical microscope under a number of conditions at a variety of magnifications. Samples were viewed whole, sectioned, crushed, or ground. Samples were mounted in air, aqueous, ethanol, or occasionally other, mediums. The range of magnifications used allowed widths up to about 3mm, or details as small as a micron to be to be viewed. Illumination was provided by transmission and/or reflection, and passed through crossed planar polarising, phase contrast, or no, filters. Although illumination for transmission studies was integral to the microscope, illumination for reflection studies was provided by a Leitz Pradovit slide projector.

The view was calibrated with a graticule from Graticules Ltd., Tonbridge, Kent, England. The graticule was marked for 1mm in 100 divisions.

Photographs of selected views were taken using a Pentax K1000 35mm camera and Kodak ISO100 colour film.

6 Texture - developing a method for quantification of

6.1 Introduction

To assess the texture of products, a quantifiable mechanical method was considered necessary. Establishing a taste panel that would remain constant for the duration of the Ph.D. project was neither desirable nor practicable. Over three years the students present within the department that would constitute a sensory panel would change. Also, many samples to be tested may be unhygienic or even toxic, neither of which should be given to a sensory panel. Additionally, crispness values allocated by humans may not remain constant over the three year period, and factors such as colour or taste may influence perceived texture. Using a mechanical technique would overcome all the above considerations. However, a technique for measuring crispness, crackliness, and crunchiness was not available, so it was necessary to develop one. The simplest mechanical test is compression of the sample in a texture analyser. For foamed low moisture content foods (e.g. expanded cereals) a response consisting of a number of sharp force peaks is obtained. Each compression curve on Figure 6-1 is one repetition performed by the mechanical method on each sample perceived by the sensory panel as most crisp, crackly and rubbery respectively; the samples, mechanical method and sensory panel are described below. There are many approaches to analysing these types of multipeak responses: for example, the determination of the power spectrum using Fourier transform analysis or the use of Richardson Plots to determine fractal dimension (Nuebel and Peleg 1993, 1994, Nixon and Peleg 1995). Similar methods of analysis can be applied successfully to recorded sound during compression (Tesch *et al.* 1994, Dacremont 1995).

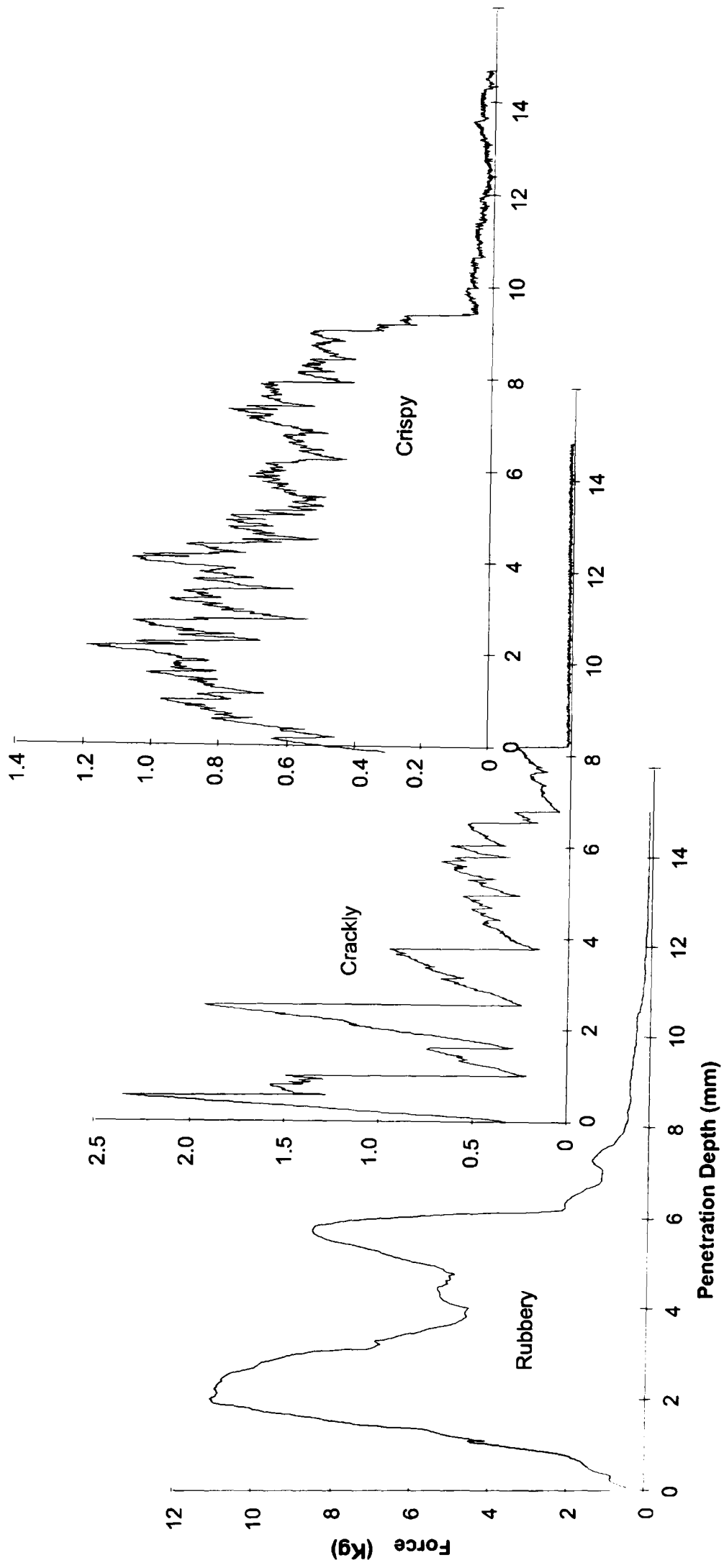

Figure 6-1 Force compression curves from three samples perceived as most rubbery, crackly, and crispy by the sensory panel. The three samples were extruded with added moistures of 23, 13, 3.7% solids feed rate respectively. Note the differences in peak height. The samples and panel are described in Section 6.1.1.

Richardson Plots are easy to visualise, develop, and apply. However it is difficult to isolate specific textural attributes from the results, as any given measurement of length is a compound effect of all lengths measured at resolutions equal to or lower than the resolution being used for measurement.

Power spectra of both force and acoustic data have the advantage that individual frequencies can be examined, hence the potential for determining a range of attributes exists. The determination of power spectra by Fast Fourier Transform (FFT) from data sets for texture analysis is not trivial (Ramirez 1985), and an external computer mathematical or statistical package is often used (Barrett *et al.* 1992). Kaye (1993) gives clear explanations about fractals and their potential applications accompanied by simple analogies.

A method to determine the contribution to overall line length of the force-compression curve by fractures of specific dimensions has been developed and demonstrated. It had the advantages of being simple and fast to apply to one or more data sets in succession. Frequencies were isolated and correlated to sensorially perceived textures. Additionally, it was simple to visualise the algorithm and results. The method was applied to a series of puffed rice samples extruded with various water contents to create different textures, and the results were compared to those obtained with a sensory panel.

6.1.1 Materials and Methods for Development of Texture Analysis

6.1.1.1 Extrusion of Samples

Mixtures of brown rice flour and distilled water were extruded on a Clextral BC-21 twin screw extruder. The barrel heating zones were 40°, 80°, 120°, and 130°C (±2°C). The screw speed was 300rpm. The twin bladed cutter rotated at 1000 rpm. The circular die was 3mm in diameter. The solids feed rate was 8 Kg hr^{-1}, and the amount of water added was increased in twelve equal increments from 0% to 23% (solids basis) to create a range of thirteen samples with different textures. Samples were collected below the cutter, allowed to cool on an aluminium table at ambient

temperature for 30 minutes, then stored in sealed plastic containers. Samples were roughly spherical; their mean lengths and widths and associated standard deviations are shown in Figure 6-2. The dimensions of 15 samples at each water content were measured. The samples were used over the following two days for sensory panel analysis, and on the third for mechanical analysis.

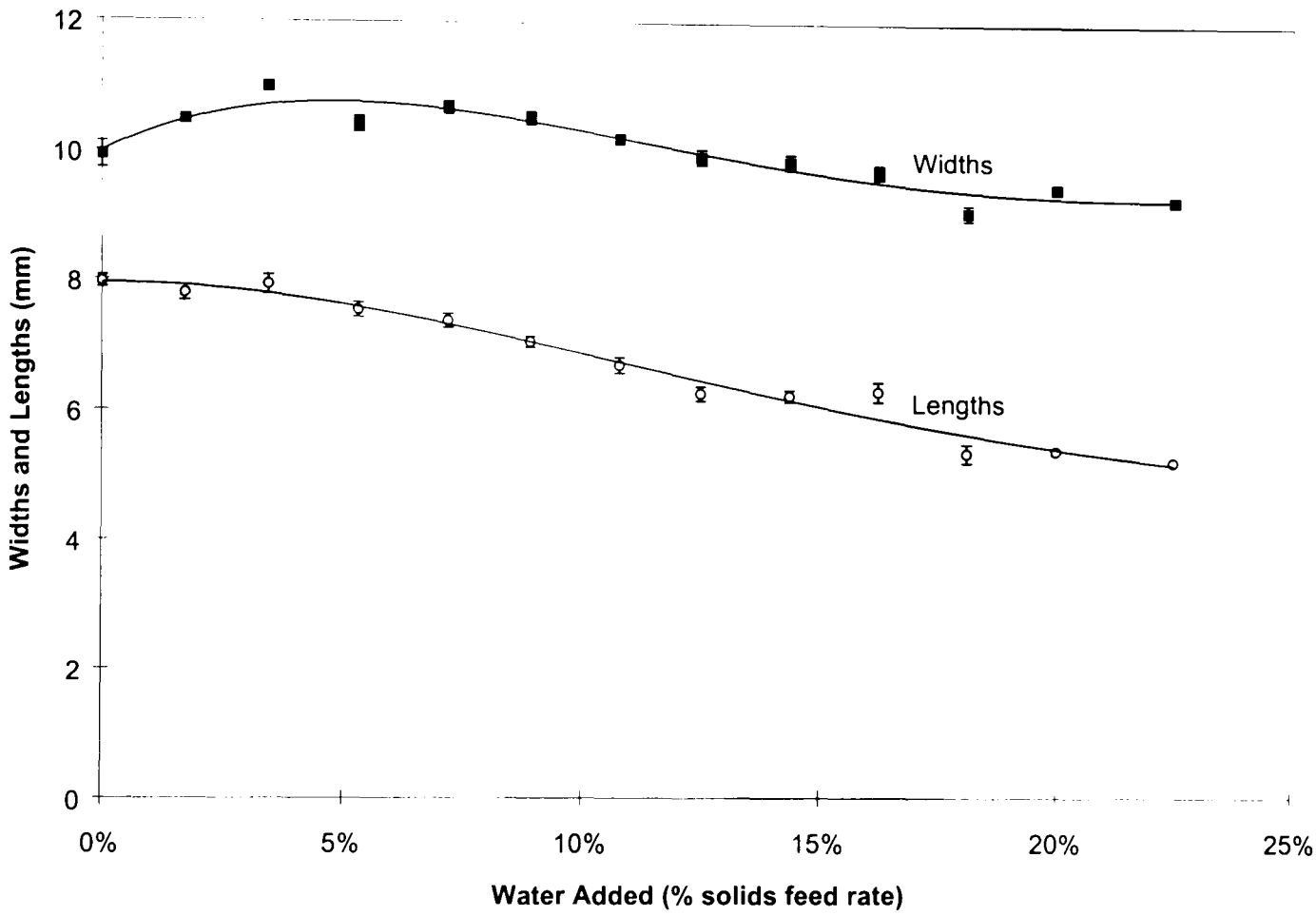

Figure 6-2 Dimensions of the samples. Bars represent standard errors in 15 repetitions.

6.1.1.2 Mechanical Method

The method being reported consists of two stages: Firstly the data acquisition, then the data processing.

6.1.1.2.1 Data Acquisition

The data was acquired on a TA-HD Texture Analyser, controlled by XTRA Dimension 3.7c software for DOS, supplied by Stable Microsystems, England, in compression mode. The samples were placed onto a metal bed, with a 75×3.5mm slit running across its length (Figure 6-3). A 70×2mm V-shaped guillotine was used to

shear the samples, and ultimately to pass through the slit. This was used in preference to compressing the samples between two parallel plates to prevent sample bulking at small plate separations and causing artefacts in the measured force. The TA-HD probed the samples at 1mm s^{-1}. After an initial force threshold of 300g was met, data was collected at a rate of 200Hz, (corresponding to a spatial resolution of 5μm) for the following 12mm. The force threshold was used because the sample was able to move along the length of the slit. Reorientation and translation of the sample within the slit often occurred at early stages of contact with the probe; the force threshold was used to avoid data being recorded during this period.

Ten repetitions were made for each sample. Data for time, distance, and force were saved in a unique file for each repetition of each sample.

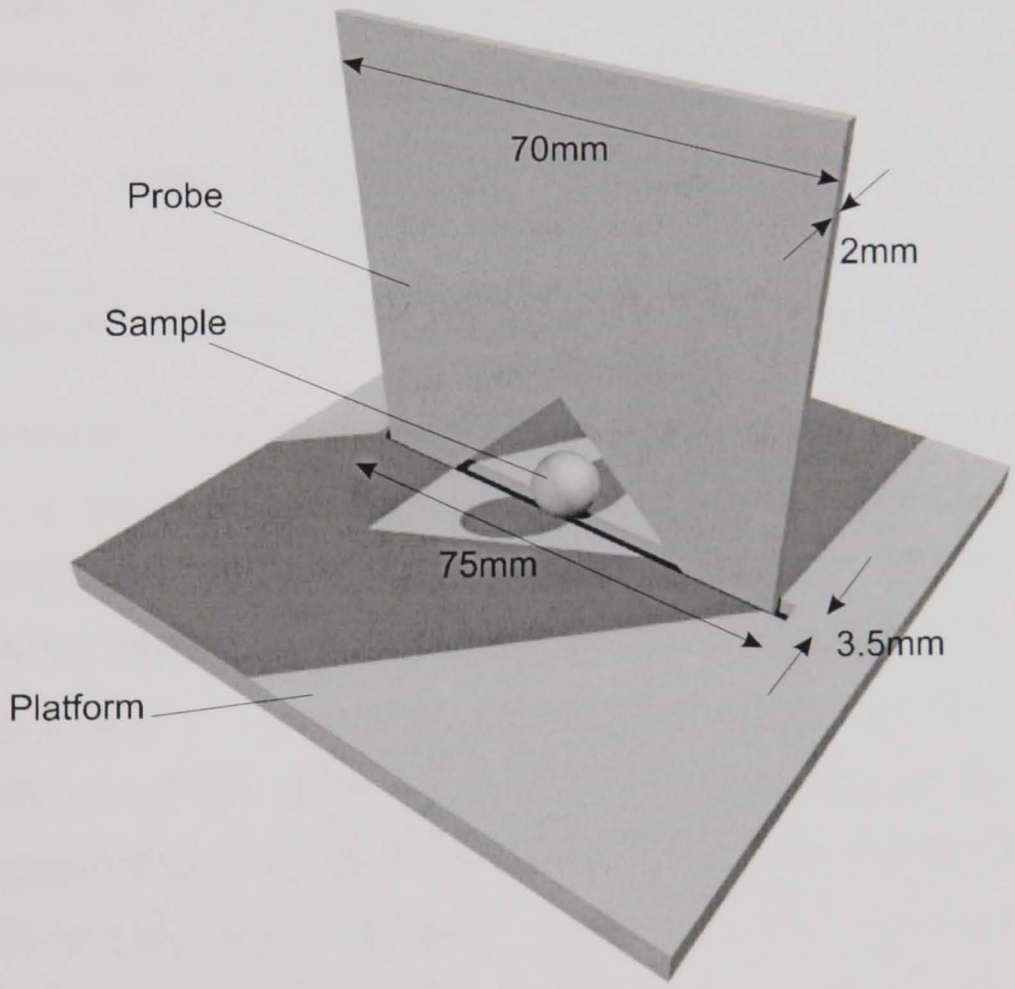

Figure 6-3 The arrangement of sample and probe

6.1.1.2.2 Data Processing

Data analysis was performed using a purposely written program, which wrote data from all calculations to a single file. Microsoft Excel 5 was used to generate graphs

from the output file, described below. The analysis program was written in PASCAL. The program performed the following on every file in the current directory.

The file was opened, and the first 28 lines discarded, which consisted of titles and parameters.

The absolute differences between the following 2049 force values were summed to calculate the length in Newtons of the line traced by the points. The 2049 values were required to bound 2048 intervals, which was the largest binary number available within the recorded 2400 values. *This step is analogous to printing the compression curve, and placing a piece of string along the length of the curve, following every peak and trough, however small. The length of string is then measured to find the length of the curve.* The measured length of the line was calculated by summing only the absolute vertical movements instead of calculating the correct distances by Pythagoras' Theorem between points. In algebraic terms, length was measured as $\sum_{0}^{n} |\Delta force|$ not as $\sum_{0}^{n} \sqrt{\Delta force^2 + \Delta length^2}$. The reason for this was to avoid a measured line length which would be unit dependent. If either the unit of distance was smaller than one metre, or the unit of force greater than one Newton, then the measured length would become disproportionately longer for non-crispy samples than for crispy ones when compared to the measured line length using both metres and Newtons. Changing axes to strain and normalised stress would eliminate unit dependency (Barrett *et al*, 1992), and is suitable for most uses. However, for the purposes of this paper, which investigated the effect of sampling resolution, the measured line lengths at very coarse resolutions were equal to the maximum strain, and independent of normalised stress. This was due to a scaling problem, not due to unit dependency.

The absolute differences between the same 2049 points were summed, using only every 2^{nd} point. Then only every 4^{th}, 8^{th}, 16^{th}... 2048^{th} point. *This is analogous to using consecutively thicker pieces of string. As the string becomes thicker, it can no longer follow the smallest peaks and troughs, and so a shorter line*

length is measured, in effect filtering out the high frequency oscillations. Figure 4 shows three lines of different thicknesses being overlaid on the crackly curve from Figure 1. If each line were straightened, the thickest line would have the shortest length.

The maximum force exerted on the sample was identified.

The sum of all 2049 data points was found, thus calculating the area under the force-deformation curve, which was converted to Joules. This measurement was useful for normalisation of measured line length, which changed the units of measured line length from Newtons to metre^{-1}. Dividing the measured line length by the area corrects for samples size, as large samples inherently give rise to longer measured line lengths without necessarily producing force-compression curves which are relatively more jagged than those from small samples.

The line length for each resolution, the maximum force and the total area were appended to a data file. The same data file was used to collate results from every sample.

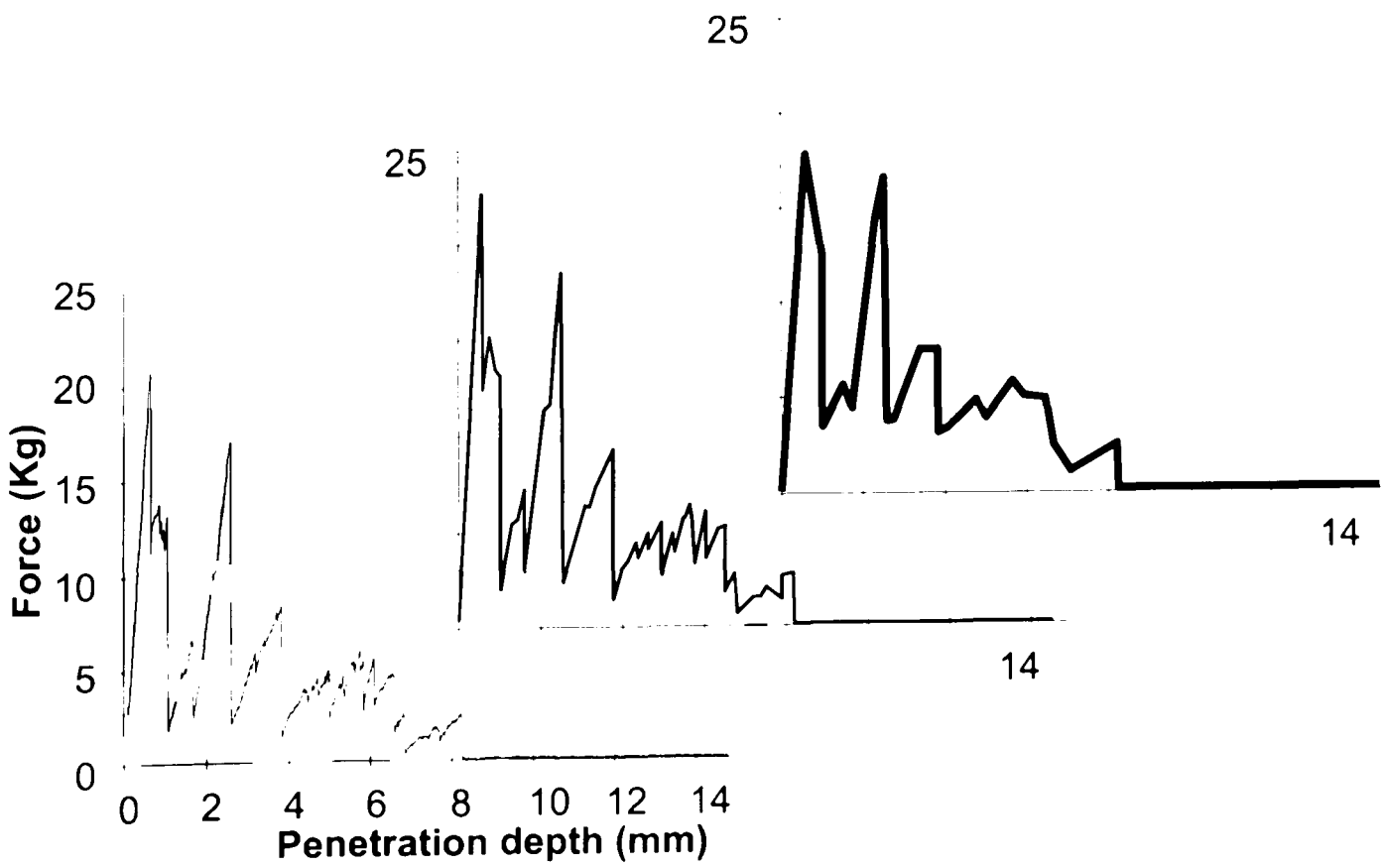

Figure 6-4 Three thicknesses of "string" following the crackly texture in Figure 6-1. The finest string follows the longest path. The thickest string follows the shortest path.

Table 6-1 shows data from one repetition of one sample; these data were later averaged with data from the other repetitions of the sample. The first row shows the sampling frequency, the last two rows show the maximum force and the total area (work done). The second row is the measured length of the line, calculated by summing absolute differences between force points. The third row contains the second row normalised to area (work done). Normalisation to area was used to compensate for the variation in sample size with changing water content. The fourth row shows the differences between adjacent columns from the normalised row. It is these changes in measured length that can be correlated to perceived texture.

Sampling resolution (μm)	5120	2560	1280	640	320	160	80	40	20	10	5
Measured length (N)	29.64	29.64	29.82	37.98	39.68	54.21	72.24	90.18	110.2	139.7	184.6
Length/area (m^{-1})	356.5	356.5	358.6	456.8	477.2	651.9	868.8	1085	1325	1680	2220
Differences (m^{-1})		0	2.1	97.4	20.4	174.7	216.9	216	240	355	540
Area (J)	0.083151										
Maximum force (N)	16.90										

Table 6-1 Example of results taken from one repetition of one sample

It is necessary to explain why the process of finding differences in consecutive line lengths is useful: The length of a force-compression curve has been calculated from the first 2049 recorded points. The curve was digitised during the acquisition process at a resolution of 5μm, so the length of the curve included all the peaks that are at least 2×5μm wide (in a manner similar to the Nyquist sampling rate for digitised waveforms (Ronayne 1986)), but any peaks narrower than this would have been filtered out, and did not contribute to the length of the line. Similarly, if only every second data point was used for analysis, data would have effectively only been obtained at a resolution of 10μm, and calculating the length of the curve from this data would include all peaks with a width of 2×10μm or more. The difference between the two lengths (the one for peaks at least 2×10μm wide, and the one for peaks at least 2×5μm wide) gave the contribution to the total measured line length by the peaks with widths between 10 and 20μm. This was repeated for 20 and 40μm, 40 and 80μm, 80 and 160μm... 5.12 and 10.24 mm. Specific features were therefore isolated by simple subtraction of consecutive lengths; it was these changes in lengths that were correlated to sensorially perceived textures.

6.1.1.3 *Sensory Panel Method*

To investigate the relationship between the mechanical method and perceived texture, samples were assessed by a sensory panel. The samples were from the same thirteen batches as the samples that were assessed mechanically. The sensory panel consisted of thirteen untrained assessors, five males and eight females, aged from 25 to 55, all of whom were English or Scottish. Although the panel had previously partaken in flavour research, most had little experience of texture quantification.

Samples from the same fifteen batches (thirteen batches plus two repetitions of two batches as controls) were given to each member of the panel, with instructions to rank the samples in separate orders of crackliness, crunchiness, crispness, hardness, and rubberiness. The samples were labelled with random letters. The sensory panel members worked individually; each member produced five sets of data as each assessor ranked the samples once for each attribute. Samples with the most amount of a given attribute were ranked in first place, and the samples with the least amount of a given attribute were ranked in last place. The panel assessed the characteristics on the first bite of the sample, not during or after mastication. The assessors were allowed to use as many samples from each batch as were needed to rank the samples. Each member of the panel was also asked to write a short description of how they perceived the five attributes, which guided them to consider the differences in texture more carefully. The sensory panel trials took each assessor between twenty and fifty minutes to complete.

6.1.2 Results

6.1.2.1 *Mechanical Method Results*

Each repetition for all samples were ranked by change in line length for each mechanical parameter; that is, 150 repetitions were ranked for the interval 5-10 μm, then the same 150 repetitions were ranked for the interval 10-20 μm, then for 20-40 μm, 5.12-10.24 μm. Repetitions were ranked with the longest change in line length first, and the shortest change in length last. As there were ten repetitions of each sample, each sample was ranked in ten places for each mechanical parameter. The mean ranked value and standard error in mean ranked value were calculated for each

sample. Standard error was calculated as *standard deviation* / $\sqrt{repetitions}$. The mean ranked orders, theoretically ranging from 5.5 to 145.5 were offset and scaled by the function *new value = (old value + 4.5) ÷ 10* to be comparable to the results from the sensory panel below, theoretically ranging from 1 to 15. The standard errors were reduced by a factor of 10 for the same reason. Figure 6-5 shows the mean ranked order and standard error in ranked order obtained for each sample for the interval 640-1280 μm, selected as it correlated well with crispness below.

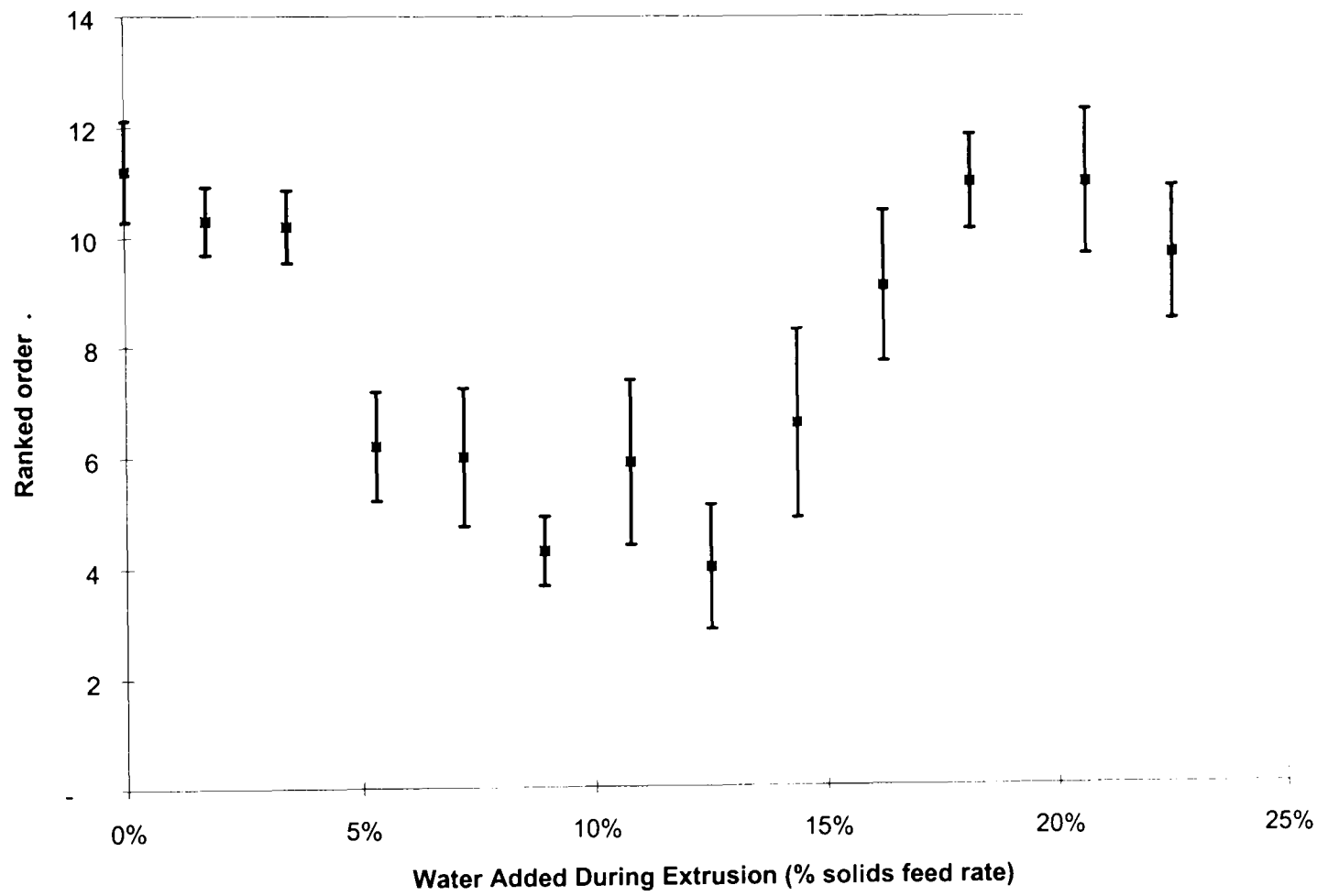

Figure 6-5 Samples ranked in order of differences between the line lengths measured at resolutions of 640 and 1280 μm by the mechanical method. Bars are standard errors.

6.1.2.2 SENSORY PANEL RESULTS

From examination of the sentences written by the panel members, it was clear that most members perceived crunchiness in the same way they perceived either crackliness or crispiness, but not both. As crunchiness had not been perceived uniquely or consistently, it was removed from further analysis. Nine of the thirteen panel members mentioned sound when describing crackliness. The typical descriptions of crispiness included the adjectives "light" or "brittle." "Force" was

commonly used when describing hardness, and "chewiness" used when describing rubberiness.

Figure 6-6 and Figure 6-7 show the data collated from the sensory panel's perceptions of crispness and crackliness. The mean ranked order and standard error in ranked order are plotted for each sample for each attribute.

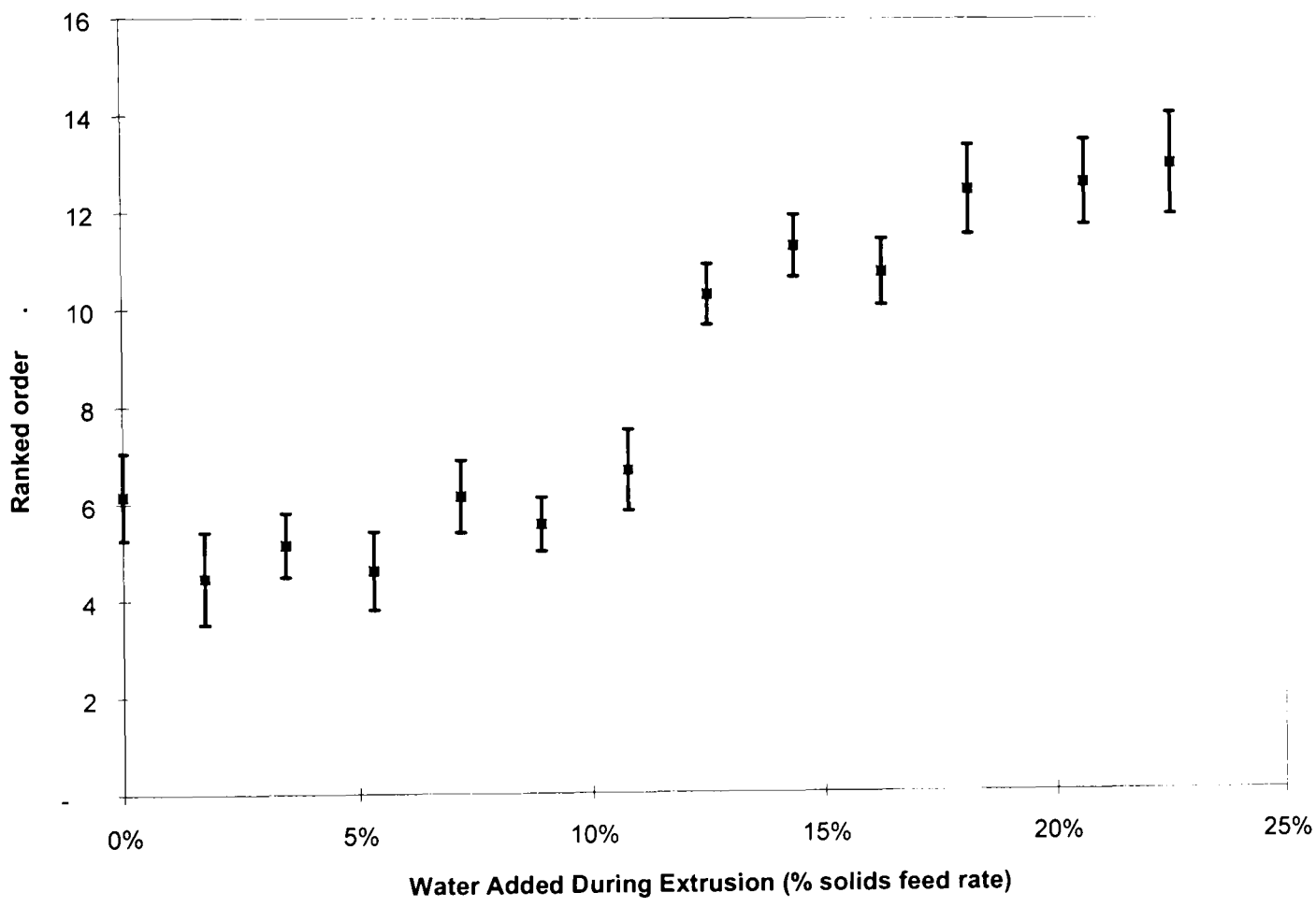

Figure 6-6 Samples ranked in order of crispness by the taste panel. Bars are standard errors.

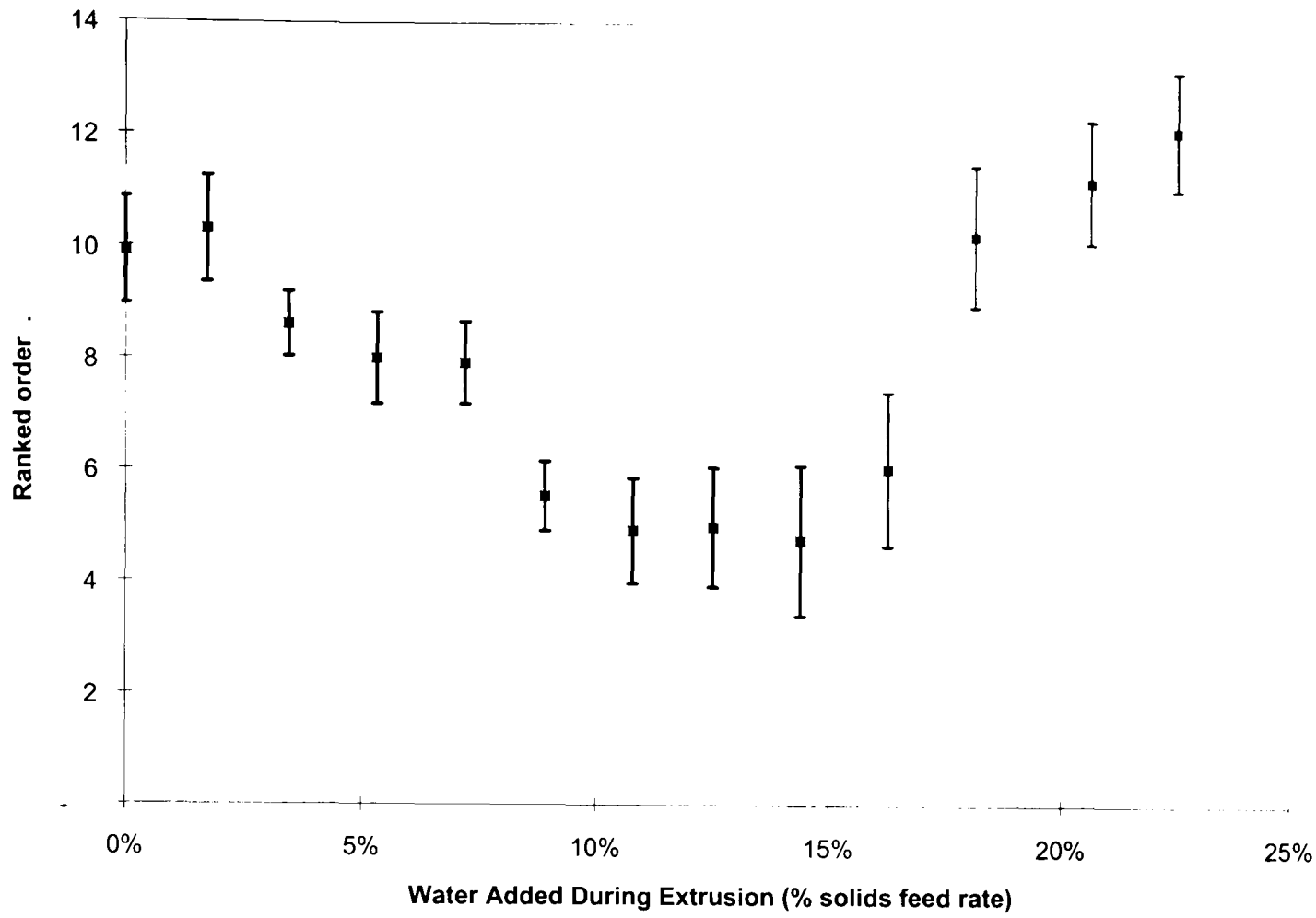

Figure 6-7 Samples ranked in order of crackliness by the taste panel. Bars are standard errors.

6.1.3 Correlation of Sensory Panel and Mechanical Data

Correlations between mean ranked order for each combination of each sensory panel attribute and each mechanical category were calculated by Spearman's coefficient of rank correlation, which is also the product moment correlation (Kendall and Buckland 1982). A graph plotting all the coefficients of rank correlation is given in Figure 6-8. By examination, it can be seen the difference in line length when going from one resolution to the next correlates better with any given perceived texture between some pairs of resolutions than with others. The highest correlations between sensory attributes and mechanical parameters are given in Table 6-2.

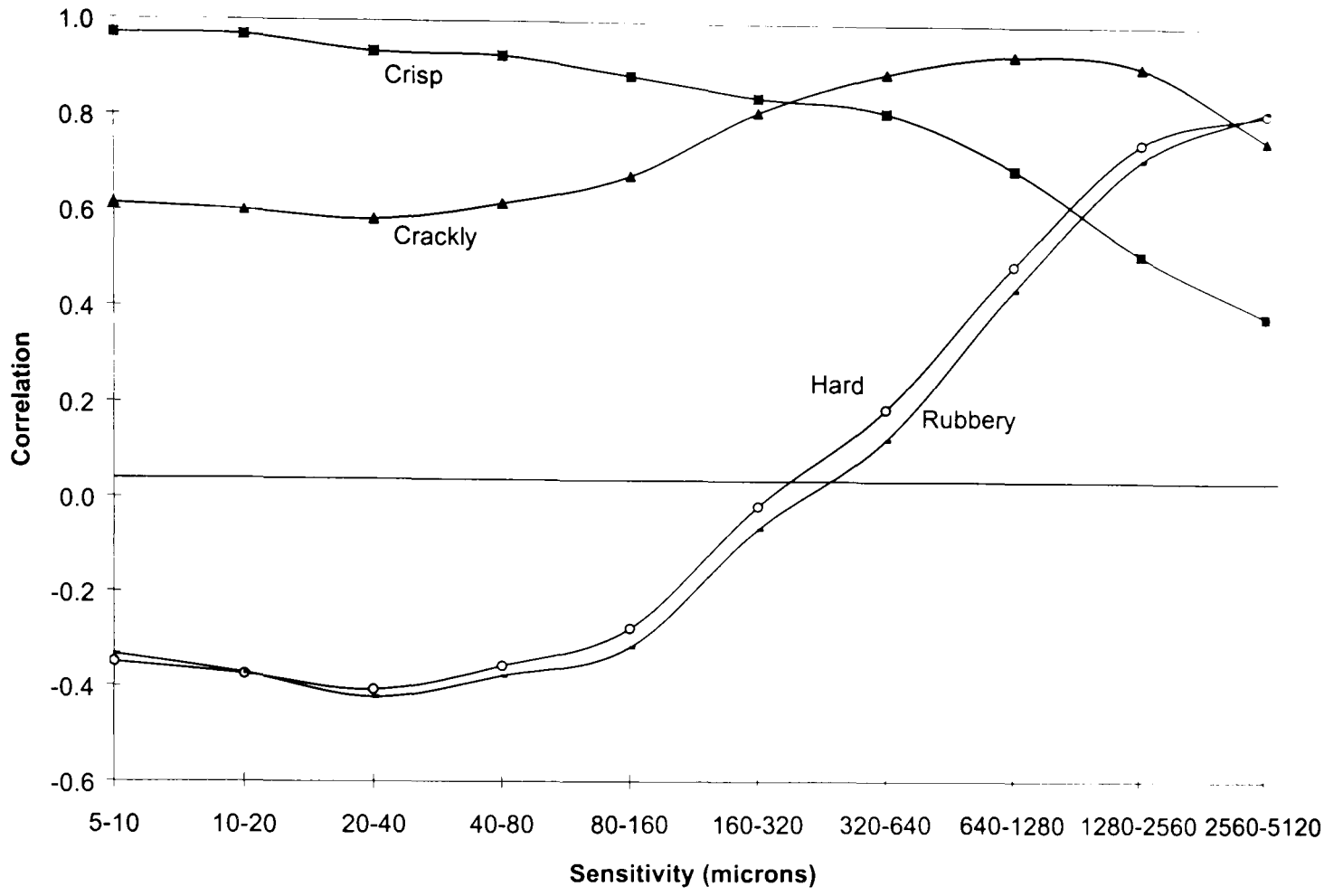

Figure 6-8 A summary of all correlations of organoleptic sensations with mechanical parameters, correlated using Spearman's Coefficiant of Rank Correlation

Textural Attribute	Sampling Resolution	Coefficient of rank correlation
Crispness	5 - 10μm	0.97
Crackliness	0.64 - 1.28mm	0.94
Rubberiness	Maximum force obtained	0.98

Table 6-2 The peak correlations between perceived texture and mechanical sensitivity.

Figure 6-8 should be used as a reference chart when analysing samples other than those used to calibrate the method to a sensory panel. For example, when mechanically analysing two or more samples, the differences between the measured line lengths for 10 and 20 μm resolutions will be indicative of the relative crispness of the samples. Similarly, the differences between the measured line lengths for 640 and 1280 μm resolutions will be indicative of the relative crackliness of the samples. By this technique, samples may be ranked in order of crispness or crackliness, compared to past results, or compared to a previously defined texture "window" for quality assurance.

A negative correlation (Spearman's coefficient = -0.22) of maximum force with crispness agreed with Seymour and Hamann (1988).

The best correlations with crispness were equally the differences between line lengths measured for 5 and 10 μm, and between 10 and 20 μm. These were the highest resolutions used, and hence give rise to the concern that the true peak may occur at a higher resolution, i.e. for displacements lower than 5μm. The assumption is being made that a peak does exist, and correlation does not increase with infinitesimal displacements. Imai *et al* (1995) found members of a sensory panel could detect particles at least as small as 6 μm, so the sensations of texture at the high resolutions used here (5μm) are not as surprising as may first appear.

Crackliness correlated best at a much coarser resolution; the peak in correlation clearly occurred as the resolution was changed from 0.64 to 1.28mm.

The sensory attributes hardness and rubberiness both correlated best with the mechanical parameter "maximum force."

This work was performed with an indigenous sensory panel, and should be recalibrated if used outside the UK (Rohm, 1990; Szczesnaik and Skinner, 1973; Bourne *et al.* 1975).

It must be remembered there is an inherent disadvantage of using a machine for sensory testing; the results are quantitative, not qualitative. It is possible to optimise the crackliness of a product as measured by the mechanical technique, but not possible to monitor the introduction of an unforeseen texture or attribute that the algorithm is not designed to identify, such as grittiness, sample integrity, or even which sample is preferred. The use of a sensory panel to assess the crackliness of the same product would simultaneously detect unforeseen attributes.

6.1.4 Conclusions

Sensory panel results for crisp and crackly type evaluations can be emulated by machine using subtraction of consecutive line lengths of traced compression-force data of different sampling resolutions.

It is trivial to emulate sensory panel results for hardness and rubberiness simultaneously.

The advantages of the technique demonstrated should be evident. A machine is faster, more convenient, immune to toxins, more reproducible, and may be cheaper over a long period than a sensory panel.

Data presented here demonstrates the suitability of the technique when analysing a range of samples which were similar in size and structure; the claim is not being made that the technique will determine which of two dissimilar samples is the most crackly. For example, it is not claimed the technique will determine the relative crackliness of a cornflake compared to a slice of toasted bread; conversely, data is not presented to invalidate such a comparison.

7 Experimentation

7.1 Overview

The overall aim of the work was to answer a question. Progress through the project was driven both by hypotheses and by discoveries made throughout the project, therefore a predefined path of research was not followed. For example it was found that both extruded and conventionally processed samples equilibrated to similar moisture contents in any given relative humidity. Despite this the extruded samples deteriorated more quickly in a confectionery bar. It was therefore seen to be important to investigate the rate of moisture gain. A much later example of an event-driven experiment began while examining samples microscopically. The curious absence of Maltese Crosses in samples made with an SME within a narrow range was noted. This led to further examinations of such samples, then finally to the development of samples that were microscopically indistinguishable from conventionally processed samples.

7.2 Initial Experimentation to Verify the Claims in the Brief.

Experimental chocolate countline bars were made using various types of expanded rice, but keeping the rest of the formulation within the specifications of the marketable product. The expanded rices used were conventional, extruded rice and two experimental extruded rices made at the university. The experimental chocolate countline bars were sealed in plastic wrappers similar to those used for production chocolate countline bars. Over the following weeks, the experimental bars were observed and eaten to assess the effects of age on the texture of the bars.

A second experiment involved removing the expanded rice from the bars after periods of storage, then drying the rice to calculate the moisture contents. However the chocolate, fat, and caramel impregnated into the rice caused measurement difficulties.

The claims in the brief were verified. The bars made with conventional expanded rice remained crisp for the duration of the trial (three months). The bars made with extruded expanded rice became swollen, cracking the enrobing chocolate and forcing caramel through some of the cracks. The swelling reached a maximum between one and two weeks, before contracting with continued storage. The crisp texture was lost from the extruded rice filling after a week.

To assess the starch in the conventionally processed and extruded puffed rice, four parameters were measured; WSI, WAI, solution viscosity, and X-ray pattern type. The results are displayed in Table 7-1. Although the WAI and WSI for the two samples are not wildly different, the solution viscosities and X-ray pattern types clearly showed the starch in the two samples had different characteristics. In particular the higher WSI and cold paste viscosity suggested that the extruded product contained more converted starch.

Sample	WSI	WAI	Dispersion Viscosity (Pa.s.) @ 1Pa	Type of amylose-lipid inclusion complex
Conventional	12.3% ± 0.2%	920% ± 20%	0.15	V
Extruded	14.1% ± 0.2%	959% ± 4%	~1	E

Table 7-1 Parameters comparing starch profiles within conventionally processed and extruded puffed rice. Three repetitions were used for the WAI and WSI data.

7.3 Extruded and Conventional Puffed Rice

7.3.1 Measuring Sorption Isotherms

7.3.1.1 Method

Moisture sorption isotherms were obtained for conventionally puffed rice and extruded krispies (Section 5.1.1). Undried samples were placed in humidity chambers for twenty days, weighed, dried in a vacuum oven for six days at 75°C, then re-weighed to calculate to moisture contents at equilibrium. The samples were not oven- or vacuum-dried before being equilibrated, as this could possibly alter the physical structure of the krispies, for example, vacuum pressure could rupture cell walls.

7.3.1.2 Results

Results are shown in Figure 7-1. Data are not shown for 100% humidity, as samples cannot be in equilibrium with such an environment.

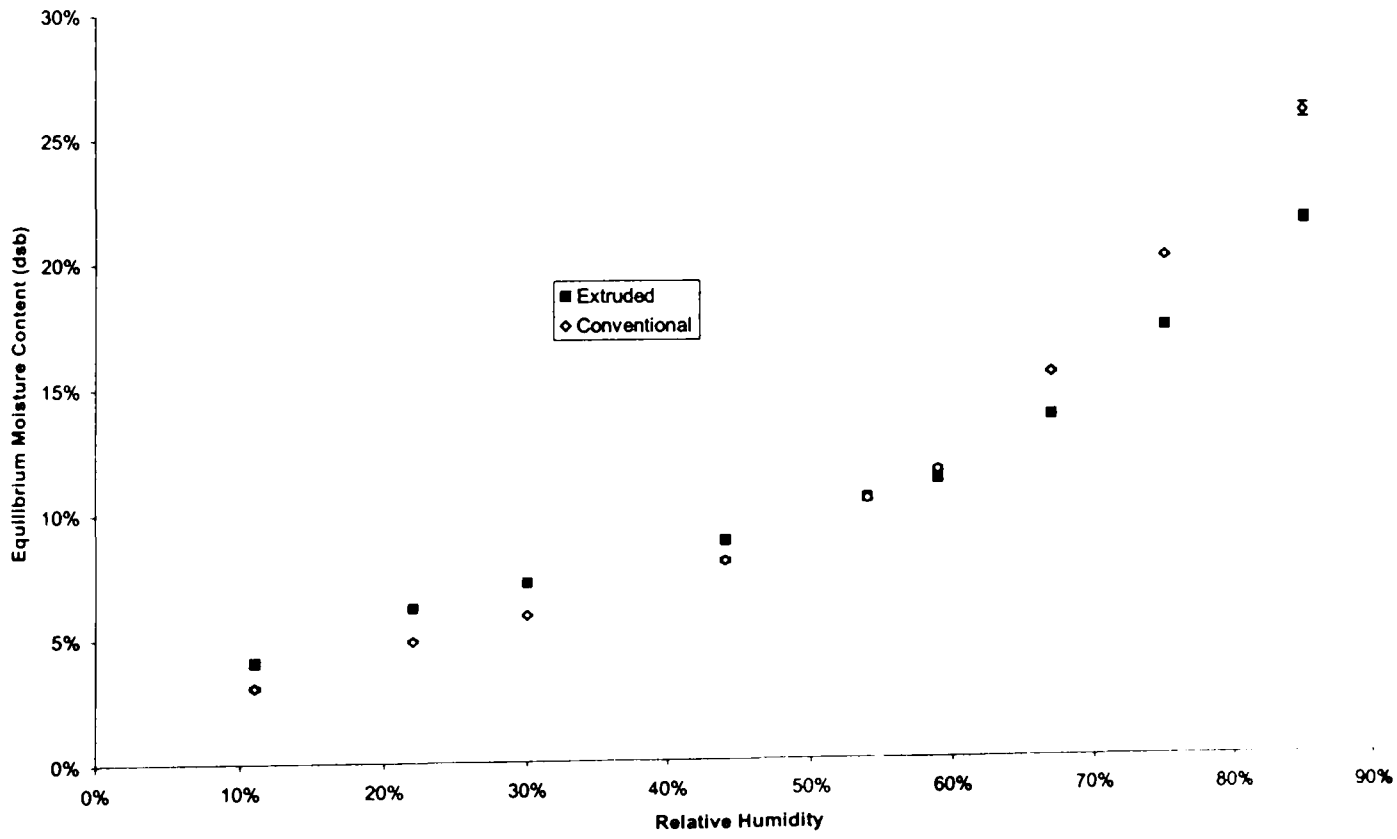

Figure 7-1 Sorption isotherms for both extruded and conventionally puffed rice. The samples were equilibrated for thirty days at ambient temperature, then dried for six days under vacuum. Bars are standard errors, but mostly hidden behind markers.

7.3.1.3 *Analysis and Conclusions*

The extruded krispies clearly had higher and lower equilibrium moisture contents than the conventionally puffed rice product at low and high relative humidities respectively, crossing at around 55% relative humidity. To assess the importance of this difference, the water activity of the other constituents (caramel, chocolate, and cocoa fat) of a chocolate countline bar were measured to determine the relative humidity within a bar. The water activity of caramel was around 0.55, which would lead to a relative humidity of around 55% within a chocolate countline bar. Having established the extruded and conventionally processed puffed rices equilibrate to similar moisture contents at this relative humidity, the equilibrium moisture contents was rejected as a cause of the poor moisture stability of extruded puffed rice within confectionery bars. The logical step was to investigate the rate at which the samples reach equilibrium.

7.3.2 Measurement of Water Adsorption Rates

7.3.2.1 *The Experiment*

Graphs showing rates of moisture sorption were created for conventionally puffed rice and extruded expanded rice for a 48 hour period (Section 5.3.3). Again, samples were not oven- or vacuum-dried before being exposed to the various humidities. The omission of drying was justified by the fact that both samples had similar moisture contents (2% moisture), so neither sample should adsorb moisture inherently faster than the other because of differences in the initial state of water.

7.3.2.2 *Results*

Figure 7-2 and Figure 7-3 show the adsorption by the conventional and extruded samples over the first 24 hours of exposure to various relative humidities. To highlight the differences in rate of moisture adsorption between the two samples, Figure 7-4 and Figure 7-5 show the extent of adsorption after 11 and 23 hours respectively, from 11% to 100% relative humidity.

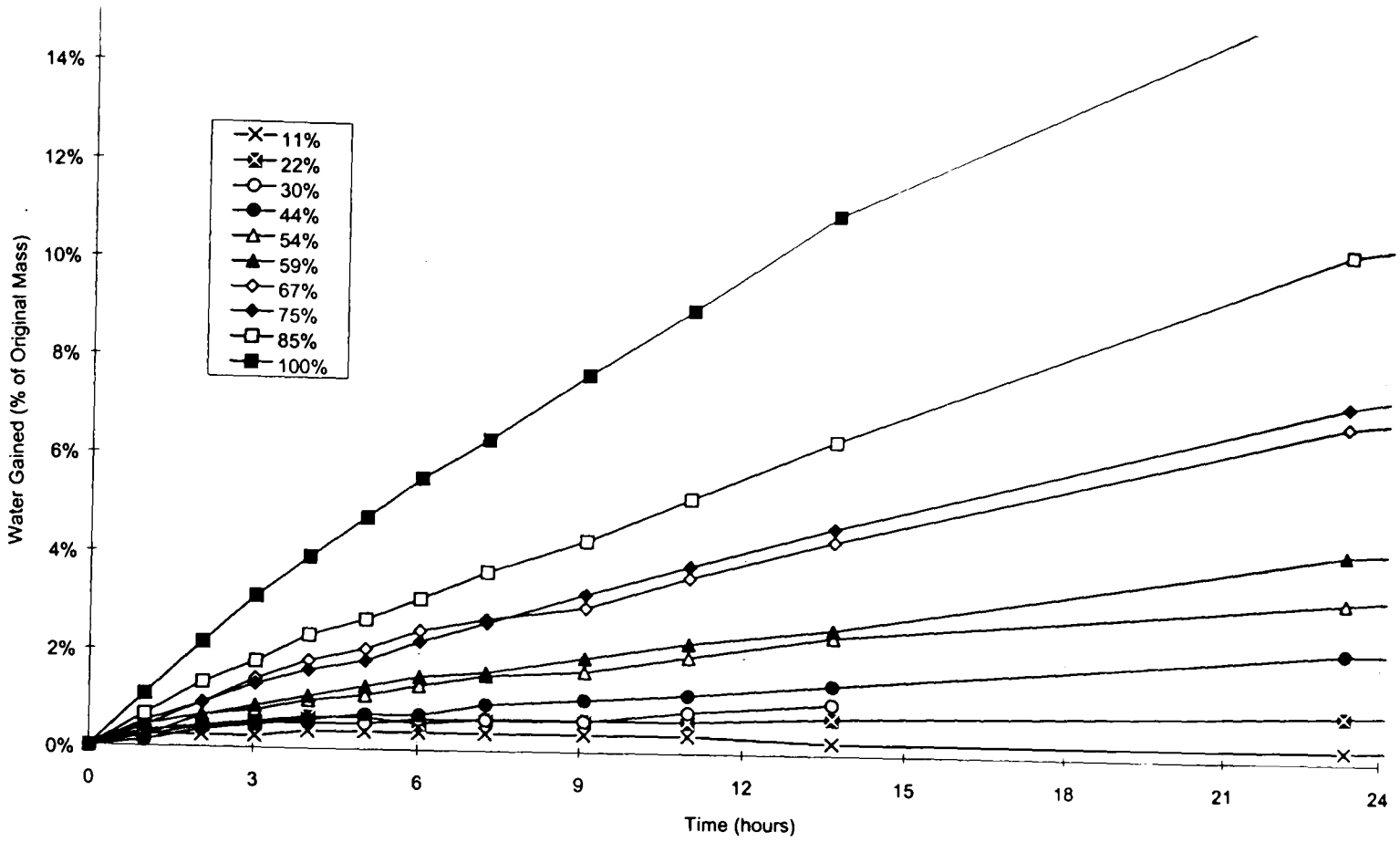

Figure 7-2 Sorption kinetics for conventionally puffed rice at ambient temperature

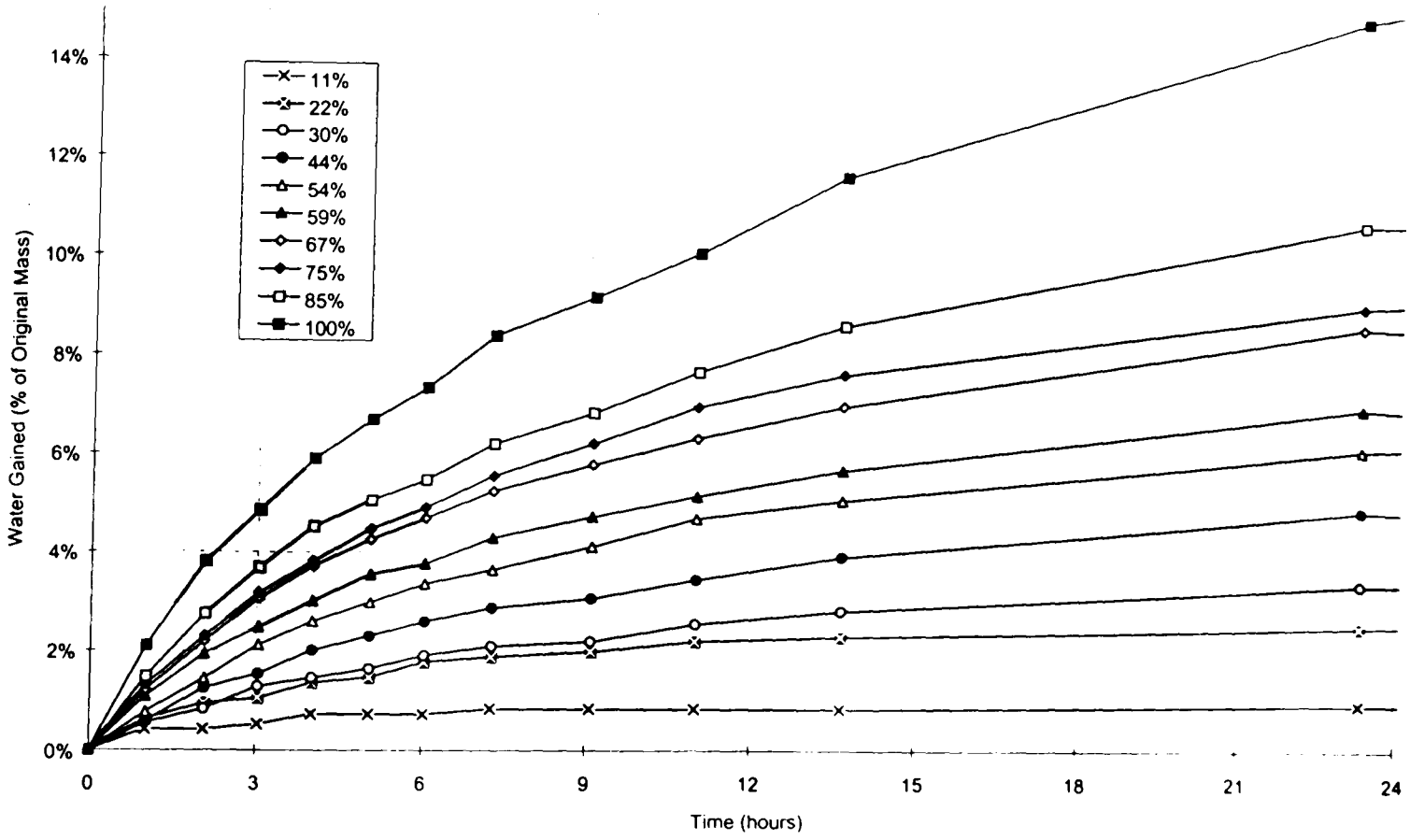

Figure 7-3 Sorption kinetics for extruded rice at ambient temperature

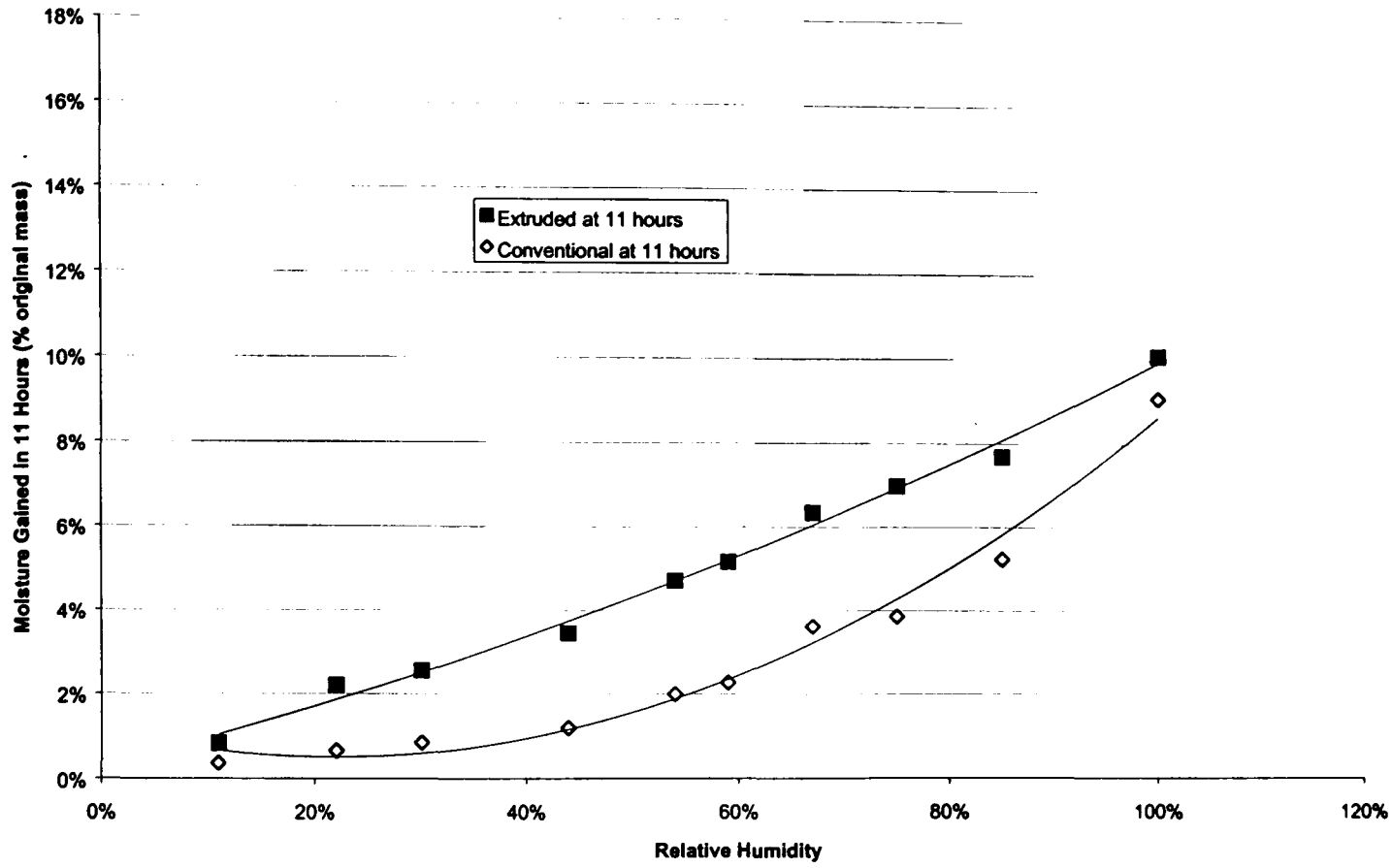

Figure 7-4 Comparison of moisture gained at 11 hours for extruded and conventionally puffed rice at ambient temperature.

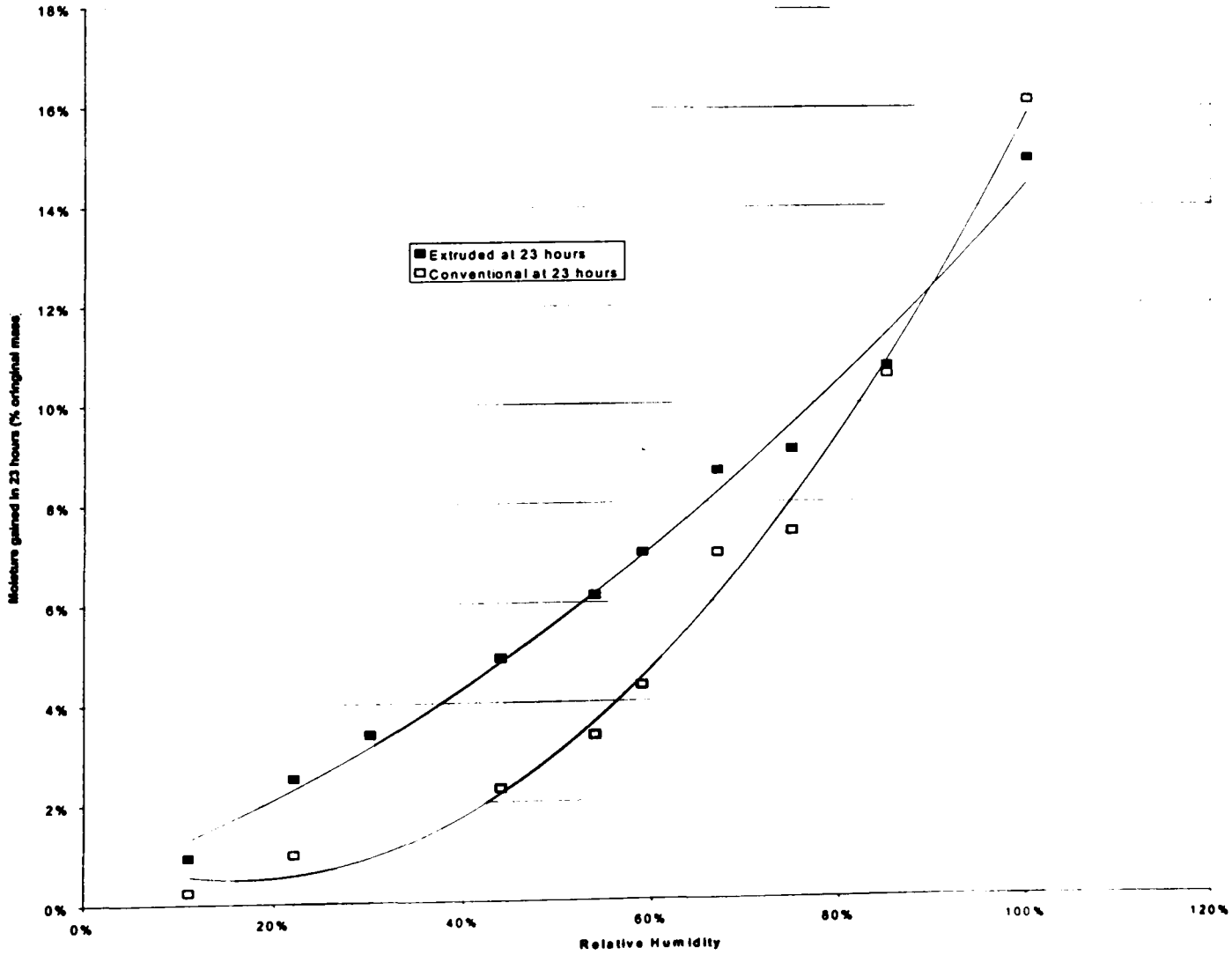

Figure 7-5 Comparison of moisture gained at 23 hours for extruded and conventionally puffed rice at ambient temperature

7.3.2.3 *Analysis and Conclusions*

It may be clear from Figure 7-2 to Figure 7-5 that the extruded samples adsorbed moisture more quickly than the conventional samples. To analyse the differences the results were fitted to Equation 7-1 to identify the rate constants for each sample across the range of relative humidities used. Data from the mathematical modelling are displayed in Figure 7-6, which shows the fitted equilibrium values, mc_∞, and in Figure 7-7, which shows the modelled rate values, k.

$$mc_t = mc_\infty\left(1 - e^{-tk}\right)$$

Equation 7-1 The equation used to model the rate of moisture vapour adsorption by the extruded and conventional samples

Where mc_t and mc_∞ are the moisture contents at time t and ∞, and k is the rate constant.

Equation 7-1 was used in preference to the standard equation for solvent adsorption by polymers (Equation 4-3) because the samples were foamed rather than a continuous homogeneous polymer. Equation 4-3 was also used during analysis, but proved unstable; values for the power constant n could fluctuate in the range 0.2 – 0.8, and the fitting program was able to adjust mc_∞ and k to adapt to the fluctuations. (n is valid from 0 to 1.) The values of mc_∞ were fixed at the equilibrium values (mc_{eq}) from Section 7.3.1.2 in an attempt to kerb the fluctuations in n, but this served only to prevent a good fit of the model to the data.

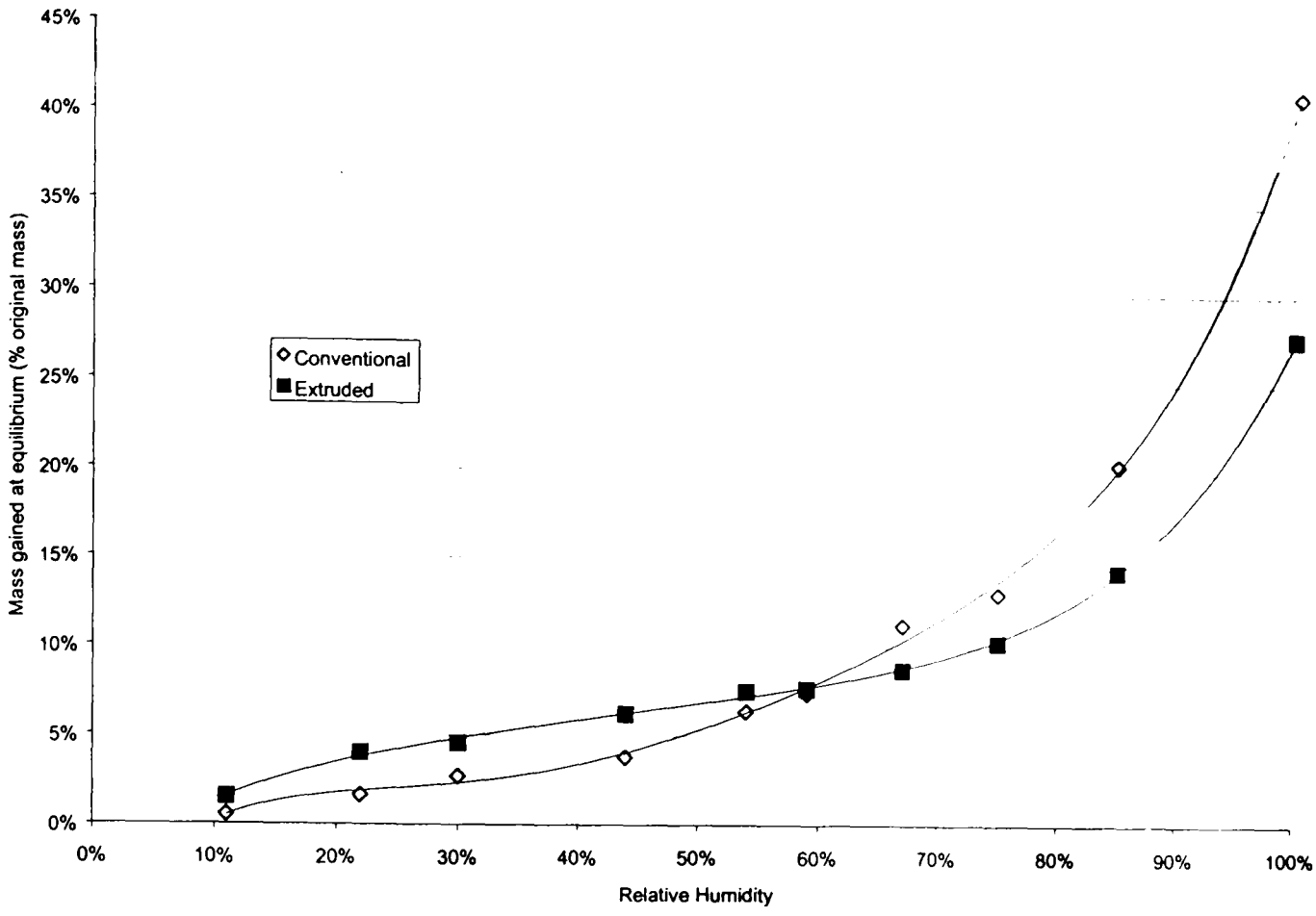

Figure 7-6 Equilibrium moisture content (mc_∞) as fitted to the data shown in Figure 7-2 and Figure 7-3. It should be noted samples cannot be in equilibrium at 100% RH.

The predicted equilibrium moisture contents in Figure 7-6 closely resemble the measured equilibrium moisture contents in Figure 7-1, indicating that Equation 7-1 is a good model. A further comparison can be made between moisture contents at 11 and 23 hours, both from measured data (Figure 7-4 and Figure 7-5) and from predicted data (Figure 7-8)

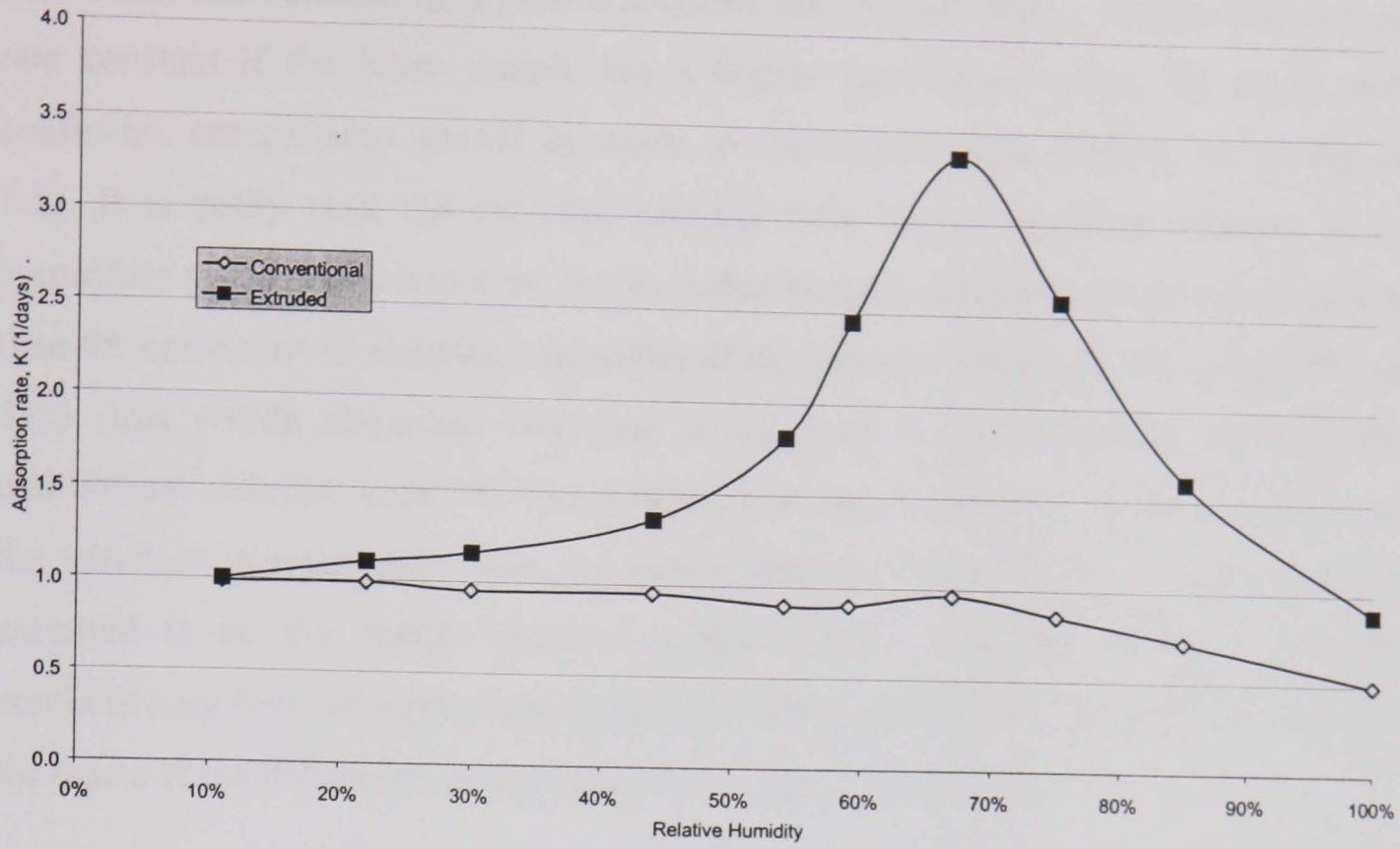

Figure 7-7 Moisture adsorption rates as fitted to the data in Figure 7-2 and Figure 7-3

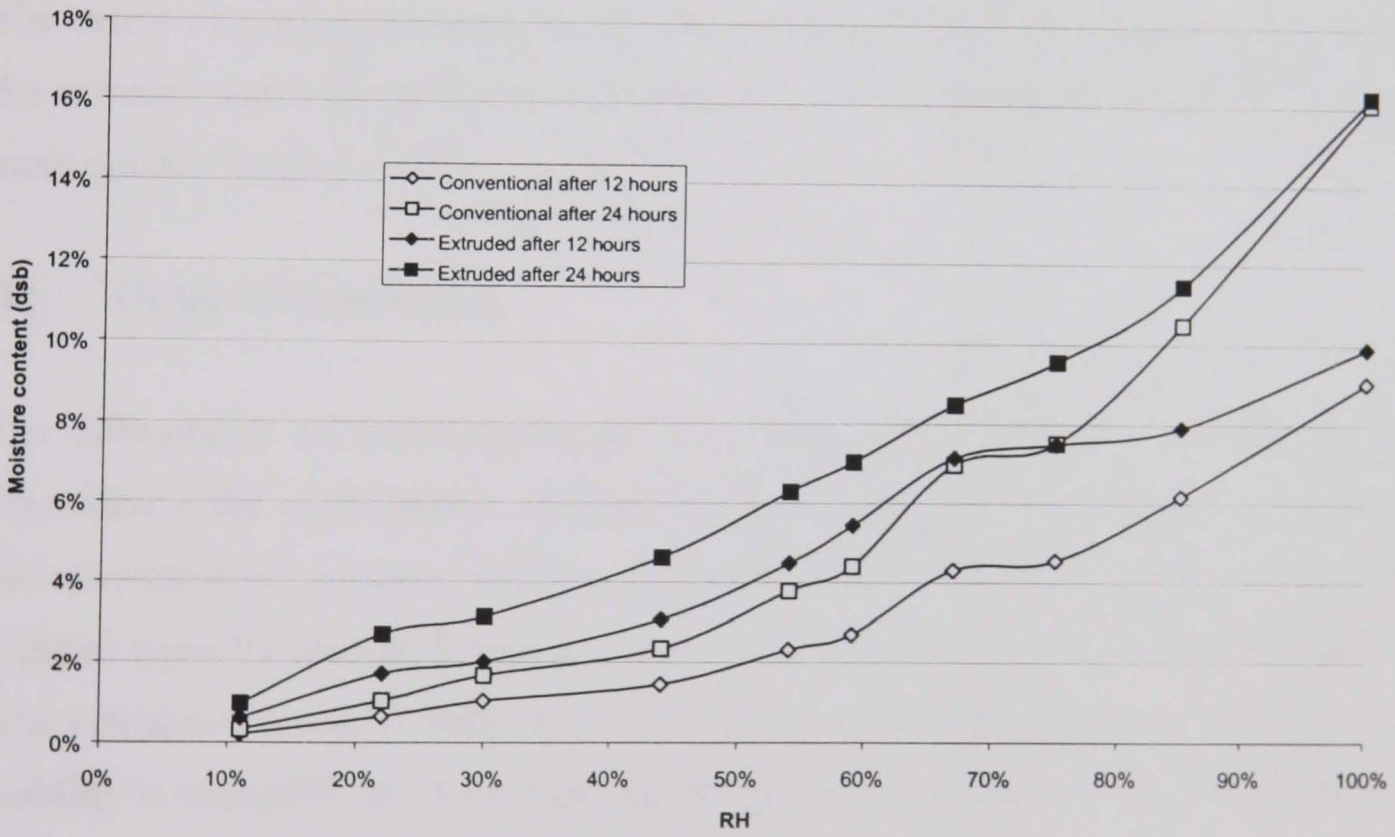

Figure 7-8 Moisture contents predicted from Equation 7-1 for extruded and conventionally puffed rice at 11 and 23 hours. Compare this to Figure 7-4 and Figure 7-5.

Figure 7-7 implies the extruded samples adsorbed moisture vapour more quickly than the conventional samples, though the variation in fitted equilibrium moisture contents between the two samples (Figure 7-6) complicates analysis. For example, a sample

with a fast rate constant may adsorb moisture less quickly than a sample with a slow rate constant if the latter sample has a higher equilibrium value. To avoid such confusion, comparisons should be made to the original data (Figure 7-2 to Figure 7-5). It is easily seen the extruded samples have higher moisture contents at all humidities at most points in time: the extruded samples adsorb moisture more quickly than the conventional samples, regardless of equilibrium values. At the critical RH of 55% (that within chocolate countline bars), there is no difference between the equilibrium moisture contents. The difference in rate constants is a true indication of the variation in water gain from the vapour phase at the product A_w. This fact was assumed to be the reason extruded puffed rice is unsuitable for use in moist confectionery bars, so further hypotheses and experimentation were needed to explain the cause of the difference in adsorption rates. Initial hypotheses were: -

(a) Starch damage

The extent of damage incurred by the starch varied between the two processes, with the extruded starch incurring most damage and as a consequence adsorbing moisture more quickly (section 4.2.2).

(b) Order of Complexing

The diffusability of moisture through the samples was determined in part by the crystalline order of the starch. Preliminary X-ray diffraction investigations revealed the conventionally produced samples displayed V-type complexes, while the extruded samples typically showed E-type responses. V-type complexes are stable, whereas E-type complexes are only stable while the sample is in a glassy state, and molecular mobility is negligible. E-type complexes can only be formed at high temperatures and low moisture contents; consequently the molecules are unable to rearrange into a stable V-type complex before cooling below their glass transition temperature. It therefore seemed reasonable that starch processed under these conditions may not have been able to realign or rearrange molecules to close microscopic pores and fissures before cooling below the glass transition temperature. Upon hydration to around 15% moisture, E-type complexes will reform to V-type complexes, also

suggesting there is an additional thermodynamic force encouraging water uptake (section 4.2.1.2).

(c) Morphology (foam and sponge structure)

If one sample were a sponge (continuous gaseous phase) while the other was a foam (discontinuous gas phase), then the spongy sample would be expected to be inherently more permeable. Such a sample would take up water more quickly through capillary action (section 4.5.4).

7.3.3 Extrusion Experiments

7.3.3.1 Technique

Samples were produced at various moisture contents, solid feed rates, barrel temperatures, and screw speeds; Table 7-2 contains details of these variables. Information about screw configuration is given in Section 5.2.1. Extrusion parameters (torque, power, and pressure) were recorded. Sample diameters and the numbers of residual granules were measured. WAI, WSI, and WVAR were obtained for samples dried to constant mass at 105°C (Methods, pages 72, 72, and 71 respectively). SME was calculated from both power and torque using Equation 4-7 and Equation 4-8.

Experiments were carried out using two different formulations. The majority of the data presented in this section will relate to extrudates prepared with rice flour and water alone (samples 1-25). A second set of experiments was carried out with samples where the solid ingredients were 100 parts rice flour, 5 parts sucrose (icing sugar), and 0.5 parts sodium bicarbonate (samples 26-49). The sucrose was used to reduce the viscosity of the extrusion melt, and therefore reduce SME. Icing sugar was used instead of granulated sugar to aid solvation. Sodium bicarbonate was used to help seed bubble growth. In practice, the effect of process variables for the two formulations turned out to be very similar. When considering the correlation between starch conversion and hydration and SME and starch conversion, the results from both formulations will be taken into account.

Sample	Added water (%)	Total water (%)	Screw speed (rpm)	Solids feed (kg/hr)	Barrel temperature (°C) Zone 1	Zone 2	Zone 3	Zone 4
To investigate effect of barrel temperature Ingredients: rice flour								
1	31	44	100	3.98	46	79	78	79
2	31	44	100	3.98	46	78	87	89
3	31	44	100	3.98	46	79	88	99
4	31	44	100	3.98	45	79	93	108
5	31	44	100	3.98	44	79	99	117
6	31	44	100	3.98	44	85	107	128
7	31	44	100	3.98	44	85	120	140
8	31	44	100	3.98	44	85	127	147
9	31	44	100	3.98	45	94	133	157
To investigate effect of screw speed Ingredients: rice flour								
10	21	34	440	3.98	43	85	124	118
11	21	34	400	3.98	44	96	117	120
12	21	34	350	3.98	44	96	119	120
13	21	34	300	3.98	43	96	118	117
14	21	34	250	3.98	42	96	119	119
15	21	34	200	3.98	43	95	119	120
16	21	34	150	3.98	42	94	118	119
17	21	34	100	3.98	41	88	119	119
18	21	34	70	3.98	40	85	120	119
19	21	34	51	3.98	40	85	120	120
20	21	34	32	3.98	40	84	120	120

Sample	Added water (%)	Total water (%)	Screw speed (rpm)	Solids feed (kg/hr)	Barrel temperature (°C) Zone 1	Zone 2	Zone 3	Zone 4
To investigate effect of moisture content Ingredients: rice flour								
21	21	34	300	3.98	43	96	118	117
22	15	28	300	3.98	42	88	120	119
23	8	21	300	3.98	41	88	120	120
24	4	17	300	3.98	42	89	120	127
25	2	15	300	3.98	41	89	120	128
To investigate effect of barrel temperature Ingredients: rice flour, sucrose, sodium bicarbonate (100:5:0.5)								
26	45	58	100	3.96	44	76	78	80
27	45	58	100	3.96	46	77	88	90
28	45	58	100	3.96	46	78	88	99
29	45	58	100	3.96	46	78	93	109
30	45	58	100	3.96	46	79	99	119
31	45	58	100	3.96	46	85	109	127
32	45	58	100	3.96	47	84	119	140
33	45	58	100	3.96	46	85	130	149
34	45	58	100	3.96	49	92	133	157
To investigate effect of screw speed Ingredients: rice flour, sucrose, sodium bicarbonate (100:5:0.5)								
35	27	40	439	3.96	43	88	115	120
36	27	40	400	3.96	54	95	116	119
37	27	40	350	3.96	50	95	118	117
38	27	40	300	3.96	48	96	118	115
39	27	40	250	3.96	48	96	119	119
40	27	40	200	3.96	46	95	118	120
41	27	40	150	3.96	46	95	119	118
42	27	40	100	3.96	44	89	118	119

Sample	Added water (%)	Total water (%)	Screw speed (rpm)	Solids feed (kg/hr)	Barrel temperature (°C)			
					Zone 1	Zone 2	Zone 3	Zone 4
43	27	40	71	3.96	42	85	119	119
44	27	40	49	3.96	41	84	121	120
To investigate effect of moisture content Ingredients: rice flour, sucrose, sodium bicarbonate (100:5:0.5)								
45	27	40	300	3.96	48	96	118	115
46	18	31	300	3.96	43	88	117	119
47	9	22	300	3.96	42	89	117	121
48	4	17	300	3.96	42	92	116	127
49	2	15	300	3.96	42	91	117	130

Table 7-2 Summary of extrusion conditions used in the following experiments

7.3.3.2 Results and Analyses

7.3.3.2.1 Effects of Barrel temperature

7.3.3.2.1.1 Effects of Barrel Temperature on SME

An opposing trend between set barrel temperature and calculated SME can be seen as expected. Such a negative correlation must be borne in mind when considering the effects of either temperature or SME on other aspects, such as the water absorption index. The similarity of the two lines (SME due to torque and power) in Figure 7-9 also supports the method of calculating SME from both Equation 4-7 and Equation 4-8. Differences between the two calculated SME's in Figure 7-9 are due to fluctuations in internal measurements within the extruder; the extruder controller records parameters sequentially rather than simultaneously. Consequently, time elapsed between the parameters "power" and "torque" being printed leads to fluctuations in the recorded parameters and calculated SME. Figure 7-9 displays the SME calculated for measurements made at a screw speed of 300rpm, solids feed rate of 4kg hr^{-1}, and a water feed rate of 1.8 kg hr^{-1}. The temperature profile was 40°C, 80°C, T_3 and T_4. T_3 and T_4 were varied and represent the temperatures of zones 3 and 4 of the extruder barrel respectively.

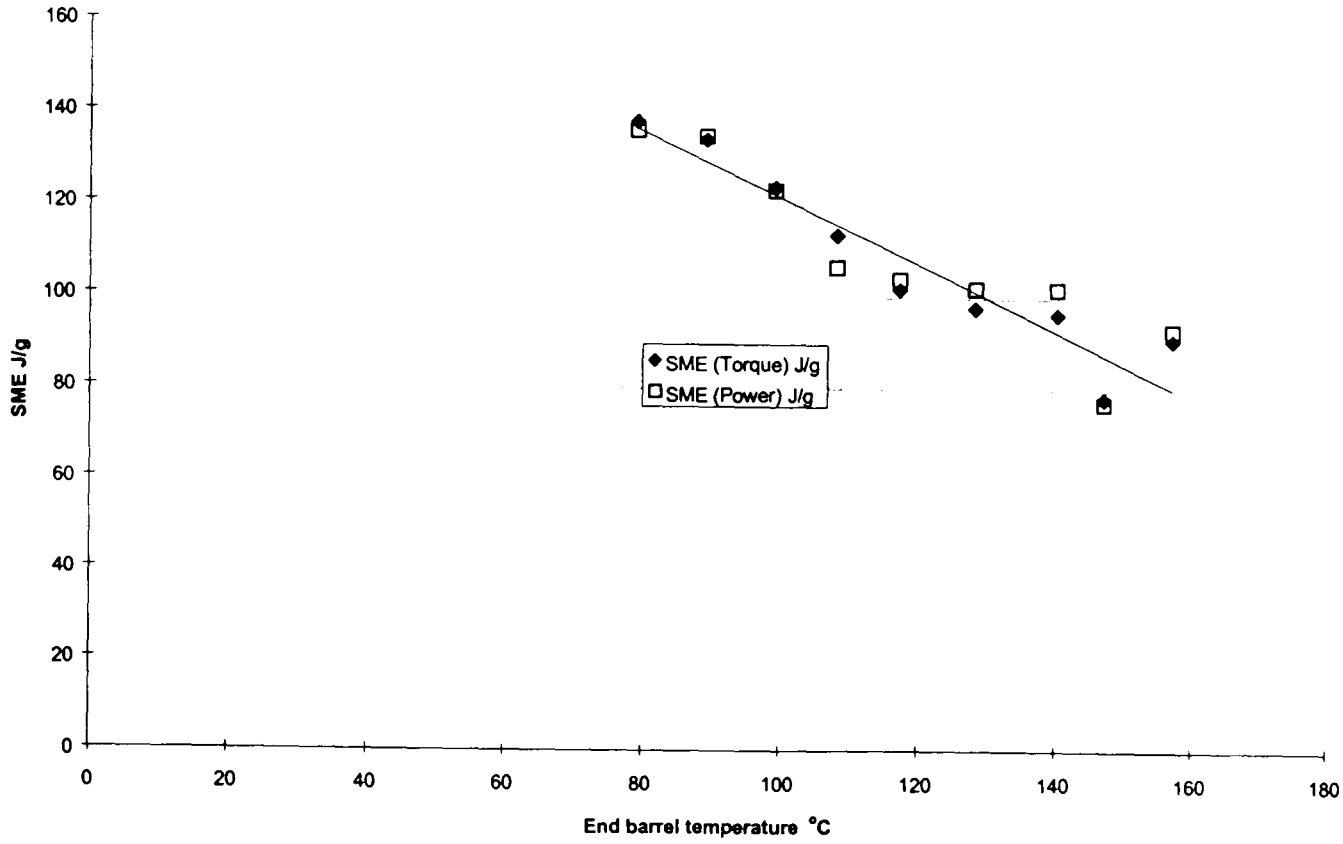

Figure 7-9 The effect barrel temperature has on SME, calculated from both measured torque and power. Samples 1-9 from Table 7-2.

7.3.3.2.1.2 Effects of Barrel Temperature on WAI and WSI

Figure 7-10 shows the relationships between barrel temperature and the water absorption and solubility indices (WAI and WSI). Clearly, the WAI and WSI increase with increasing temperature, indicating a greater gelatinisation of the starch granules leading to the increased susceptibility to water vapour adsorption. Combining Figure 7-10 with Figure 7-9 shows negative correlations between SME and both WAI and WSI. However, it should be noted the calculated SME is lower than for other ranges in this thesis (80-160 Jg^{-1} compared to 300-1000 Jg^{-1}), and the temperature range is greater (80°-160° C compared to 120°-130° C). Therefore the relative magnitudes of the SME and thermal energy inputs are more biased towards the thermal input than usual, decreasing the dependency of the gelatinisation on the SME. Additionally, the low SME suggests less generation of heat internally within the sample than normally occurs. This difference in internal heat generation leads to a greater thermal input from the barrel heaters to maintain the barrel temperature, biasing the thermal energy and SME ratio further towards a thermal energy only dependency.

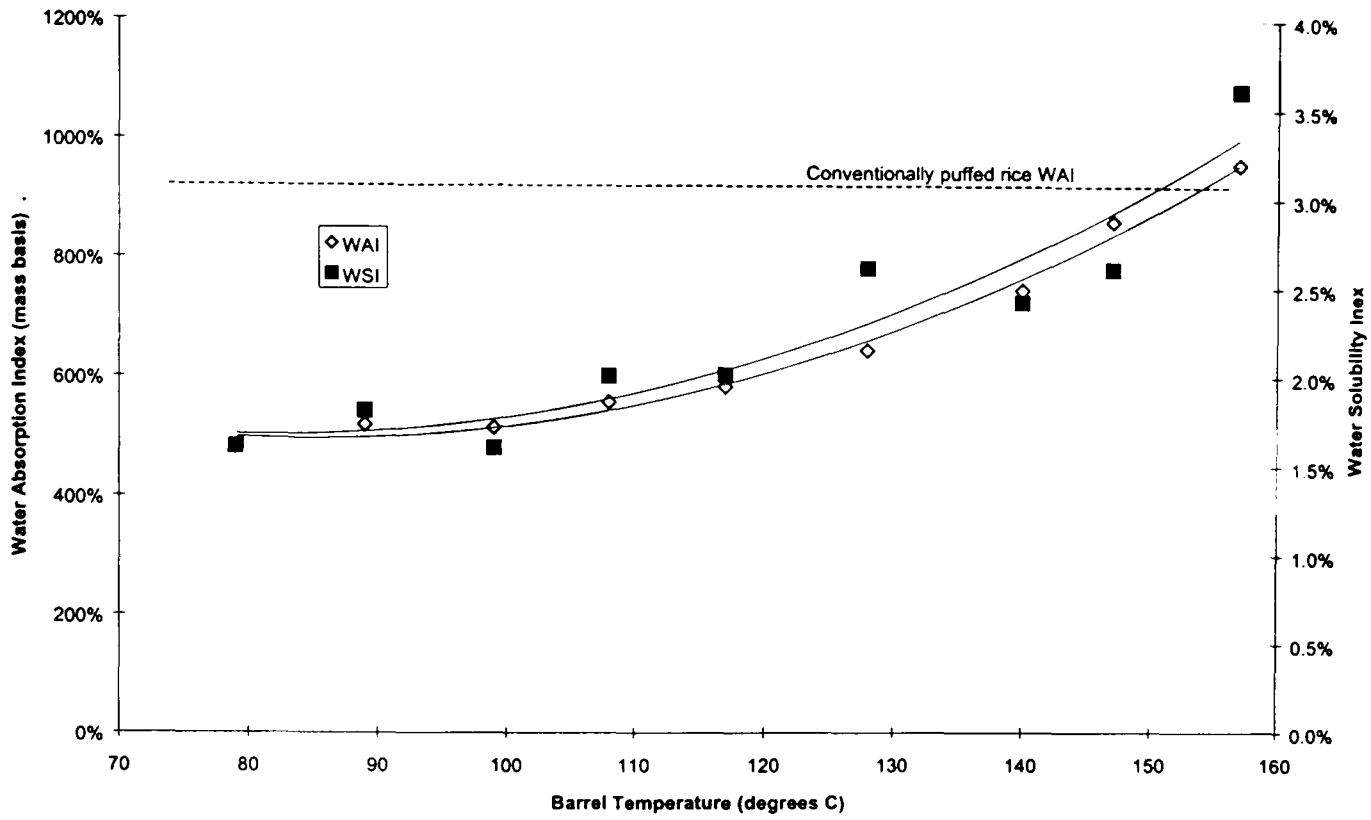

Figure 7-10 Effect of barrel (zone four) temperature on WAI and WSI. Samples 1-9 from Table 7-2. Conventionally puffed rice WSI corresponds to 12.3%.

7.3.3.2.1.3 Effect of Barrel Temperature on Water Vapour Adsorption Rate

Figure 7-11 shows little effect of barrel temperature on the rate at which water vapour is adsorbed. This is despite increased expansion to about the middle of the temperature range, followed by higher temperatures the formation of porous sponge structures (Section 7.3.3.2.1.4). This observation is very important as the degree of cook, gelatinisation, and expansion can be controlled without affecting the rate at with water vapour is adsorbed. The reasons for this phenomenon are shown later within the microscopy section (Section 7.5).

Figure 7-11 also shows there is little change in the equilibrium moisture content with variations in barrel temperature, eliminating the possibility of faster moisture adsorption despite a constant rate coefficient.

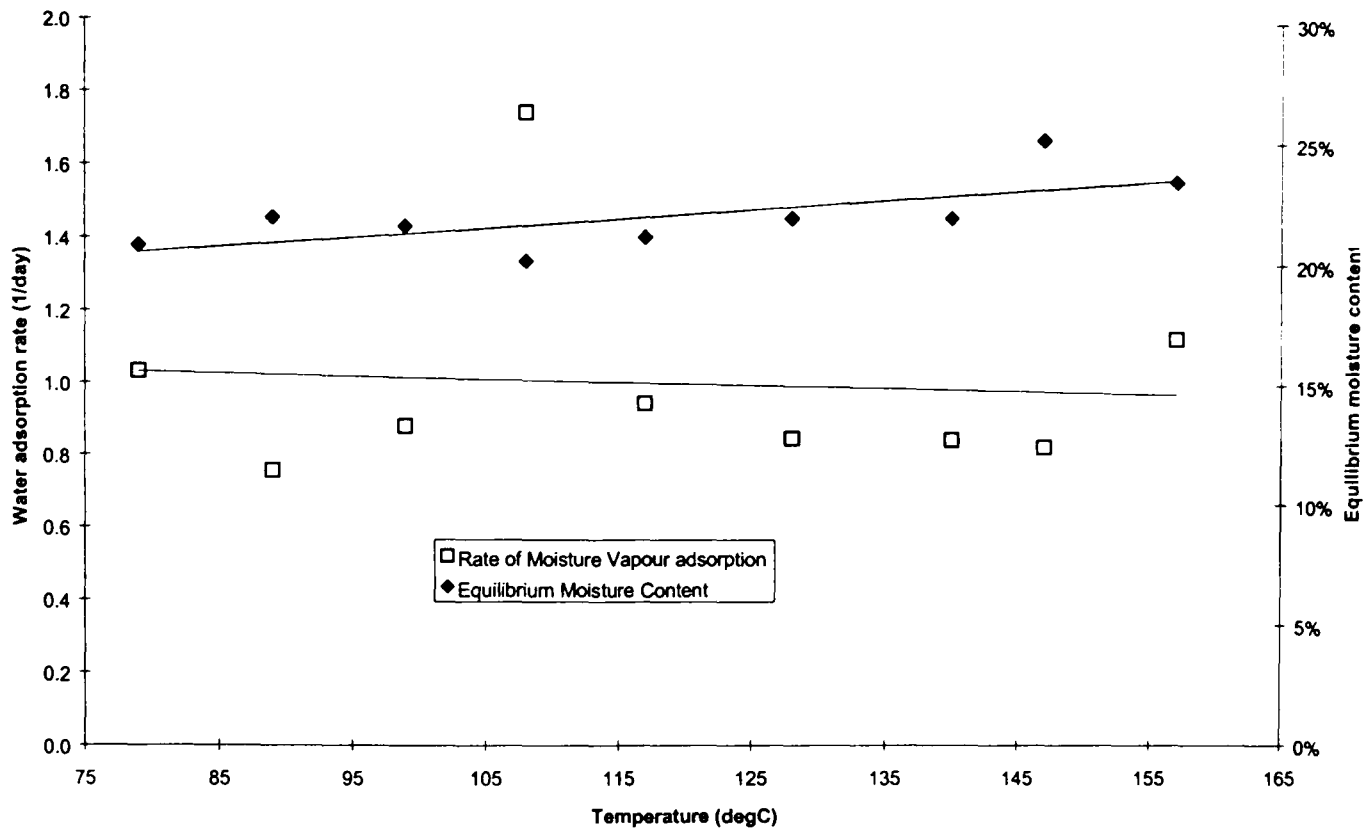

Figure 7-11 Effect of barrel temperature on moisture adsorption rate and equilibria obtained from adsorption in an environment of 100% RH. Samples 1-9 from Table 7-2. Comparable values for conventionally puffed rice samples are a water adsorption rate of 0.5 day^{-1}, and equilibrium moisture content of 42%.

7.3.3.2.1.4 Effect of Barrel Temperature on Expansion

As expected, Figure 7-12 shows an increase in zone 4 temperature from 80 to 120°C causes an increase in expansion. At higher temperatures, the expansion decreased. Visual examination of the sectioned product suggested that this decrease was due to the formation of a sponge rather than foam structure at the higher temperature. A sponge is less able to hold internal vapour pressure that is necessary for expansion, thus explaining the decrease in expansion. The increase in expansion with temperature at lower temperatures can be explained by the higher driving force (water vapour pressure) for expansion and lower resistance (viscosity) to expansion. The influence of these two factors on expansion has been modelled by Fan et al. (1994).

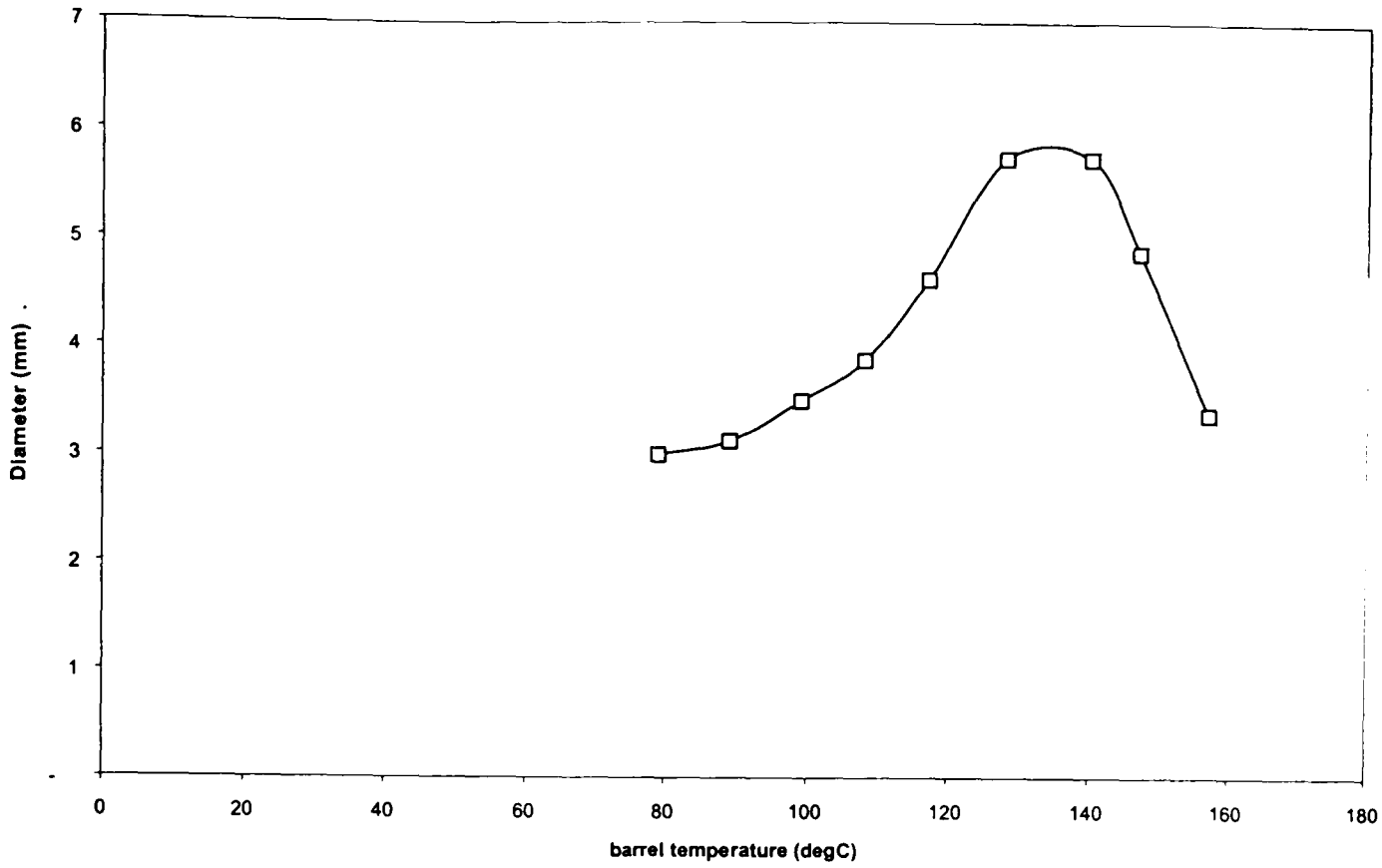

Figure 7-12 The effect of barrel temperature on product diameter (the die was 3mm in diameter). Samples 1-9 from Table 7-2.

7.3.3.2.1.5 The Effect of Barrel Temperature on Starch Crystallinity and Starch/Lipid Complexes

Figure 7-13 shows how the barrel temperature affected the molecular ordering of the starch in the extrudate. At low barrel temperatures (80°, 90°, and 100°C), evidence was seen for native starch by X-ray diffraction (Figure 7-13) (peaks at 15° and 22° 2θ). This was backed up by microscopic examination (Section 7.5) which noted a large number of residual Maltese Crosses under these conditions. As the barrel temperature rose from 80° to 130°C, the amount of V-type starch lipid complexes, which are found in processed starch, increased (peaks at 13° and 20° 2θ). As the barrel temperature rose beyond 130°C to 160°C, all ordered structure decreased, terminating in the amorphous trace recorded for 160°C (no peaks). A possible interpretation for the lack of structure is that cooling and water loss when material at this high temperature exits the die was so extensive and rapid that there was insufficient mobility or time for the amylose-lipid helical complex to form.

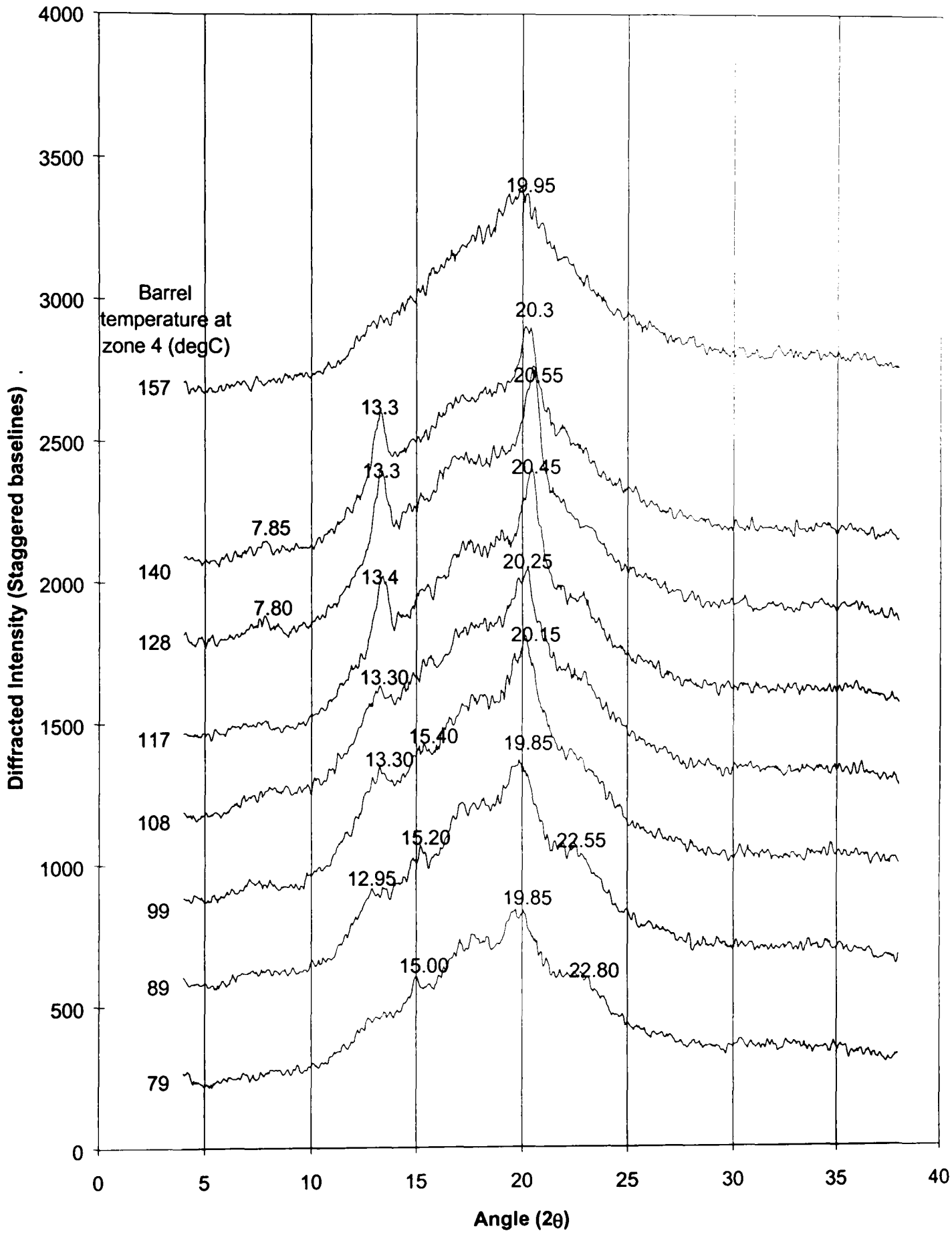

Figure 7-13 Effect of barrel temperature on X-ray diffraction by ground extrudate. Samples 1-9 from Table 7-2. A comparable spectra for conventionally puffed rice is presented in Figure 7-14.

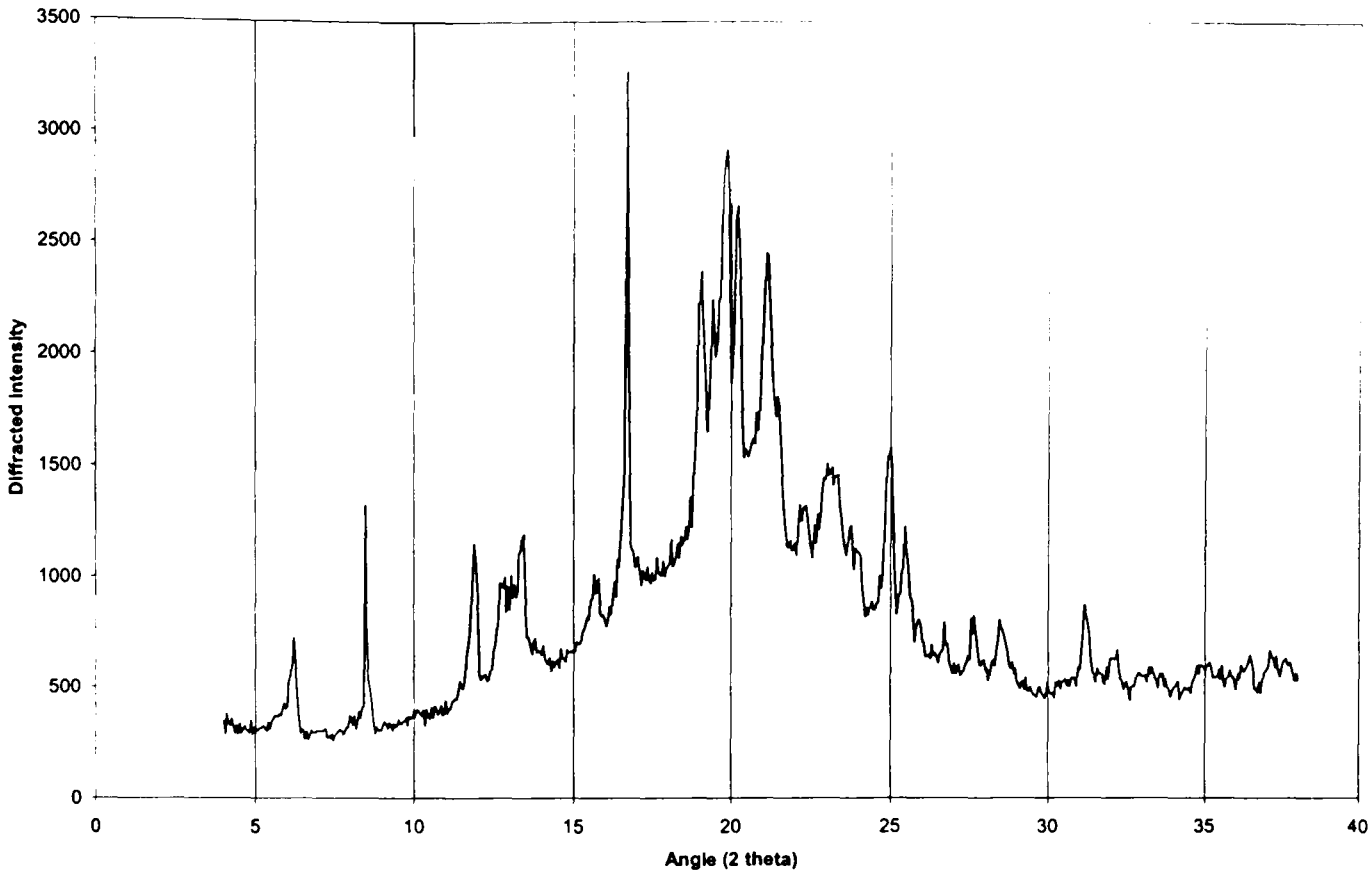

Figure 7-14 X-ray diffraction by conventionally puffed rice. Peaks near 17° and 23° are indicative of native unprocessed starch. Narrow peaks across the spectra are indicative of crystalline sucrose or sodium chloride.

7.3.3.2.2 Effects of Added Moisture

7.3.3.2.2.1 Effect of Added Moisture on SME

Figure 7-15 shows a decrease in calculated SME as the amount of added water is increased. This is a direct result of the plasticisation effect of the water on the starch, reducing the viscosity, therefore reducing the torque. As in Section 7.3.3.2.1.1, the SME calculated from the measured powers and torques coincide, again verifying the suitability of Equation 4-7 and Equation 4-8.

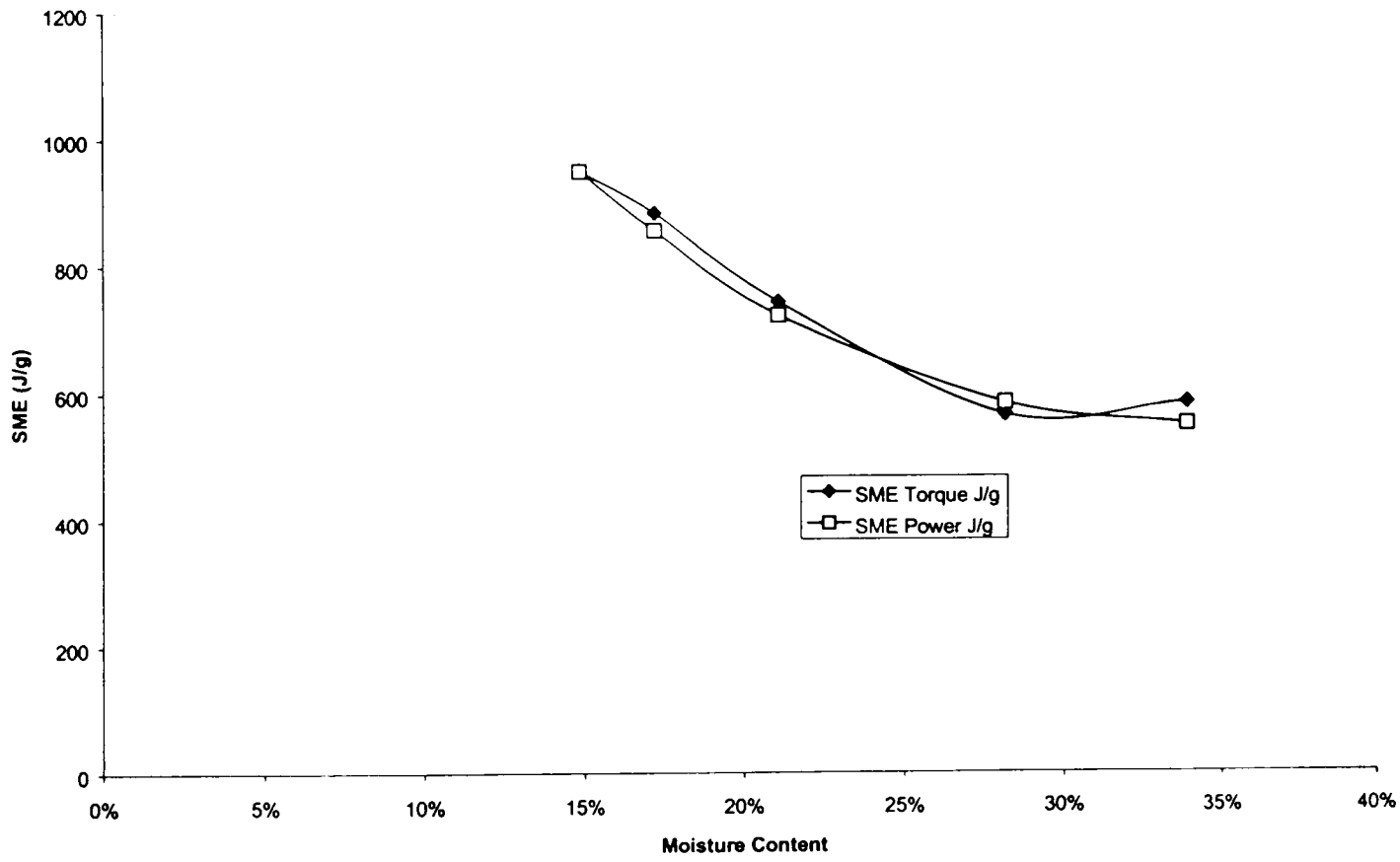

Figure 7-15 Effect of added moisture on SME (moisture content expressed as total feed moisture as a percentage of dry material.) Samples 21-25 from Table 7-2.

It can be seen from Figure 7-16 that increasing water content reduces product diameter. This has been found for maize by a number of workers, Fan et al (1996a), Whalen et al (1997), and has been interpreted as due to enhanced collapse at the higher water contents (lower viscosities) or due to the reduced degree of starch conversion resulting in a lower cell wall stability. There is some evidence that the hydration rate increases with decreasing moisture content (Figure 7-17), whereas the equilibrium moisture content is unaffected.

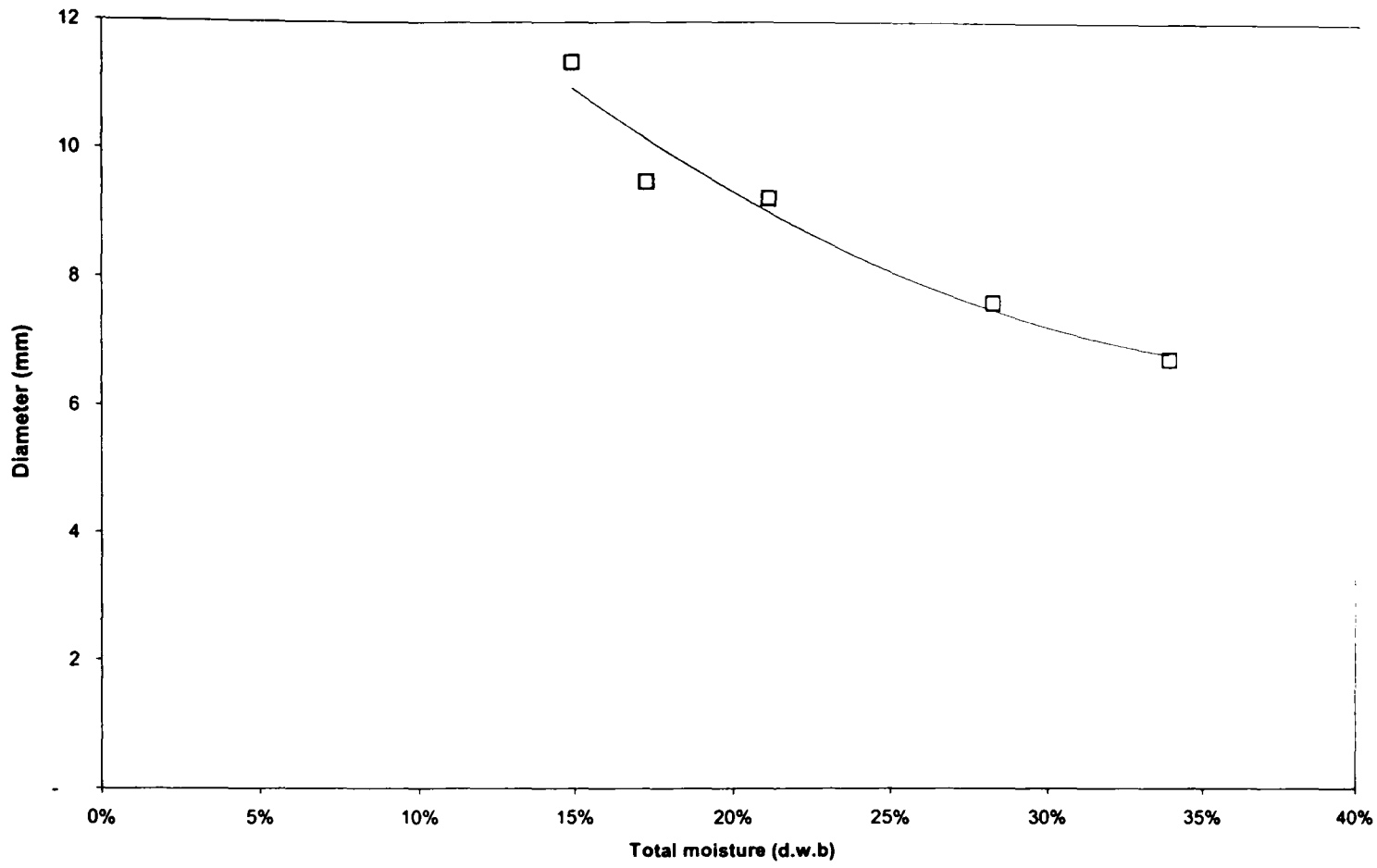

Figure 7-16 Effect of moisture on product diameter (3mm die). Samples 21-25 from Table 7-2.

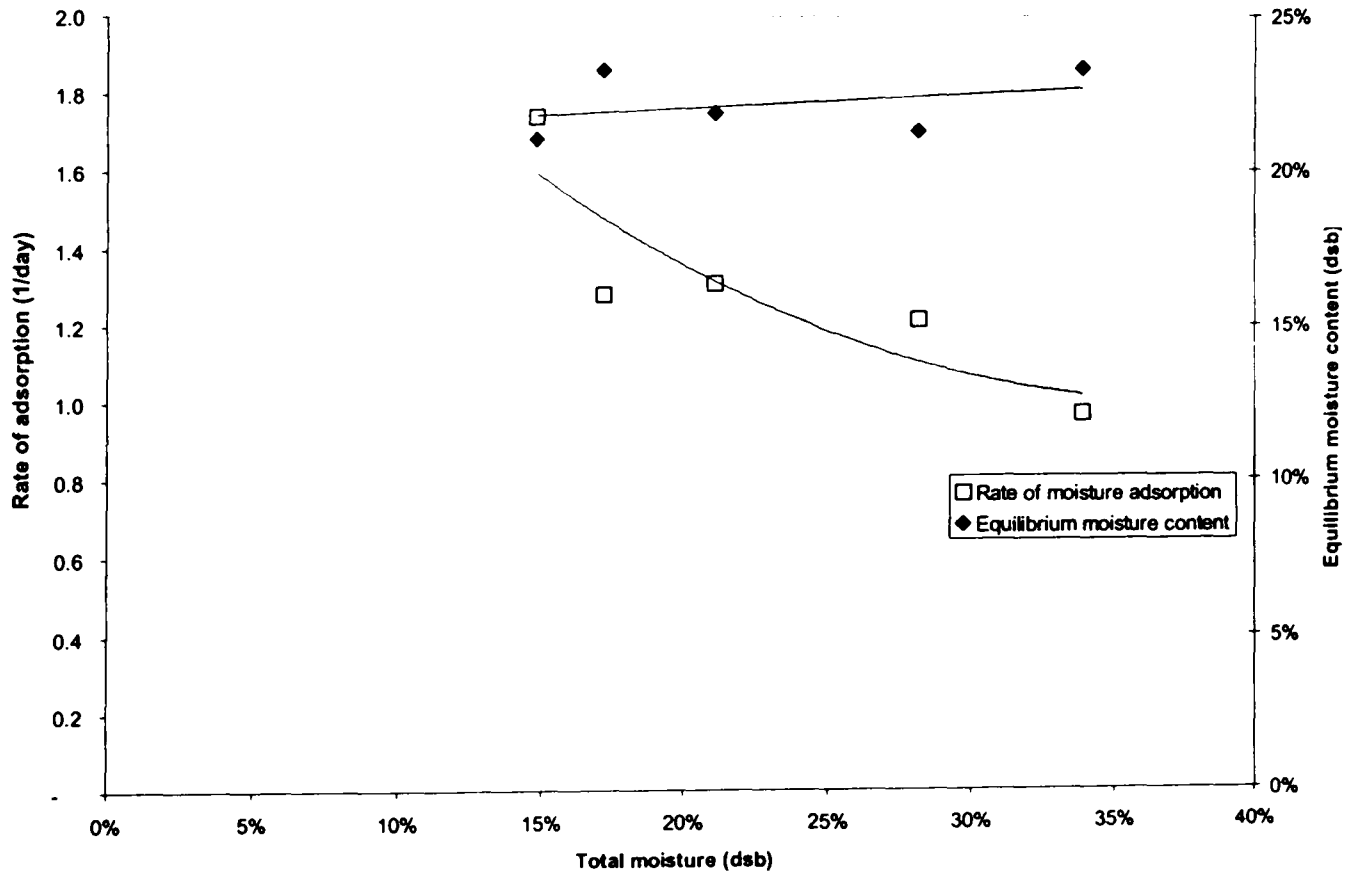

Figure 7-17 Effect of moisture on hydration behaviour. Samples 21-25 from Table 7-2. Comparable values for conventionally puffed rice are a rate of 0.5 day^{-1}, and 42% moisture content.

The extent of starch conversion as monitored by WAI and WSI is shown in Figure 7-18. The increase in WSI as added moisture decreases reflects the increasing starch

conversion. This is a consequence of the increase in SME with decreasing water content (Figure 7-15). The variable moisture content experiments would therefore be consistent with the hypothesis that the hydration rate increases with increasing starch conversion whereas the equilibrium moisture content is independent of the parameter.

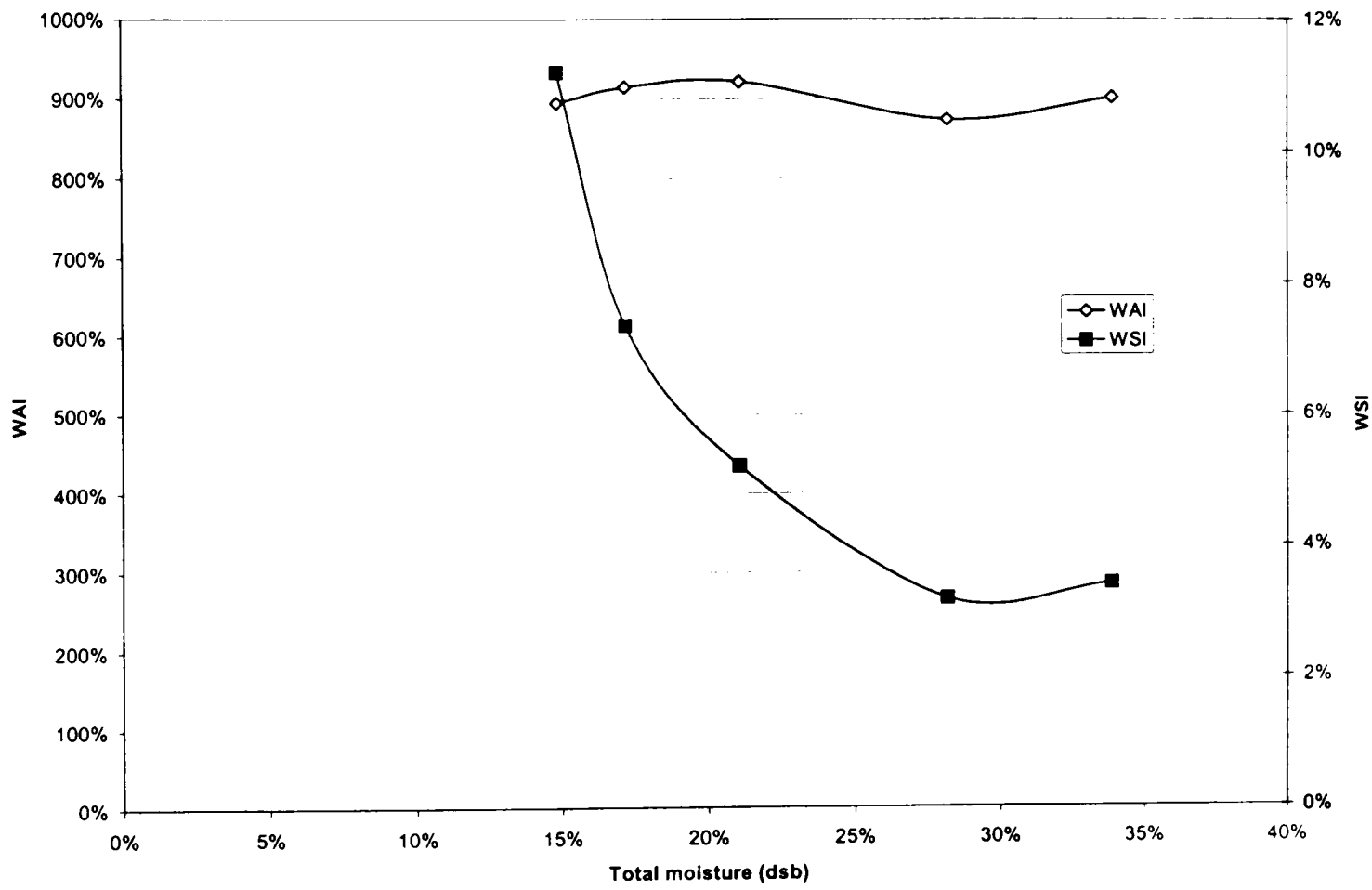

Figure 7-18 Effect of moisture on WAI and WSI. Samples 21-25 from Table 7-2. Comparable conventionally puffed rice data are 920% WAI, and 12.3% WSI.

7.3.3.2.3 Effects of Screw Speed

7.3.3.2.3.1 Effect of screw speed on SME

Figure 7-19 shows the relationship between screw speed and SME. As expected SME increases with increasing screw speed.

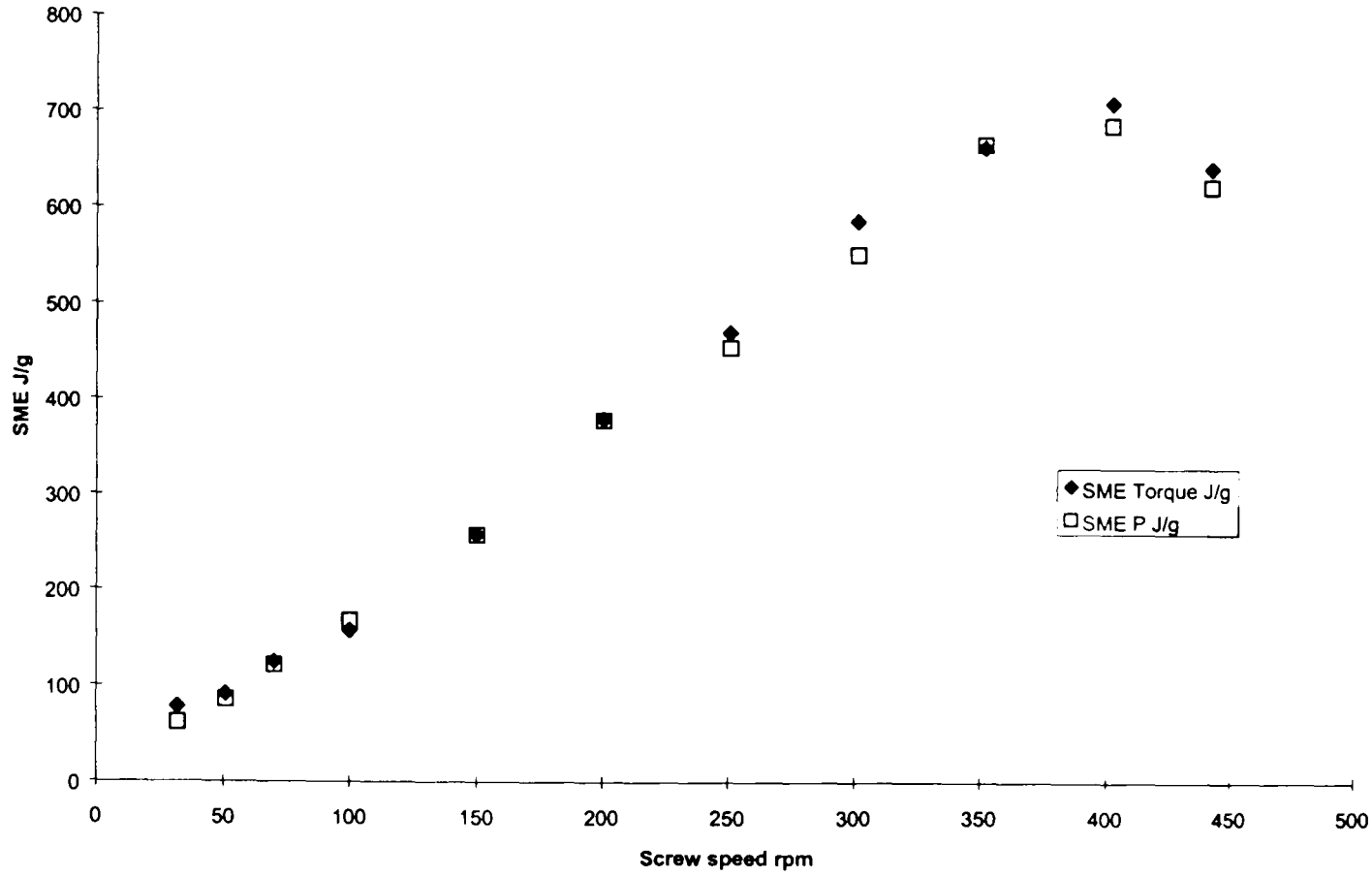

Figure 7-19 Effect of screw speed on SME. Samples 10-20 from Table 7-2.

Product diameter also increases with screw speed (Figure 7-20) which is consistent with more energy being transferred into the extrusion melt. This will enhance both starch conversion, improving cell wall stability and probably also the melt temperature, increasing the driving force (water vapour pressure) for expansion. Evidence for increased starch conversion comes from the WSI data, which show an increase with screw speed (Figure 7-21). The data at 440 rpm are not consistent with this. This may be due to extensive shear thinning or possibly slip. There is an accompanying reduction in SME for the data at 440rpm as well (Figure 7-19).

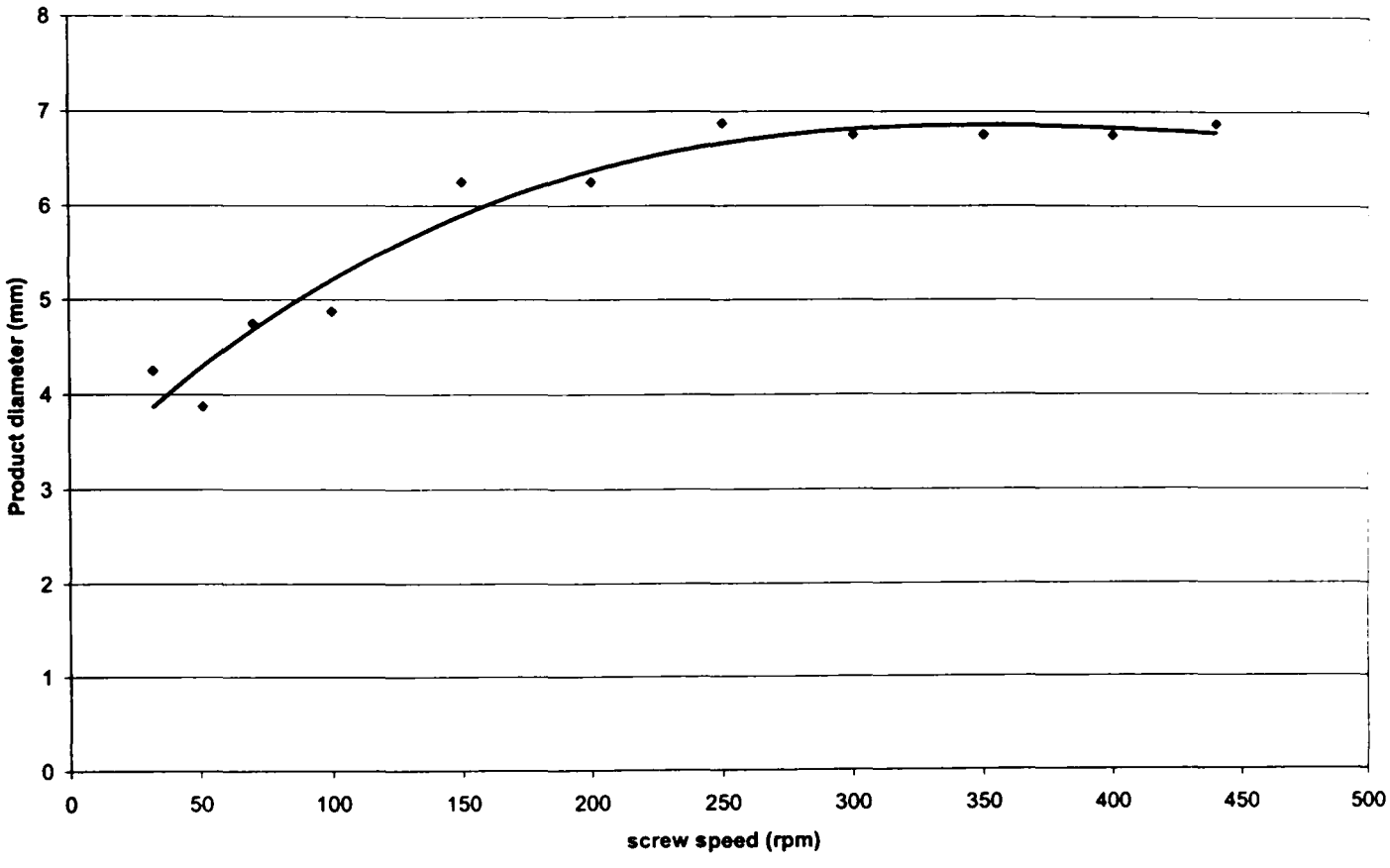

Figure 7-20 Effect of screw speed on product diameter (3mm die). Samples 10-20 from Table 7-2.

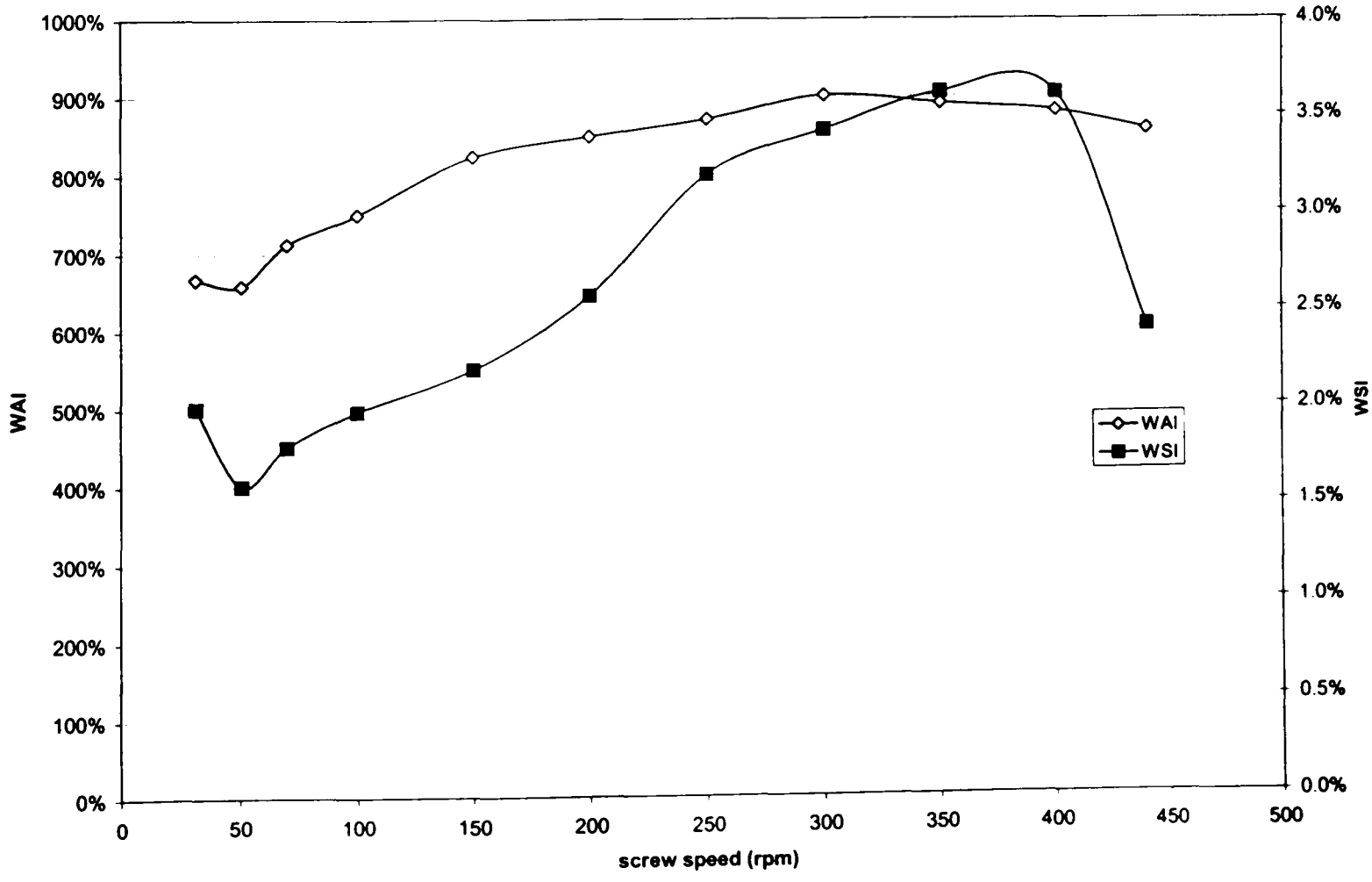

Figure 7-21 Effect of screw speed on WAI and WSI. Samples 10-20 from Table 7-2. Comparable conventionally puffed rice data are 920% WAI, and 12.3% WSI.

The influence of screw speed on hydration is shown in Figure 7-22. There appears to be a correlation between the rate of water adsorption and the WSI (compare Figure 7-21 and Figure 7-22) which is consistent with a relationship between hydration and starch conversion. The increase in equilibrium moisture may be explained by the additional work making more water binding sites available on the starch granules. The moisture absorption will therefore be related to the microstructures in the cell walls of the extrudate.

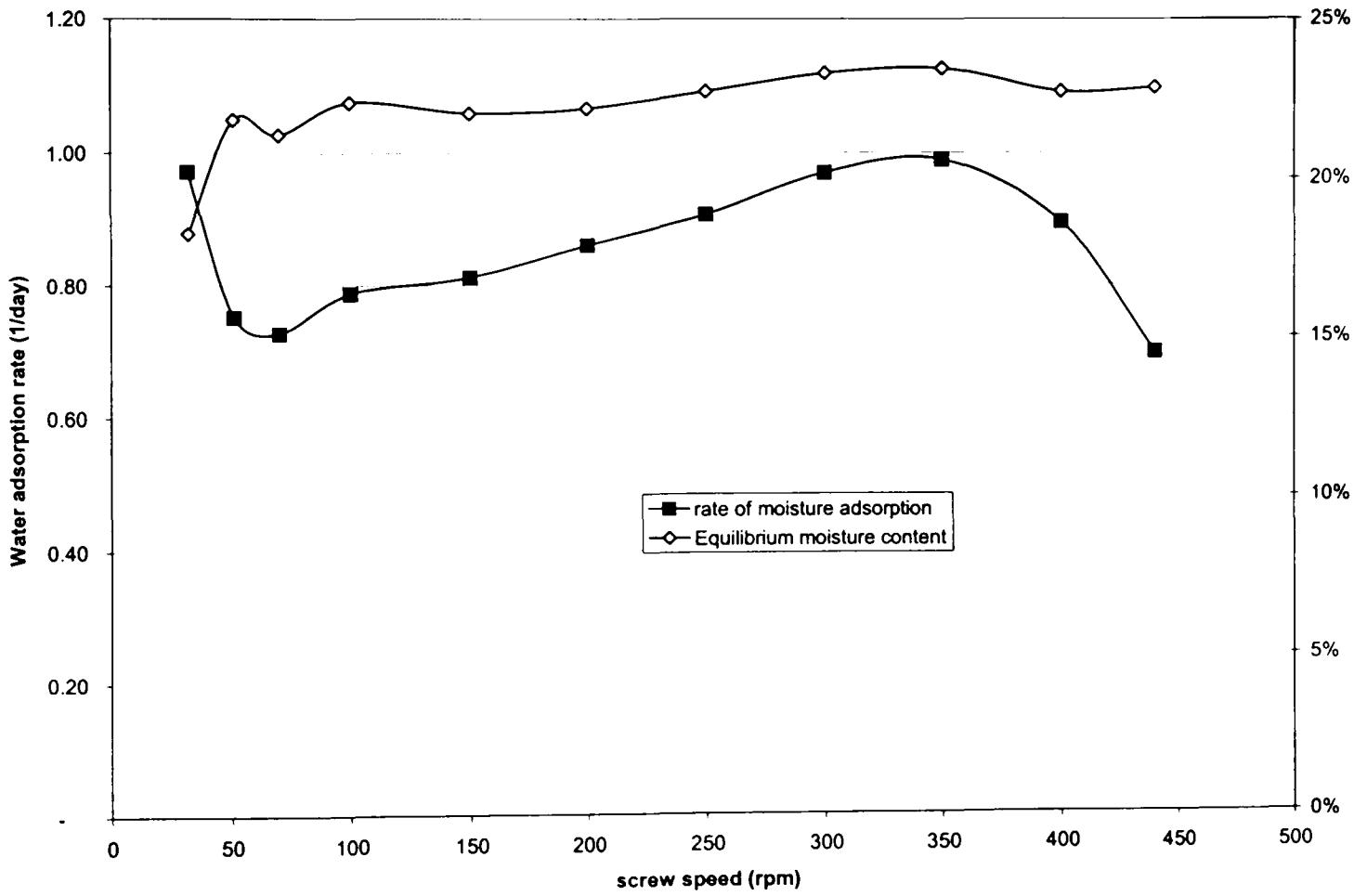

Figure 7-22 Effect of screw speed on hydration behaviour. Samples 10-20 from Table 7-2. Comparable conventionally puffed rice data are a rate of 0.5 day^{-1}, and 42% moisture content.

The X-ray diffraction patterns are independent of screw speed (Figure 7-23). The slight shifts in angle are an artefact of orientation effects within the instrument. In all cases a V-type pattern was found.

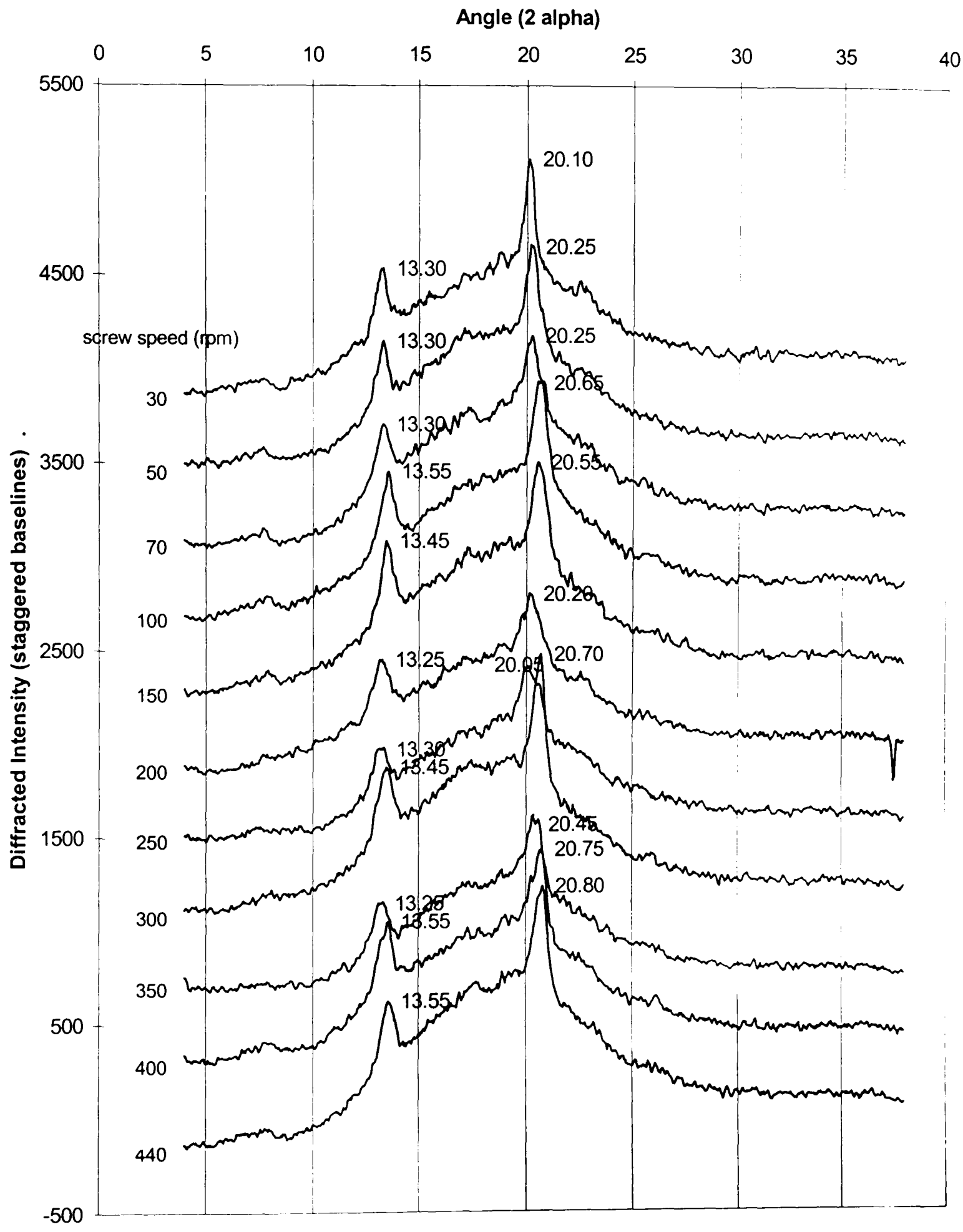

Figure 7-23 Effect of screw speed on X-ray diffractogram. Samples 10-20 from Table 7-2. Comparable data for conventionally puffed rice are presented in Figure 7-14.

7.3.3.2.4 Generalisation of product attributes.

7.3.3.2.4.1 Are WAI and WSI related to moisture adsorption rate or equilibrium moisture content?

It has been postulated that there was a relationship between hydration characteristics of the dried product and the degree of starch conversion. Indeed, results from the previous sections discussing effects varying barrel temperature, moisture content and screw speed independently indicate that such links are likely. Figure 7-24 and Figure 7-25 show the relation between moisture adsorption rate and WAI or WSI when results are compounded from experiments using all extrusion variables. Results are presented for the samples prepared with (Figure 7-25) and without (Figure 7-24) sucrose and sodium bicarbonate. It can be seen that for both sets of samples there is a significant positive correlation between adsorption rate and the water solubility index. For the samples containing sucrose and bicarbonate there is also a positive correlation between WAI and the hydration rate. No such correlation is found for the samples not containing sucrose and sodium bicarbonate. A possible interpretation for this difference in behaviour is that the presence of the plasticisers reduces the SME, moving to a range where WAI increases with increasing degree of starch conversion. At higher SME's, it is suggested that the peak experienced in the WAI - starch conversion relationship prevents correlation with other parameters. It is surprising and interesting to note the WSI in Figure 7-25 is not about 5% greater than that in Figure 7-24 even though 5% extra soluble material (sucrose) is present in the sample.

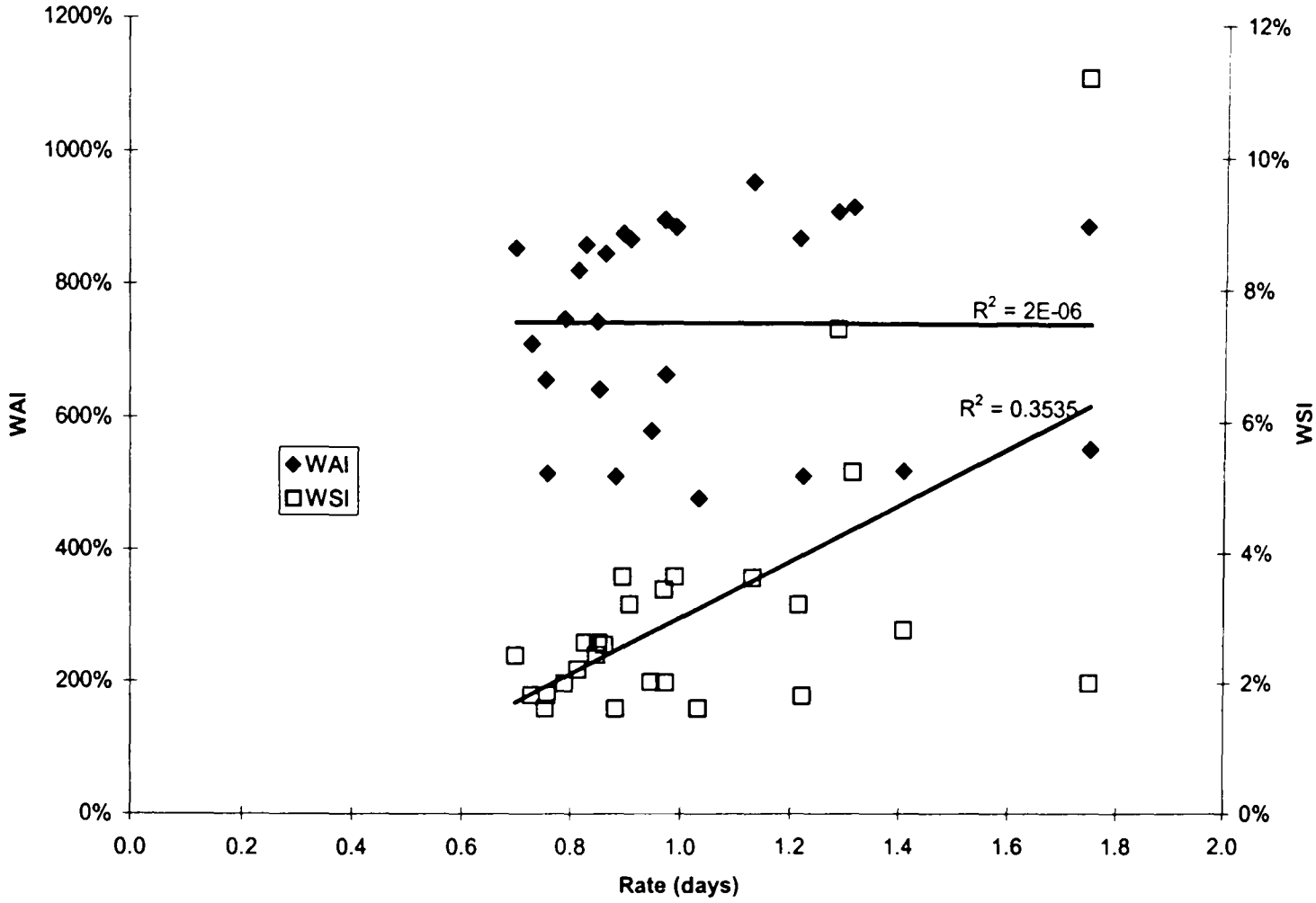

Figure 7-24 Relationship between moisture adsoption rate, WAI, and WSI. Samples 1-25 from Table 7-2. Comparable data for conventionally puffed rice samples are a rate of 0.5 day^{-1}, 920% WAI, and 12.3% WSI.

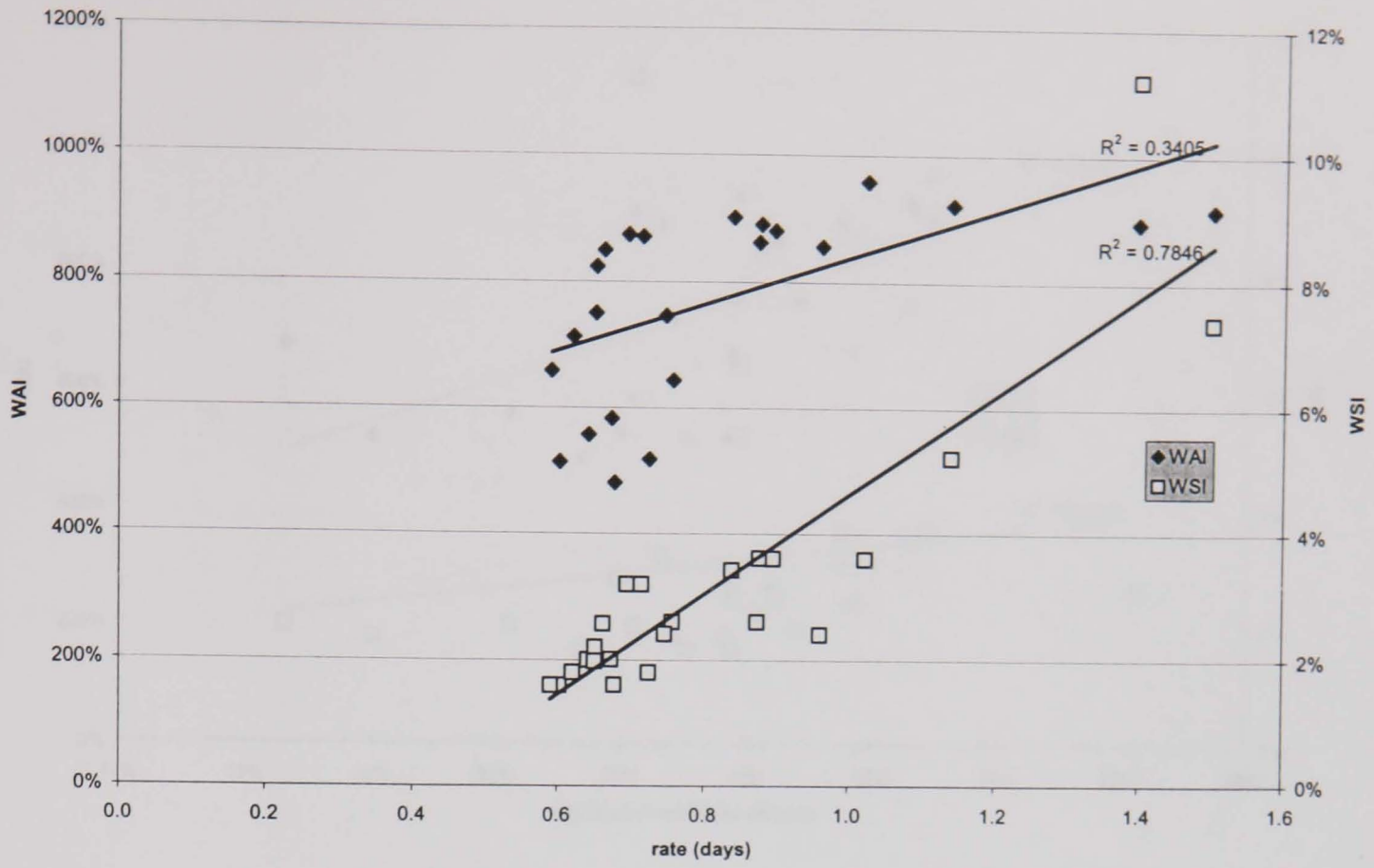

Figure 7-25 Relationship between moisture adsoption rate, WAI, and WSI. Samples 26-49 from Table 7-2. Comparable data for conventionally puffed rice samples are a rate of 0.5 day^{-1}, 920% WAI, and 12.3% WSI.

Similarly to Figure 7-24, Figure 7-26 shows that there is also only a weak correlation between equilibrium moisture content and WAI or WSI when results are compounded from experiments using all extrusion variables. As might be expected intuitively, the WAI shows the stronger correlation with equilibrium moisture content, and the WSI shows the stronger correlation with rate of moisture adsorption. The correlations between the equilibrium moisture content, WSI and WAI are shown in Figure 7-26. As might be expected these are significantly weaker than the correlation with the rate of water adsorption, although a significant positive correlation is found with the WAI for the sample with no sucrose or sodium bicarbonate.

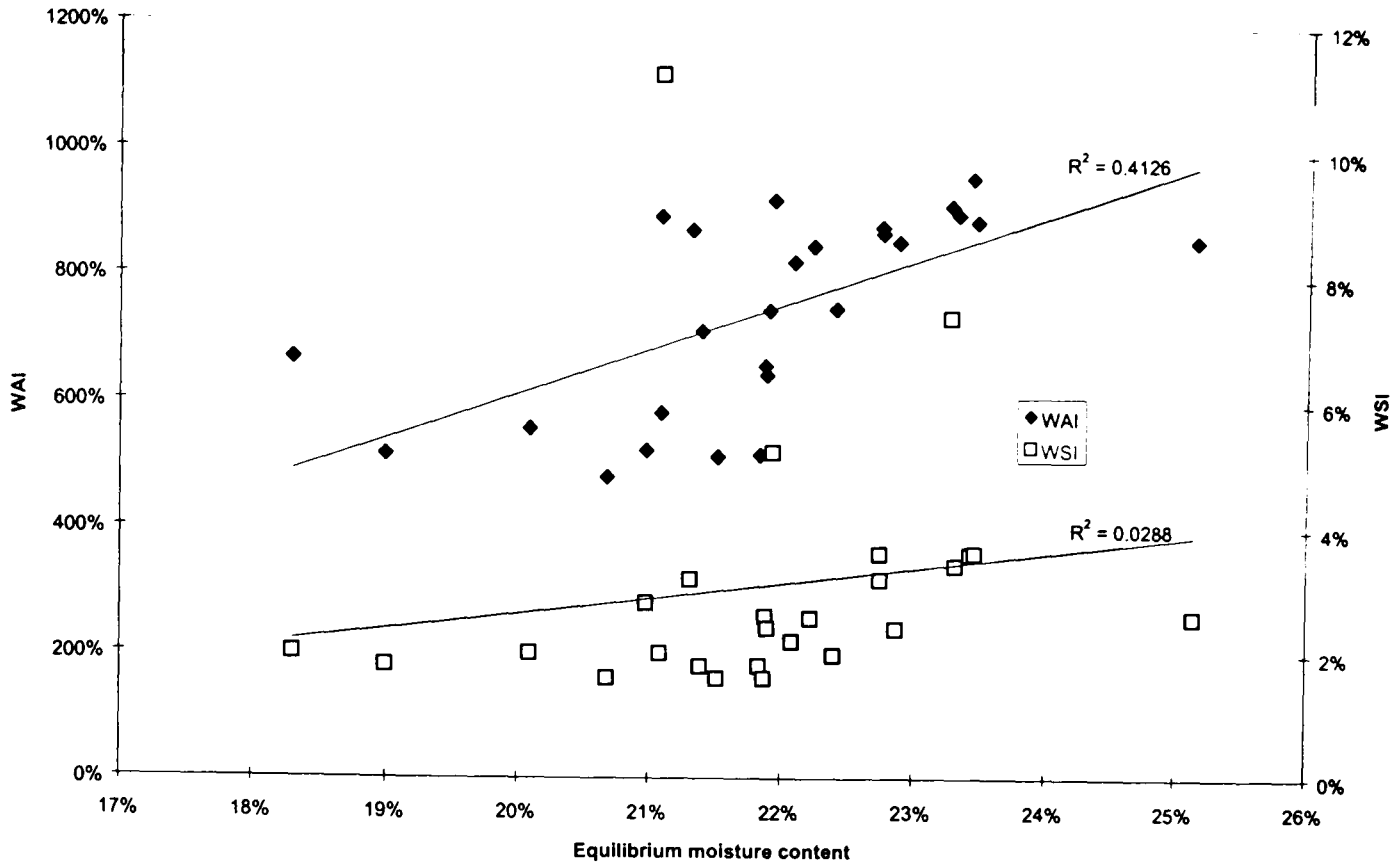

Figure 7-26 WAI, WSI, and equilibrium moisture content. Samples 1-25 from Table 7-2. Comparable data for conventionally puffed rice samples are a moisture content of 42%, WAI of 920%, and WSI of 12.3%.

7.3.3.2.4.2 Can SME be used to generalise product attributes?

Figure 7-27 and Figure 7-28 show the relationship between SME and the starch conversion parameters (WAI and WSI) for both sets of samples (without and with sucrose respectively). The similarity between the two data sets is immediately apparent. As seen over the previous sections (4.6.4.1 - 4.6.4.3), a clear distinction can be made between the trends when changes in SME are a result of barrel temperature changes, of screw speed changes, or of added moisture changes. WAI and WSI cannot be generalised in terms of SME. As the effects of moisture changes and screw speed changes appear to align with one another but not with the effects of temperature, these graphs imply that using SME as a judge of product attributes due to processing are only valid for any given temperature.

Figure 7-29 shows a similar phenomenon with moisture adsorption rate and equilibrium moisture content. Clear trends were visible between these characteristics and parameters when discussed individually in earlier sections, but when superimposed, neither characteristic can be generalised in terms of SME.

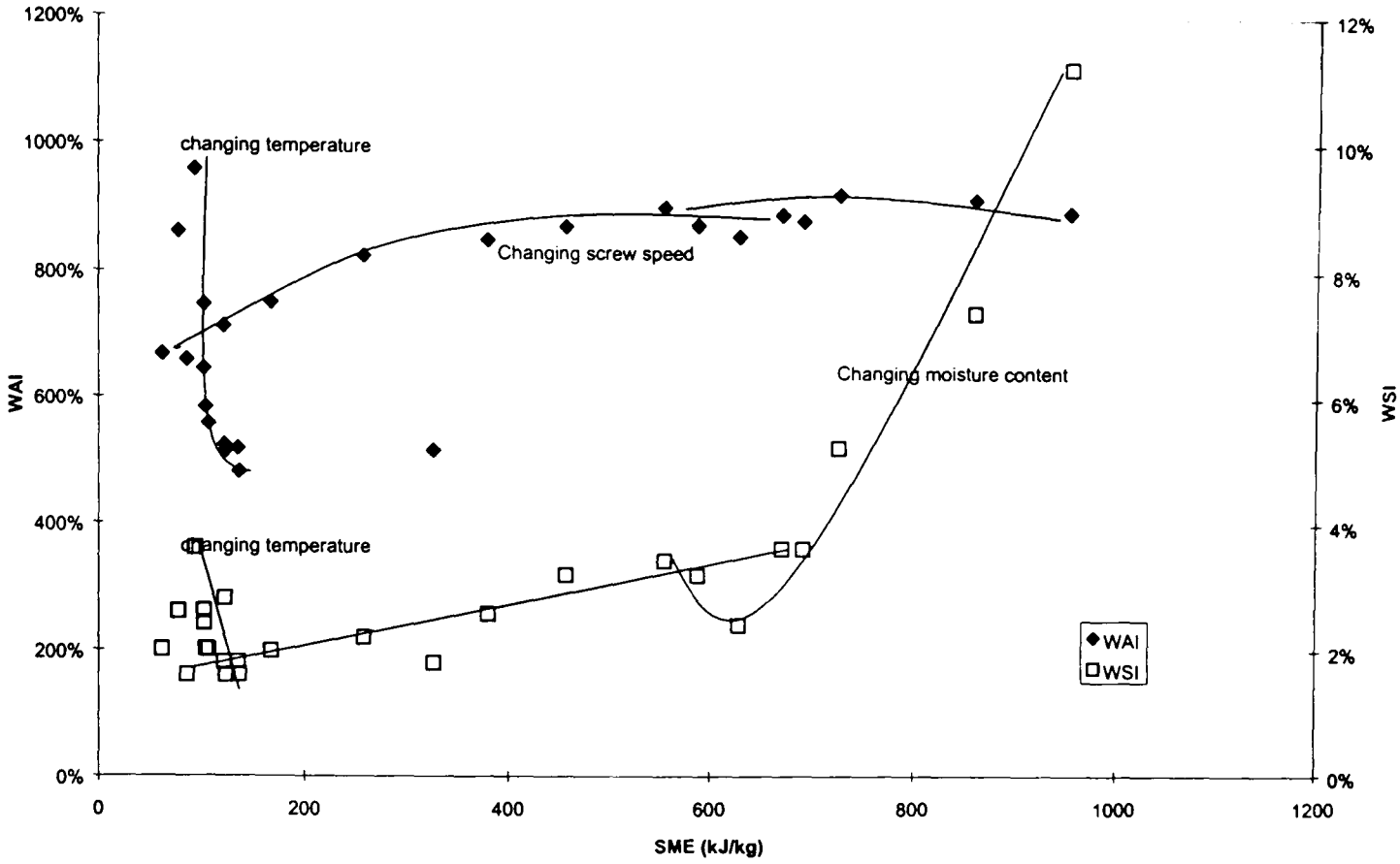

Figure 7-27 WAI, WSI, and SME. Samples 1-25 from Table 7-2. Samples 1-9 vary temperature, samples 10-20 vary screw speed, samples 21-25 vary moisture content.

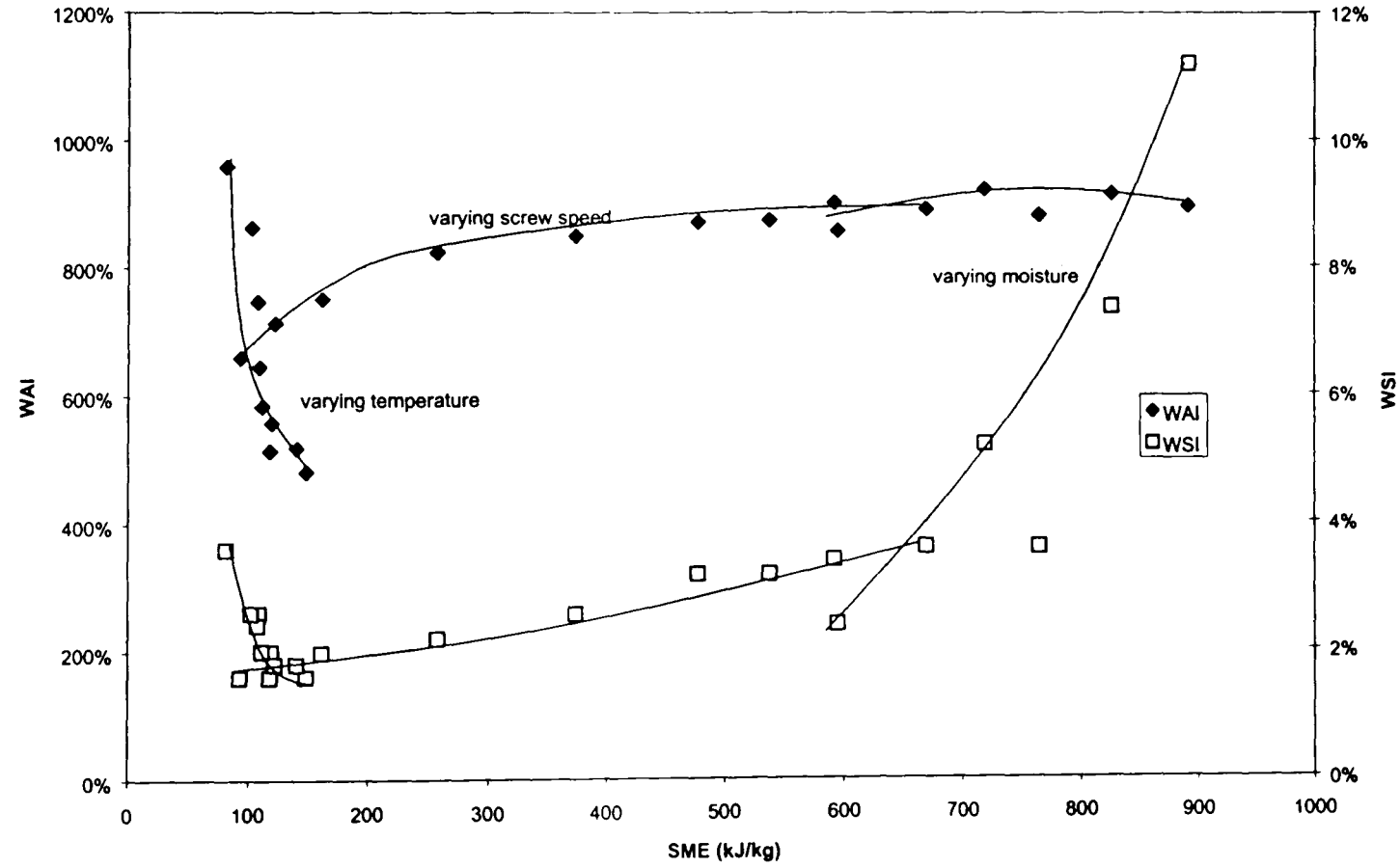

Figure 7-28 The effect of SME on WAI and WSI. Samples 26-49 from Table 7-2. Samples 26-34 vary temperature, samples 35-44 vary screw speed, samples 45-49 vary moisture content.

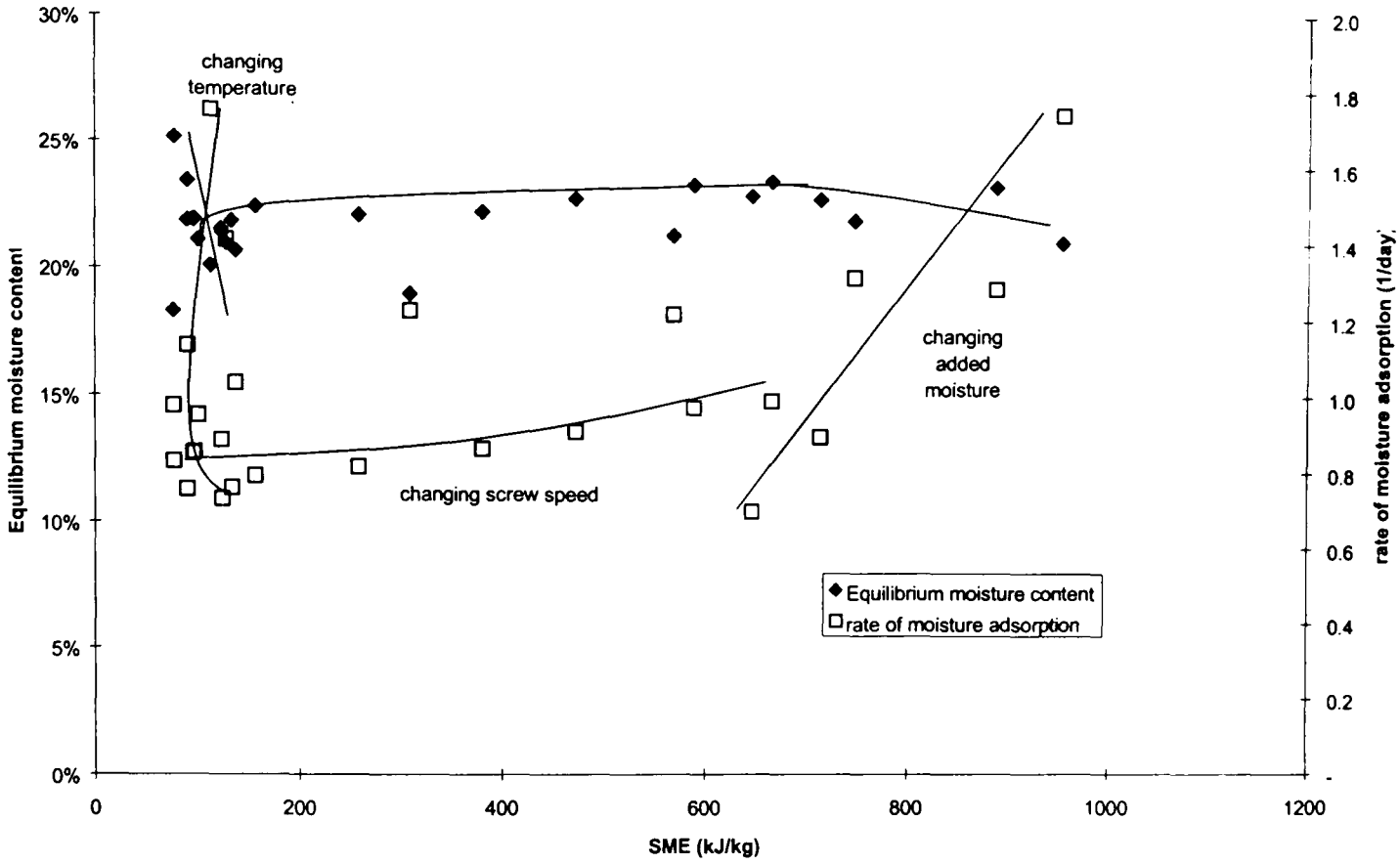

Figure 7-29 The relationship between SME, rate of moisture adsorption, and equilibrium moisture content. Samples 1-25 from Table 7-2. Samples 1-9 vary temperature, samples 10-20 vary screw speed, samples 21-25 vary moisture content. These data correspond to those in Figure 7-27.

7.4 Influence of Ageing and Amylose-Lipid Complexes

7.4.1 Overview

It was hypothesised that samples may hydrate more slowly as they age because of a contraction in structure which is known to occur when glasses are stored below their Tg. For starch, it is possible that this "physical ageing" is associated with the formation of some helical order (Livings *et al.*, 1997). This should however not be confused with retrogradation that cannot occur at these low moisture contents (Farhat et al, 1997). It is possible that this contraction will decrease the diffusability of water. Additionally, it was shown by Mercier *et al.* (1979) that the E-type complex was only metastable, and should the T_g of the sample fall to ambient temperature, then the E-type complex would transcend to a V-type complex, a less energetic state. It then seemed reasonable that E-type and amorphous starches would have a high affinity with water in order to change to the lower energy state accessible on hydration. This high affinity may lead to a fast rate of hydration of the product.

The rate of hydration of samples was monitored with age, as were their X-ray diffraction patterns. Samples were extruded at eleven moisture contents from 13% to 25% to produce extremes of sample properties (extrusion conditions

Figure 7-30). The samples were vacuum-dried (70°C overnight) rather than oven dried before hydration began. Samples were exposed to 100% RH environments for six hours at six different ages. The mass gained by all samples was averaged for each age interval. It was found that samples absorbed water more slowly as they became older (

Figure 7-30).

The X-ray diffraction patterns were analysed to determine total complexing, and to determine the relative amounts of E-type and V-type complexing. Figure 7-31 shows the effect of extrusion moisture content on the relative quantities of V-type complex in the extrudate. The ratio of V-type to E-type complexes clearly increase with

increasing moisture during extrusion, as would be expected due to milder processing and higher molecular mobility (Fan *et al.*, 1996b). However, there is no change in this trend with time. Figure 7-32 shows the relationship between the ratio of V-type to all complexes, and the absolute X-ray counts due to V-type complexes. The straight line fitted through the data and the origin indicates that the total level of complexes was constant, and that this value was independent of the proportions of V-type and E-type complexes that were formed.

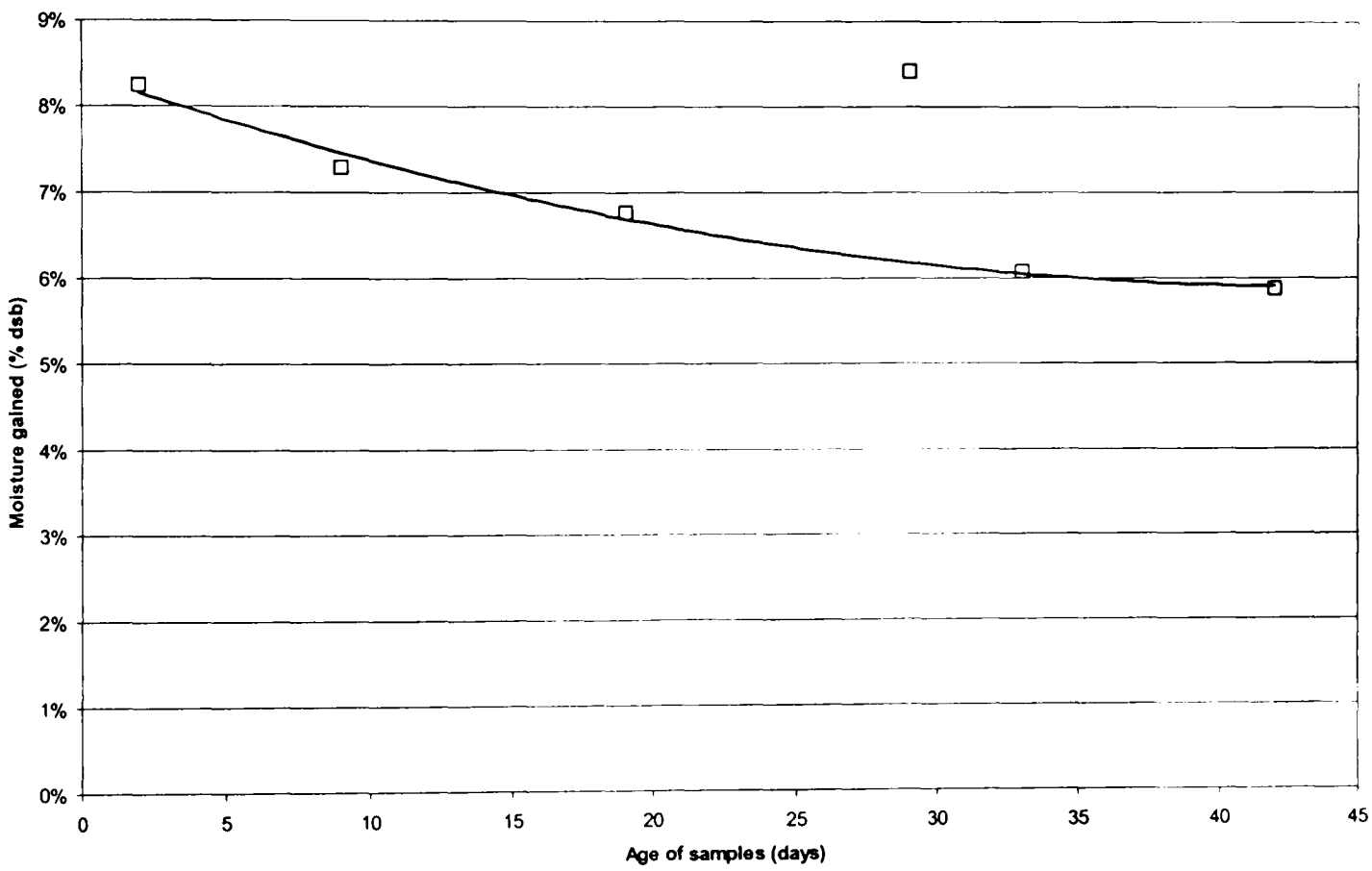

Figure 7-30 The effect of age on the average moisture gained in six hours by a range of 13 samples extruded with moisture contents ranging in twelve equal steps from from 13% to 25%. Extrusion conditions were feedrate 12 kg hr^{-1}, 300 rpm screw speed, barrel heater zones 40°, 110°, 150°, and 160°C. For comparison, conventionally puffed rice would gain about 5.7% moisture.

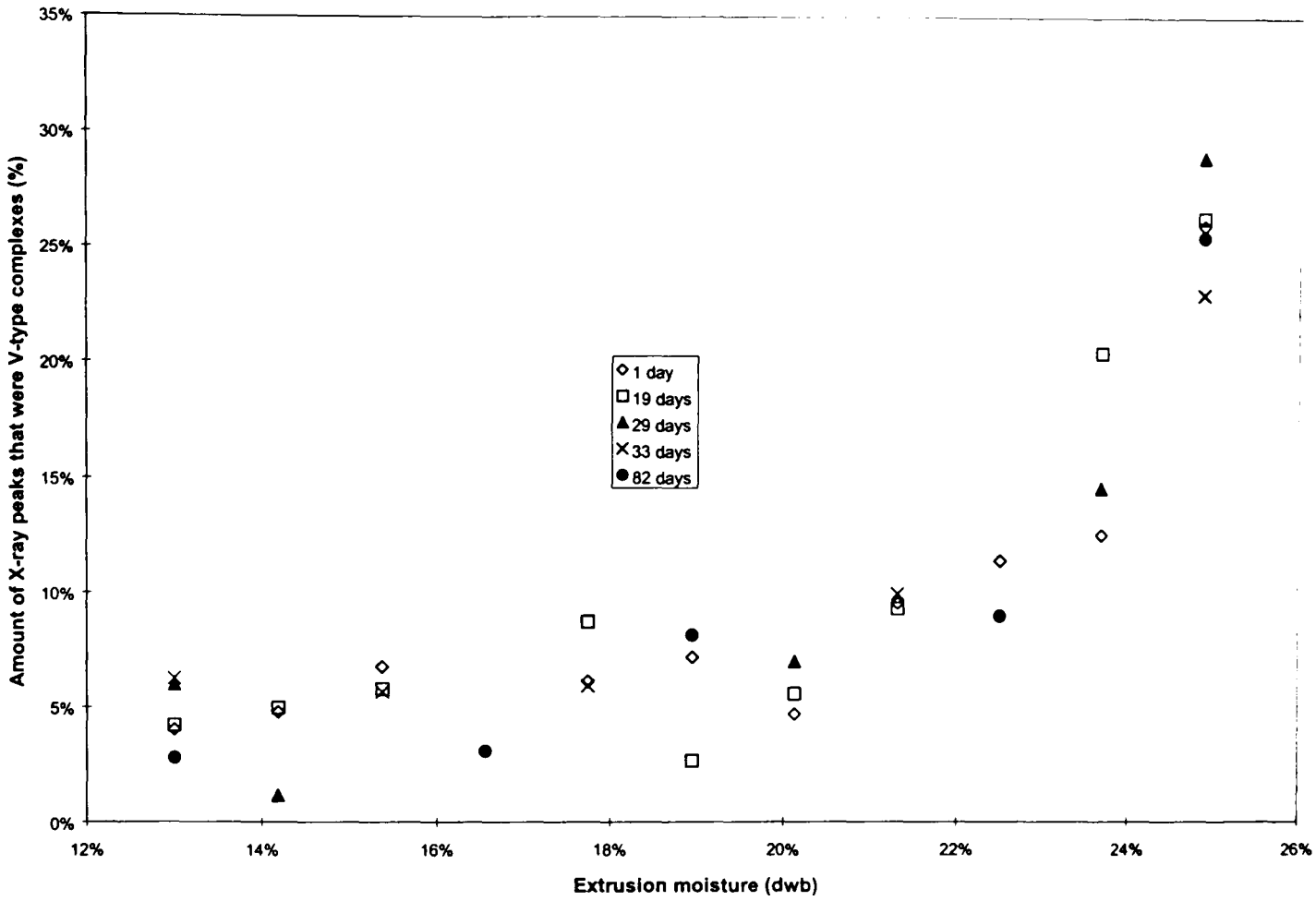

Figure 7-31 Effect of extrusion moisture content and age on the ratio of V-type to E-type complexes. Although increasing moisture clearly increases the relative amounts of V-type complexes, age has little or no effect.

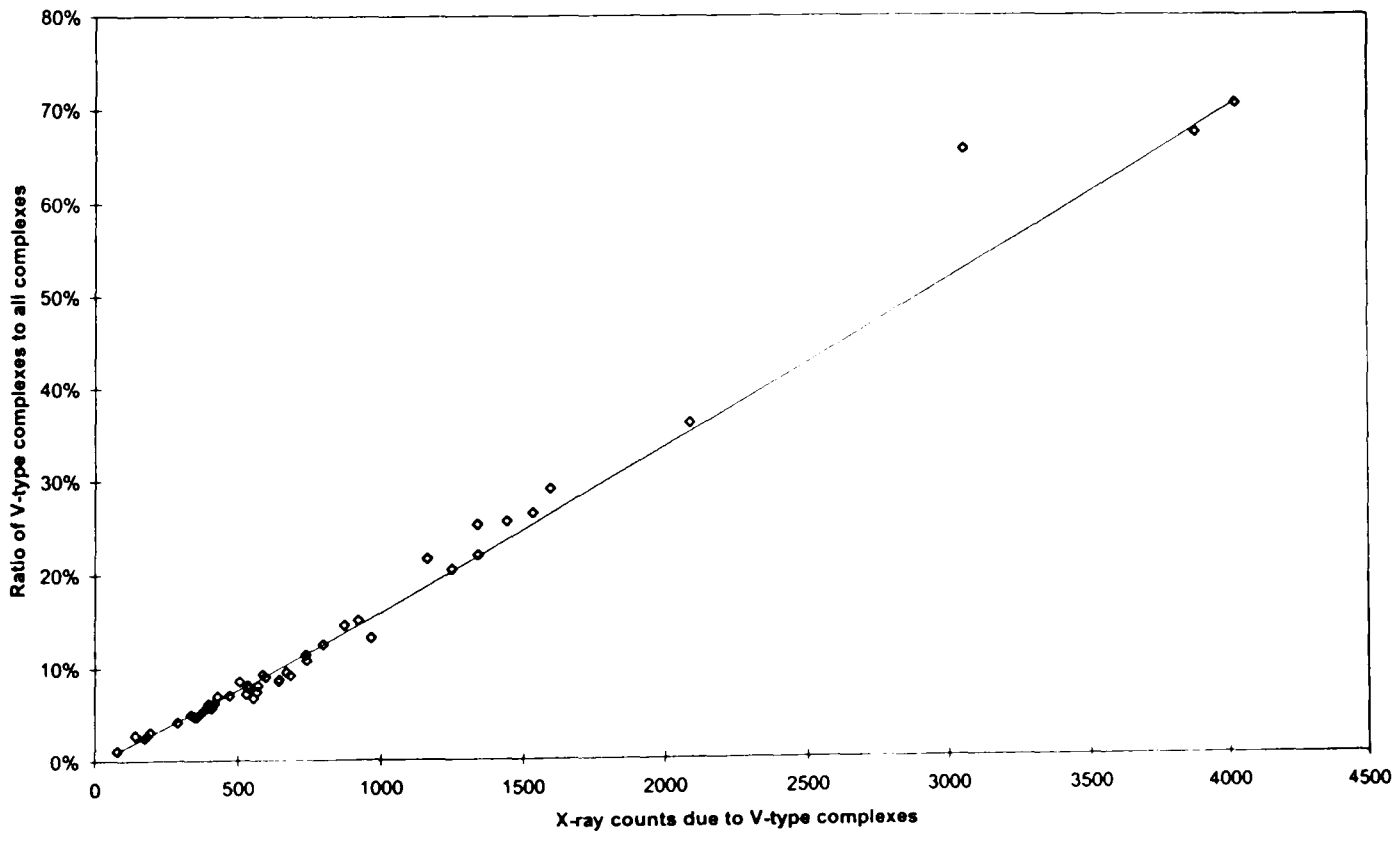

Figure 7-32 Relationship between ratio of V-type to total complexes and the absolute number of V-type complexes. The straight line through the origin indicates the total complexing is constant and independent of the ratio of V-type to E-type complexing.

The samples produced at higher moisture contents had larger proportions of V-type complexes and slower rates of hydration (Figure 7-31 and Figure 7-17). Although there appears to be a connection between the type of crystallinity in the starch and the rate of water vapour adsorption, the link is not exclusive as other variables were also present. Complexes or types of crystallinity and hydration behaviour of samples are both effects of processing conditions, and are not causal of or to one-another.

Further, while the rate of adsorption decreased with time, the type and extent of crystallinity remained unaltered. The proposal was that the ratio of $\frac{E}{E+V}$ would decrease with time at a similar rate to the decrease of water absorption rates with time. This did not occur.

7.5 Microscopy

7.5.1 Overview

During the project, samples were examined using an optical microscope. Results for samples with and without sucrose were similar. As described previously (Section 4.6.4.3) extruded samples usually showed no birefringence, or evidence of starch granules. On the occasions when evidence of starch granules in the form of birefringent patches or even Maltese Crosses (Figure 4-10) was present in samples, those samples were made at the cooler and less severely processed limit of any range, where the severity was reduced either by reducing the screw speed from 300 rpm to as low as 30 rpm, or by increasing the added water during extrusion, from none to as high as 20%. These samples were chewy due to the high percentage of water and were only slightly expanded. As such they were not desirable products.

Conventionally puffed rice samples however, show the bulk of the structure to be a homogeneously refracting mass, again showing no evidence of complete or gelatinised granules (Figure 7-33). This difference was noted and thought to be due to an inherent difference between the two processing methods, and therefore unavoidable.

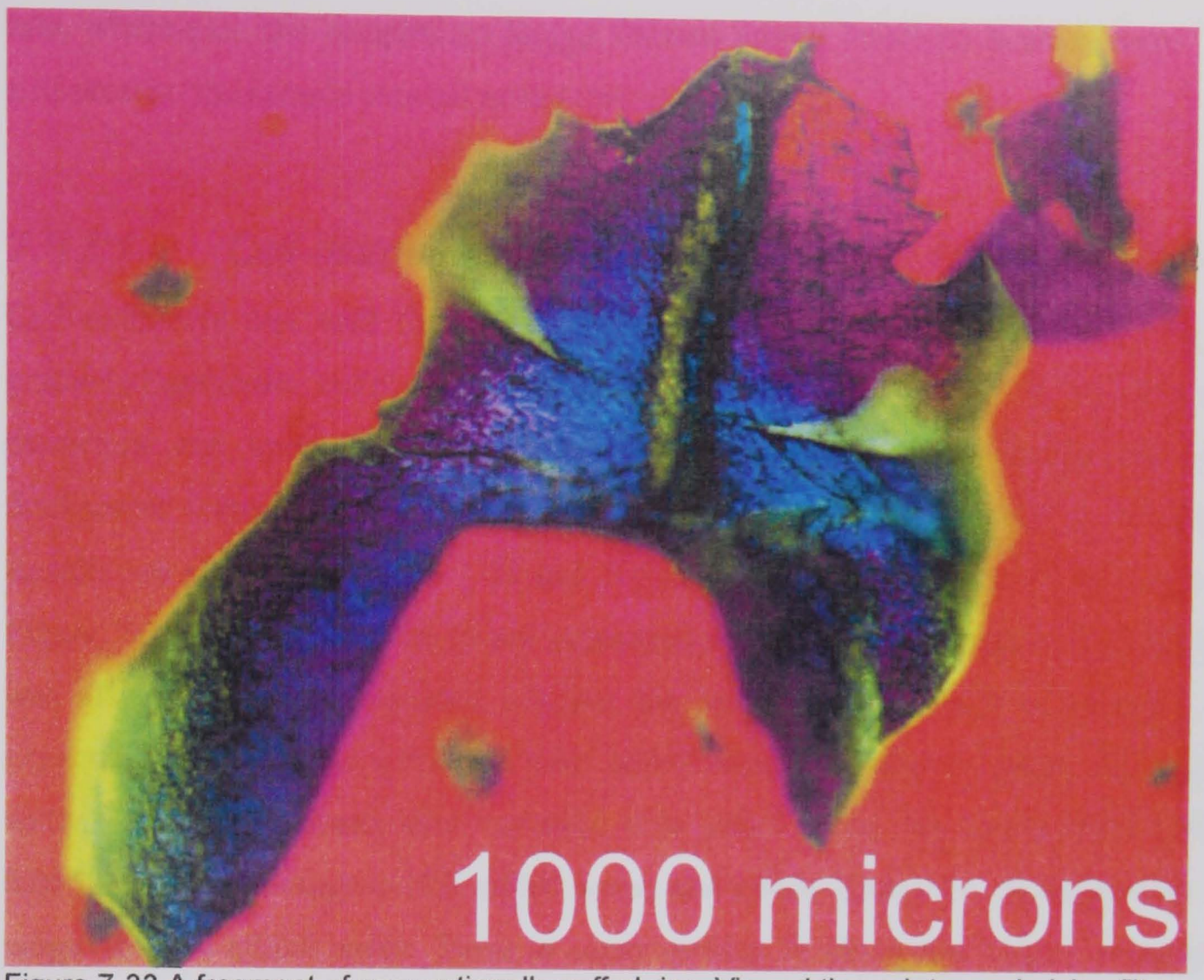

Figure 7-33 A fragment of conventionally puffed rice. Viewed through two polarising filters and a quarter wave plate.

The reason the difference was thought unavoidable was as the SME imparted to the extruded samples was reduced, the occurrence of Maltese Crosses increased. As the conventionally puffed rice samples contain no birefringent patches or Maltese Crosses, this reduction in SME was thought to be undesirable. Additionally, the conventionally puffed rice samples appeared to have large-scale crystalline order, as fragments of sample refracted light smoothly. To obtain this order, starch must have leached from the granules and recombined. This is certainly not possible in samples where granular order remained. As SME used to produce the extruded samples was further reduced fewer samples gelatinised, and the chance of creating a homogeneous birefringent mass was assumed to decrease.

In order to calibrate the texture measuring method, samples were made with wildly varied amounts of added water during extrusion, ranging from 0 to 23% of the feed

rate, whereupon the samples no longer foamed (some localised bubbles were still present, the sample was not completely continuous).

7.5.1.1 Cell diameter, cell wall thickness and foam/sponginess

Cell diameters and wall thicknesses were estimated by comparing the sample to graduated graticules under a microscope. Standard errors calculated for the measured diameters are understandably large. Estimated errors in measuring the wall thicknesses were considered to be larger than the actual fluctuations in thickness. Results are plotted on Figure 7-36 and Figure 7-37. Example samples are shown in Figure 7-34 and Figure 7-35 to aid visualisation. From microscopic examination, it was also possible to determine whether the samples were foams or sponges. As expected, cell diameter increased with added water, peaking at about 18% added water. Cell wall thickness also increased with added water, but slowly from 0.008 - 0.015mm over the range 0-12% added water, and slowly from 0.11 - 0.33mm over the range 10-23% added water. There is some overlap in those two ranges as samples with 10-12% added water showed both thick and thin cell walls. There is a rapid decrease in sample diameter above 12% added water. Samples with 0% water formed a sponge structure (both air and starch phases continuous). Samples with 1% water formed a foam (Figure 7-36), but most cell walls were ruptured, creating a sponge. All other samples formed closed cells (foams at low water additions, or masses of starch with localised expansion at high water additions).

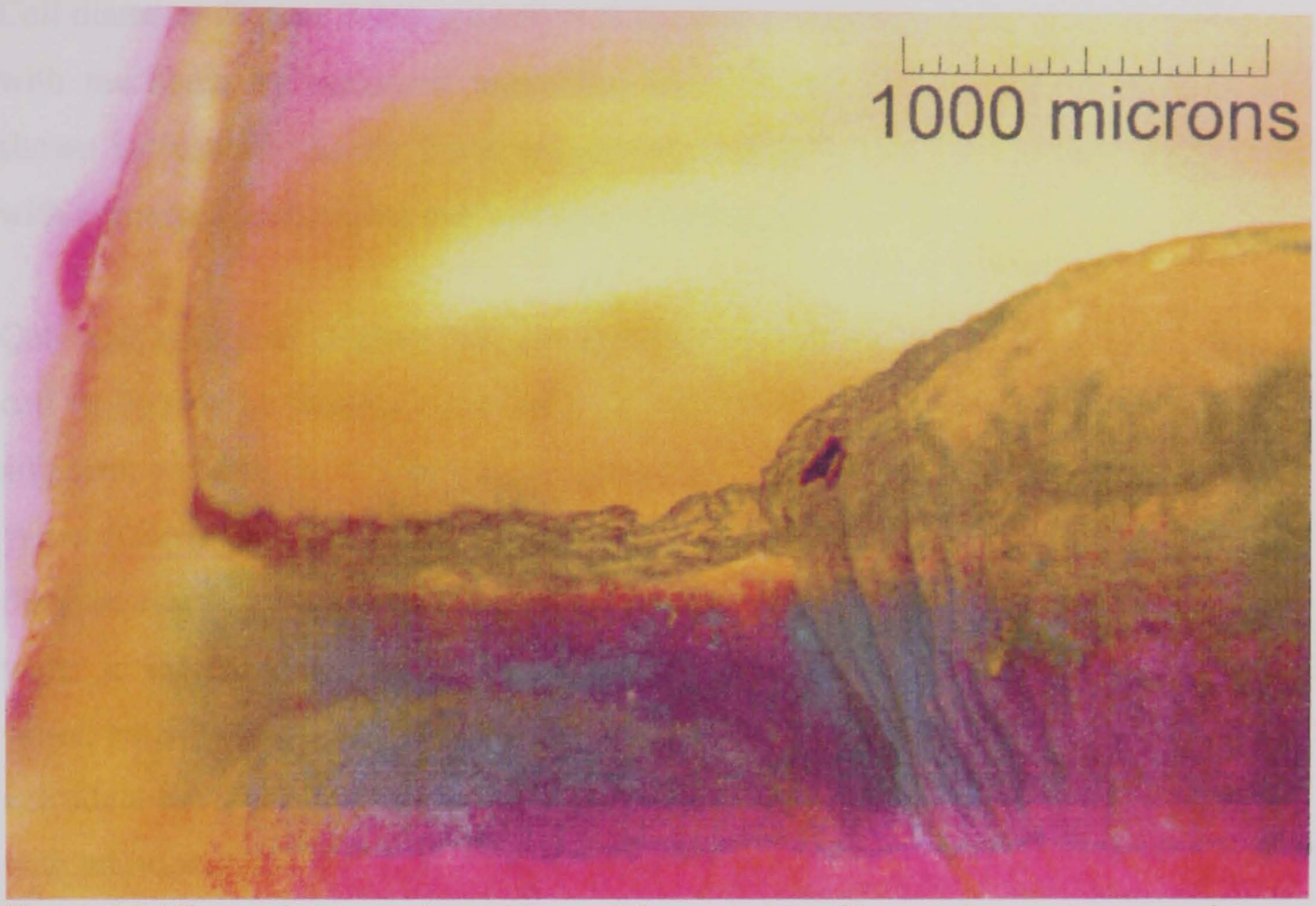

Figure 7-34 Foam structure. Viewed through two polarising filters and a quarter wave plate.

Figure 7-35 Sponge structure. Viewed through two polarising filters and a quarter wave plate.

Cell diameter (Figure 7-36) and cell wall thickness (Figure 7-37) correlated well with mechanically measured maximum force during compressive shear. This was shown incidentally during the development of texture measurement to correlate well with perceived rubberiness and hardness (Chapter 6).

Cell wall thickness (Figure 7-37) is recorded as thick and thin cell walls. The thick cell walls may be thought of as the inter-cell distance in samples where cells are not adjacent, whereas the thin cell walls are dividers between adjacent cells (Figure 7-38). When little moisture is added, expansion is prolific, there is no measurable inter-cell distance (thick walls), and cell dividers (thin walls) are at their narrowest. As added water is increased to about 12%, cell dividers become wider. Beyond 12% added water, cells do not appear in adjacent positions. Inter-cellular regions of unexpanded extrudate become apparent when 9% or more water is added. These regions widen with additional water.

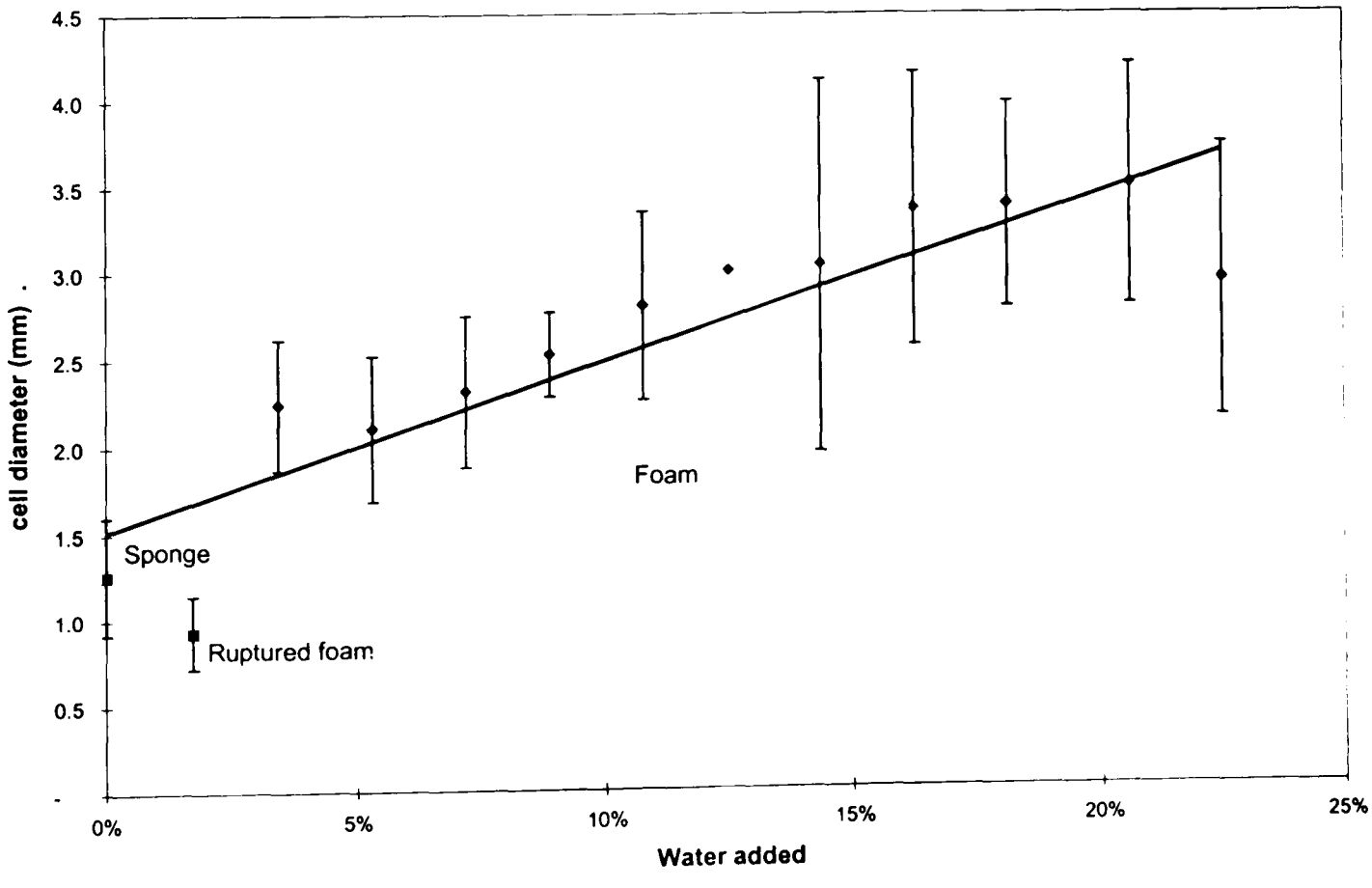

Figure 7-36 Graph of cell size with varying extrusion moisture. Bars are standard errors.

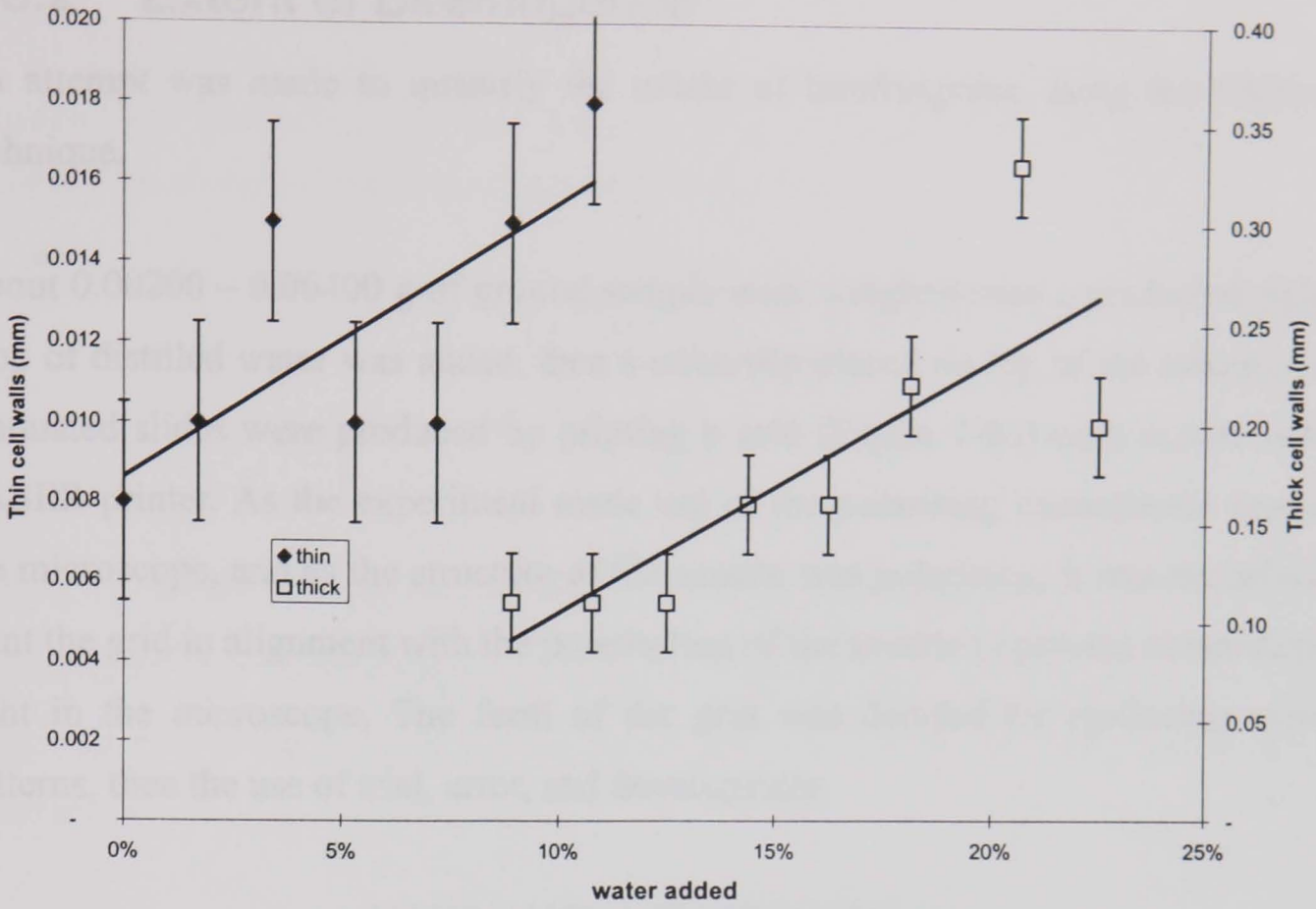

Figure 7-37 Graph of cell wall thickness. Extrusion conditions as for Figure 7-36. Bars are estimated error in measurements, as these errors were larger than the fluctuations in wall thickness.

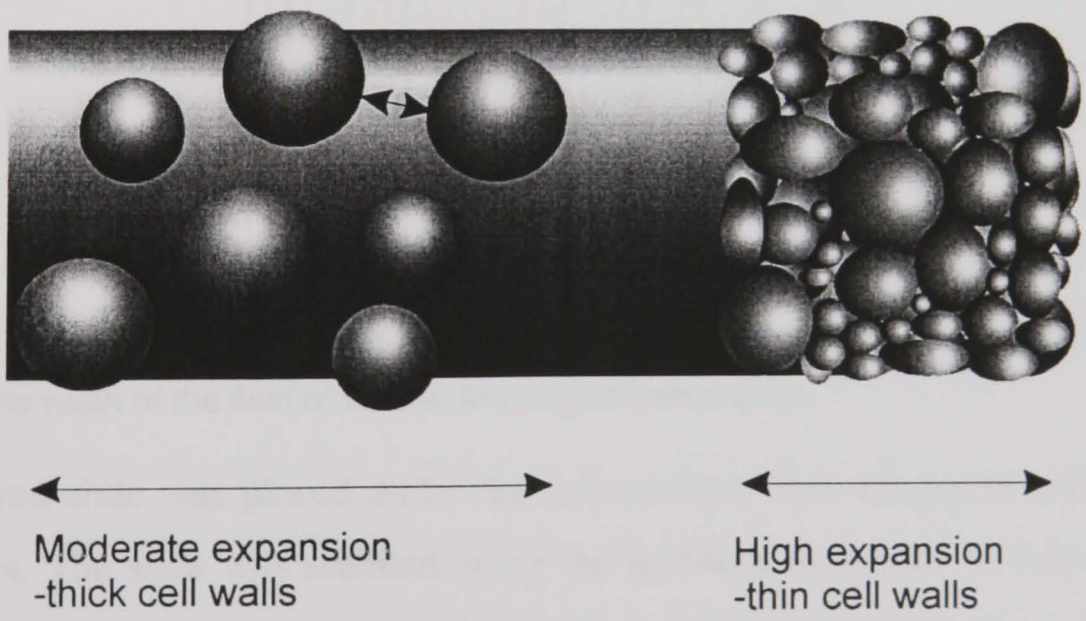

Figure 7-38 Thick and thin cell walls

7.5.2 Extent of Birefringence

An attempt was made to quantify the extent of birefringence using the following technique.

About 0.00200 – 0.00400 g of ground sample were weighed onto a graduated slide, a drop of distilled water was added, then a coverslip placed on top of the mixture. The graduated slides were produced by printing a grid (Figure 7-39) onto acetate with a LASER printer. As the experiment made use of the polarising transmission mode of the microscope, and as the structure of the acetate was polarising, it was necessary to print the grid in alignment with the polarisation of the acetate to prevent attenuation of light in the microscope. The form of the grid was decided by producing various patterns, then the use of trial, error, and development.

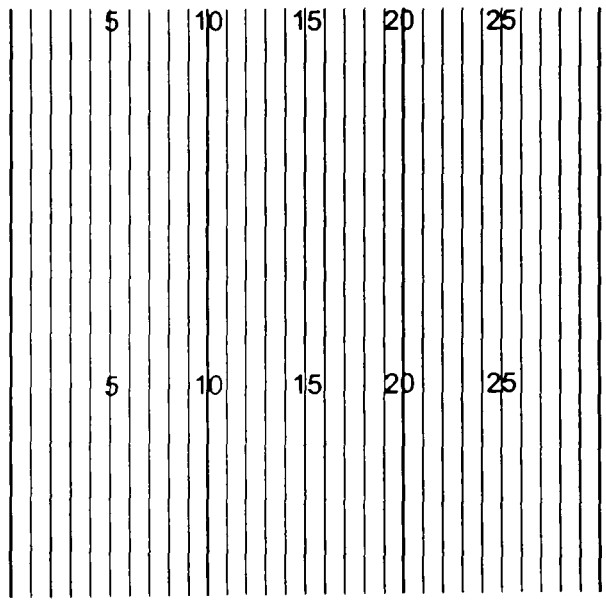

Figure 7-39 The grid used to graduate the slides (not actual size). Each interval was 0.75mm, about half the width of the field of view at the magnification used.

The prepared slide was placed under the microscope, then examined using crossed polar filters. The slide was scanned using the gridlines as guides to help ensure all Maltese Crosses were counted, and that each cross was counted only once. As the gridlines were only used as guides, their exact form was not critical. Trial and error revealed parallel lines with a spacing of about 0.75mm, half the field of view at the magnification used, were easiest to work with. The concentration of residual Maltese Crosses in the sample and the associated errors were calculated by

$$C_x = \frac{counted_x}{mass_{sample}}$$

Equation 7-2 Converting Maltese Crosses counted under the microscope into the concentration of residual Maltese crosses in the sample.

$$\overline{C_x} = \sqrt{\frac{counted_x}{mass_{sample}}}$$

Equation 7-3 Calculating the error in calculating the number of Maltese Crosses residual in the sample.

Where C_x is the number of Maltese Crosses in one gram of sample; $\overline{C_x}$ is the estimated error in calculating C_x; $counted_x$ is the number of Maltese Crosses counted under the microscope, and $mass_{sample}$ is the mass of the sample examined under the microscope.

After all crosses had been counted, the quarter wavelength filter was used in addition to the crossed polarisers to show polarising fragments residual in the sample. Typically, these fragments were a green colour in contrast to the ambient pink seen when using the quarter wave filter and polarisers. The polarising fragments were thought to be partly gelatinised granules as no other polarising fragments (e.g. husk, cellular tissue) were evident in the unprocessed flour. The slide was scanned again to count the fragments, which were converted to a concentration in a similar manner to Equation 7-2.

Figure 7-40 shows the number of residual starch granules per gram of extrudate, as determined by counting Maltese Crosses. The expected trend was for the number of Maltese Crosses to fall off with increasing SME (in the case of Figure 7-40, this is represented by screw speed). Unexpectedly, it was found the number of Maltese Crosses was substantially lowered around a screw of 50 rpm. Because of the wholly unexpected nature of this result, the range of samples was reproduced by extrusion, again showing reduced crosses around 50 rpm. Sampling at 50 rpm to count residual crosses was repeated in triplicate, and with larger samples than for other points. It was

this additional sampling, coupled with the low count, that led to low error bars for the number of crosses at 50 rpm. The errors were assumed to be plus or minus the square root of the number of crosses before normalisation to 1 gram.

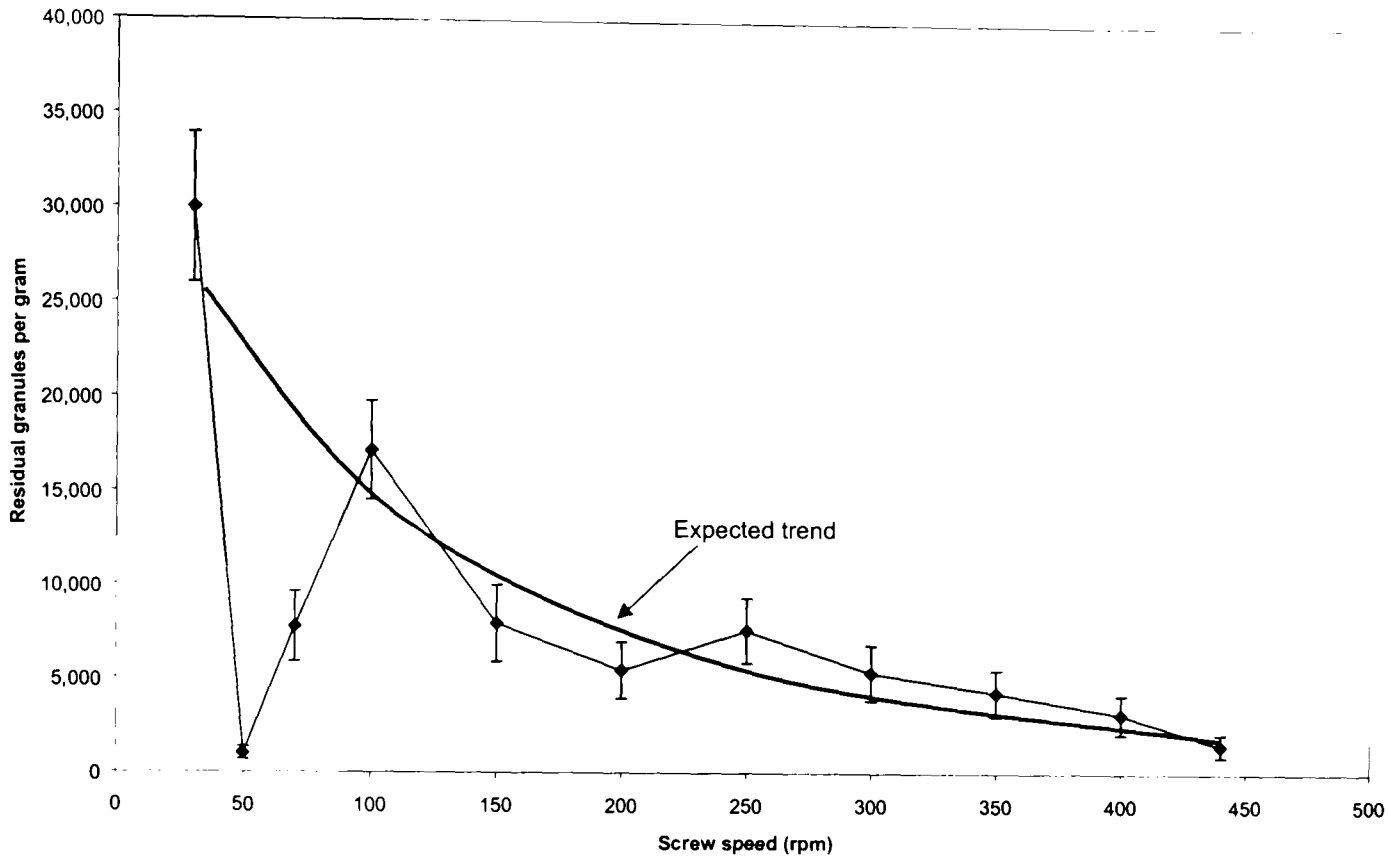

Figure 7-40 Residual Maltese Crosses. Samples 10-20 from Table 7-2. Conventionally puffed rice samples show no visible Maltese Crosses.

A reasonable hypothesis to explain the phenomenon is that as screw speed falls, the shear forces fall, allowing more Maltese Crosses to reside in the extrudate. However, as the screw speed becomes very low, the residence time within the barrel becomes sufficiently long that the granules may be gelatinised by thermal input, leading to elimination of the granules. At the lowest screw speeds, where granules are also residual, it is hypothesised that the screw speed and mixing are so low that regions of the extrusion melt are isolated from the thermal and mechanical inputs, leading to regions or clusters of negligible gelatinisation.

7.5.3 Very low SME products

It was considered that these samples prepared at 50 rpm had starch that was in a similar state to the conventionally puffed rice product. Another approach that was used to prepare samples of this type was to increase the amount of added water to greater than 20% and raise the screw speed to 100rpm.

7.5.3.1 Overview

While using the microscope to analyse the origin of different textures, it was noted that samples with the lowest SME displayed unusual behaviour. Some of the samples showed residual starch granules, as would be expected, though others produced under similar conditions showed no intact granules. Additionally, it was noted that when smashed, both conventionally processed puffed rice and these very low SME samples looked similar under polarised and/or quarter wave plates.

Because of these phenomena, more samples were made at low SME and low temperature. The solid ingredients were 100 parts rice flour, 5 parts sucrose (icing sugar), and 0.5 parts sodium bicarbonate as used previously (Section 0). Samples were extruded, then immediately placed in a 260°C oven for 60 seconds. This slightly increased expansion, and reinflated collapsed cells. While in the 260°C oven, vapour pressure was sufficient to create expansion while the moisture contents of the cell walls dropped, causing the T_g to rise, preventing cell collapse in accordance with Mitchell *et al.*, (1994).

7.5.4 Loss of Granule Birefringence Due Solely to Thermal Input.

7.5.4.1 Overview

While determining the extent of birefringence (section 7.5), it was noted that at low temperatures or low rpm the flour occasionally clustered, and did not become

processed in the extruder (Figure 7-41). The clusters could be interpreted as plant cells, but as these do not appear in the unprocessed flour, they cannot be present in the extrudate. Additionally, a few of the clusters were partly processed, which could not be due to mechanical input (or the clusters [not granules] would fragment) and so must be heat-only input (Figure 7-42 and Figure 7-43).

7.5.4.2 *Description of Thermally Gelatinised Granules*

To explain how a cluster of granules can be partly processed is difficult, and for this reason, photographs of various stages of heat conversion have been prepared. The granules appear as Maltese Crosses, as transparent spheres resembling wet jelly beans, or at an intermediate stage. The transparent granules do not appear larger than the Maltese Crosses, eliminating swelling/hydration, again pointing to thermal gelatinisation as the cause of this effect. Within any one cluster, there may be granules showing Maltese Crosses, transparent granules, or a mixture of both.

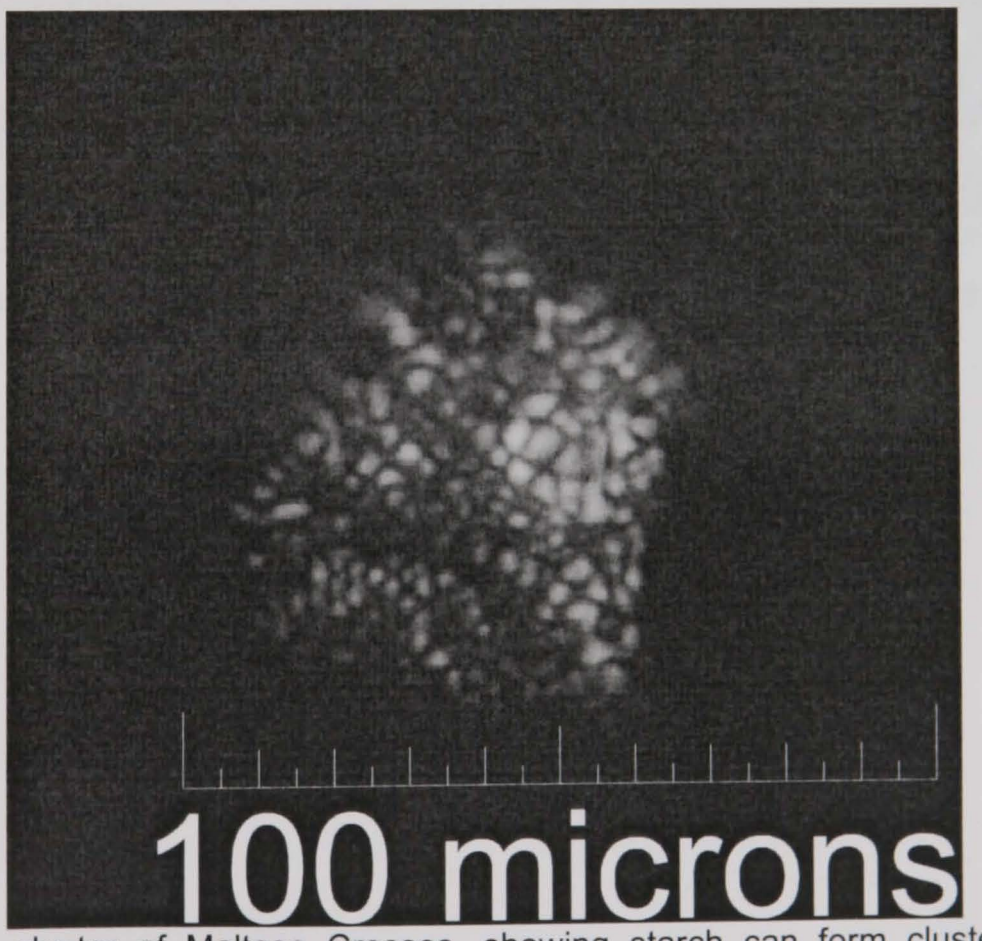

Figure 7-41 A cluster of Maltese Crosses, showing starch can form clusters and avoid processing during extrusion. Suspended in water, and viewed through two polarising filters.

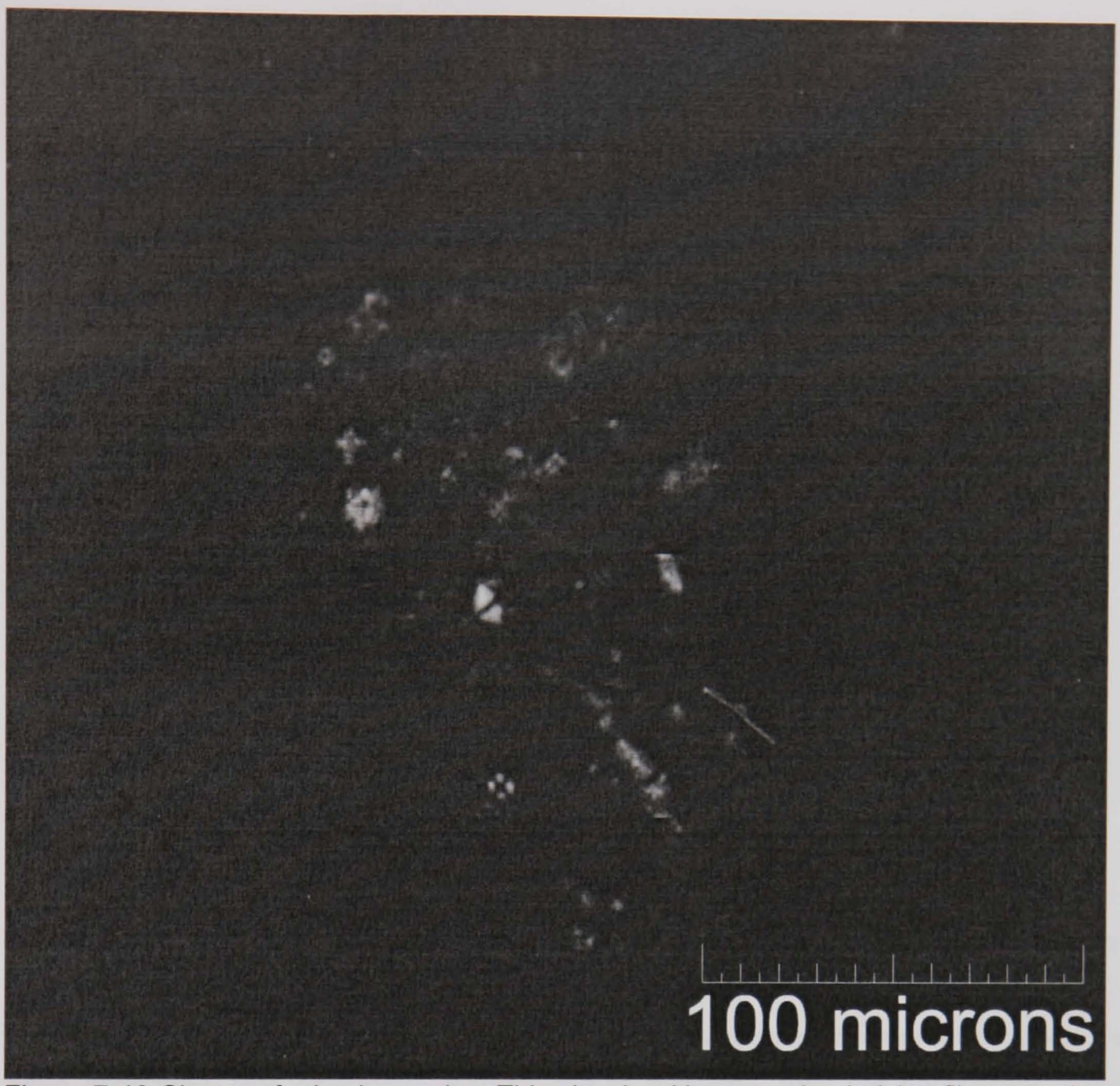

Figure 7-42 Cluster of mixed granules. This view is with crossed polarising filters, so the only material visible is the ungelatinised crystalline granules, which can be seen as Maltese Crosses.

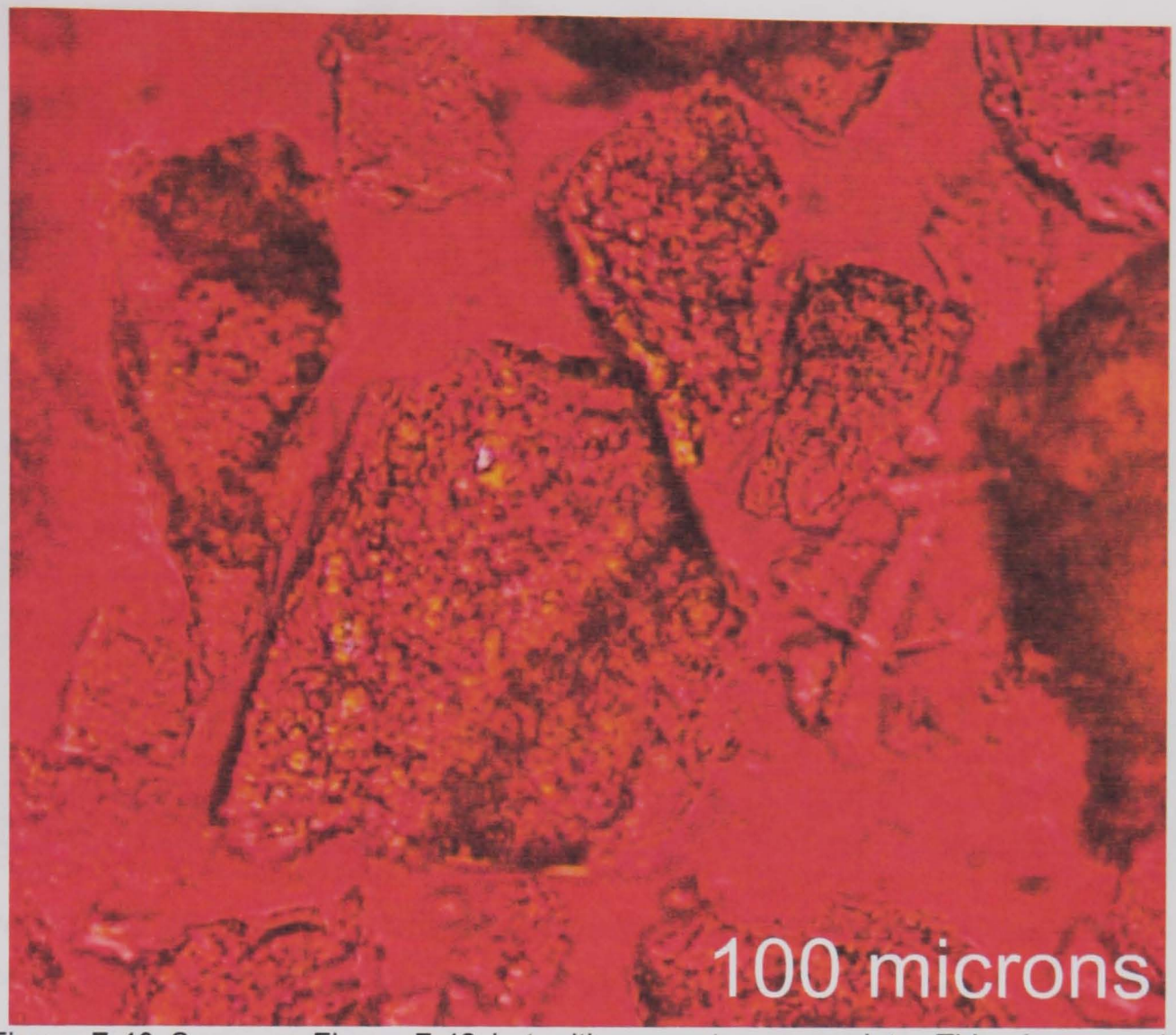

Figure 7-43 Same as Figure 7-42 but with a quarter wave plate. This view reveals many gelatinised but intact granules surrounding the crystalline granules seen in Figure 7-42. Had gelatinisation been due or partly due to mechanical forces then these granules would have been separated. Had gelatinisation been due to hydration, then the transparent granules would be expected to be significantly larger than the crystalline granules. These observations imply the gelatinisation is due only to thermal effects.

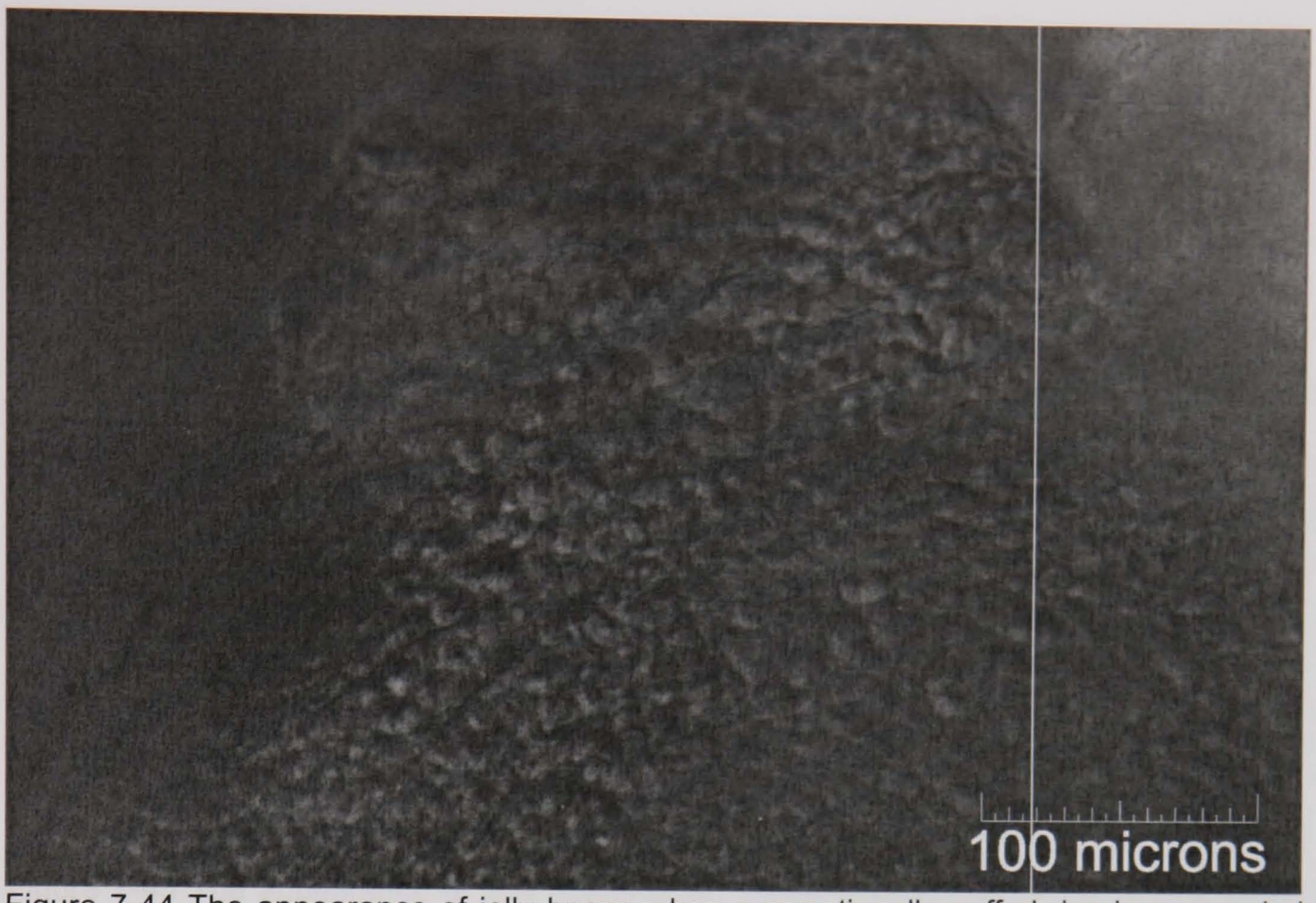

Figure 7-44 The appearance of jelly beans when conventionally puffed rice is suspended in water. The jelly beans are thermally gelatinised but intact starch granules. Viewed through two polarising filters and a quarter wave plate.

7.5.4.3 Viewing Conditions

To view the jelly beans, the samples must be viewed under crossed polarising filters, and dispersed in water. A different positive effect can be obtained using ethanol as the dispersing medium (Figure 7-45), whereas jellybeans could not be seen when using acetone or molar sodium hydroxide. In addition, a quarter wave filter is being used to create colours relating to the direction and regularity of molecular alignment. The quarter wave filter may also produce spurious effects by refraction through samples without parallel top and bottom surfaces.

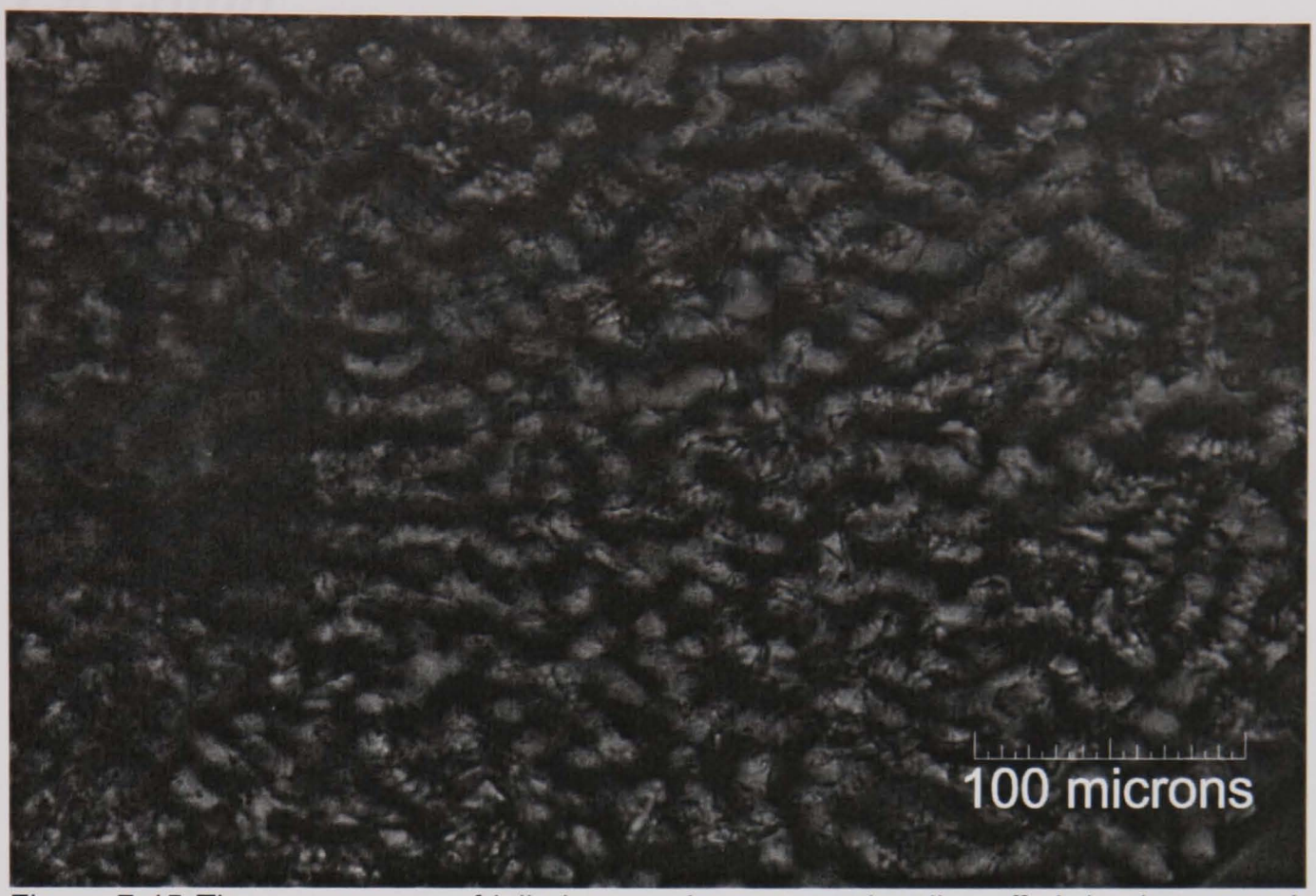

Figure 7-45 The appearance of jelly beans when conventionally puffed rice is suspended in ethanol. Viewed through two polarising filters and a quarter wave plate.

With only the two plane polarising filters, sample and non-sample is black. Intact starch granules appear as white spheres with a black cross-aligned with the two polarising filters.

With the addition of the quarter wave filter, non-sample is pink. Gelatinised sample is also the same colour pink, and is transparent, though the edges of the sample fragments are visible.

7.6 Chitin

7.6.1 Introduction

As crab shells are predominantly chitin, and as crabs do not become soggy when exposed to moisture, the idea formed that adding chitin to the rice flour prior to extrusion could form a product that did not lose texture on hydration.

Chitin is a polymer of N-acetyl-β-D-glucosamine, differing from cellulose only by the replacement of a hydroxyl group by an acetylated amino group. The most common role of chitin is as the exoskeleton in invertebrate animals (Mathews and van Holde, 1990), and may be refined from crab or prawn shells.

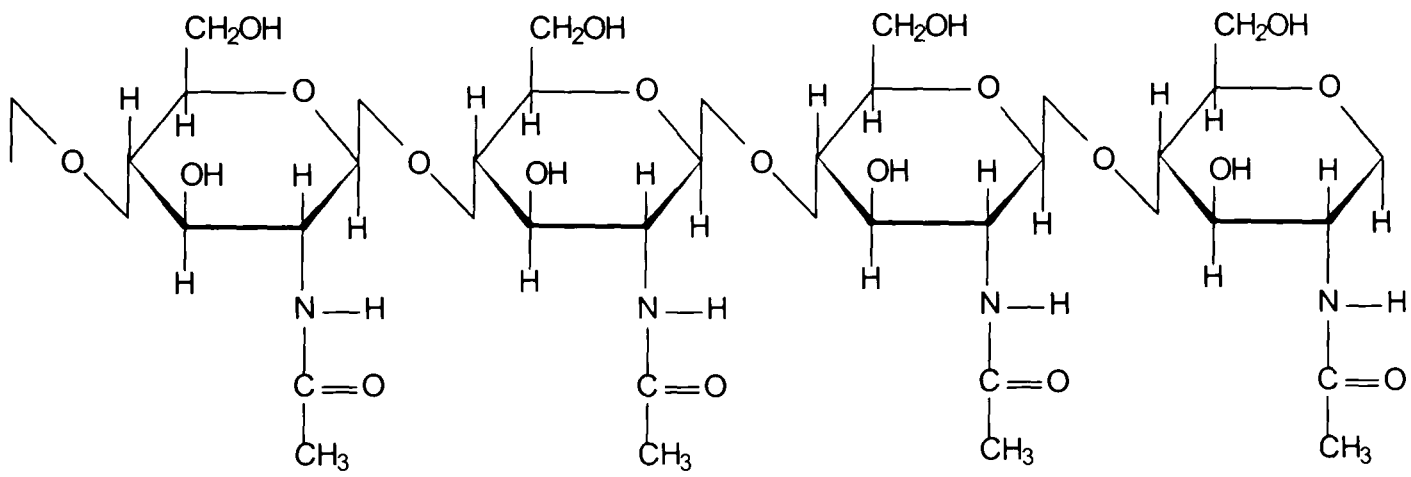

Figure 7-46 A section of the chitin polymer.

7.6.2 Experiment

Expanded samples were extruded with chitin contents of 0, 0.5, 1, and 2% dwb. The remainder of the solids were rice flour. The extrusion parameters were 300rpm, 6kg hr^{-1} feed rate, heater zones 40°, 80°, 120° and 120°C. Extrusion moisture content was 25%. The samples were analysed by the mechanical texture measuring technique for comparison (Chapter 6). The samples were exposed to 44, 54, 65, and 100% humidities for 24 hours, then the textures were measured again. As the level of added chitin was varied, it became apparent the longitudinal and radial expansion of the extrudate at the die were no longer equal as had been the case with the starch and starch/sugar blends previously used. To overcome effects of sample orientation during testing, half the repetitions were placed with axial expansion perpendicular to the

guillotine, and half were placed with their longitudinal expansion perpendicular to the guillotine. The measured textures were compared to identify increases or decreases in the susceptibility of texture to moisture vapour.

As a secondary experiment, samples were also placed in contact with water to empirically observe the hydration behaviour.

7.6.3 Results

The results showed a small decrease in crispness and crackliness in the fresh samples as the chitin content increased. However, after 24 hours exposure to various humidities, the samples with chitin showed a large loss in texture (Figure 7-47).

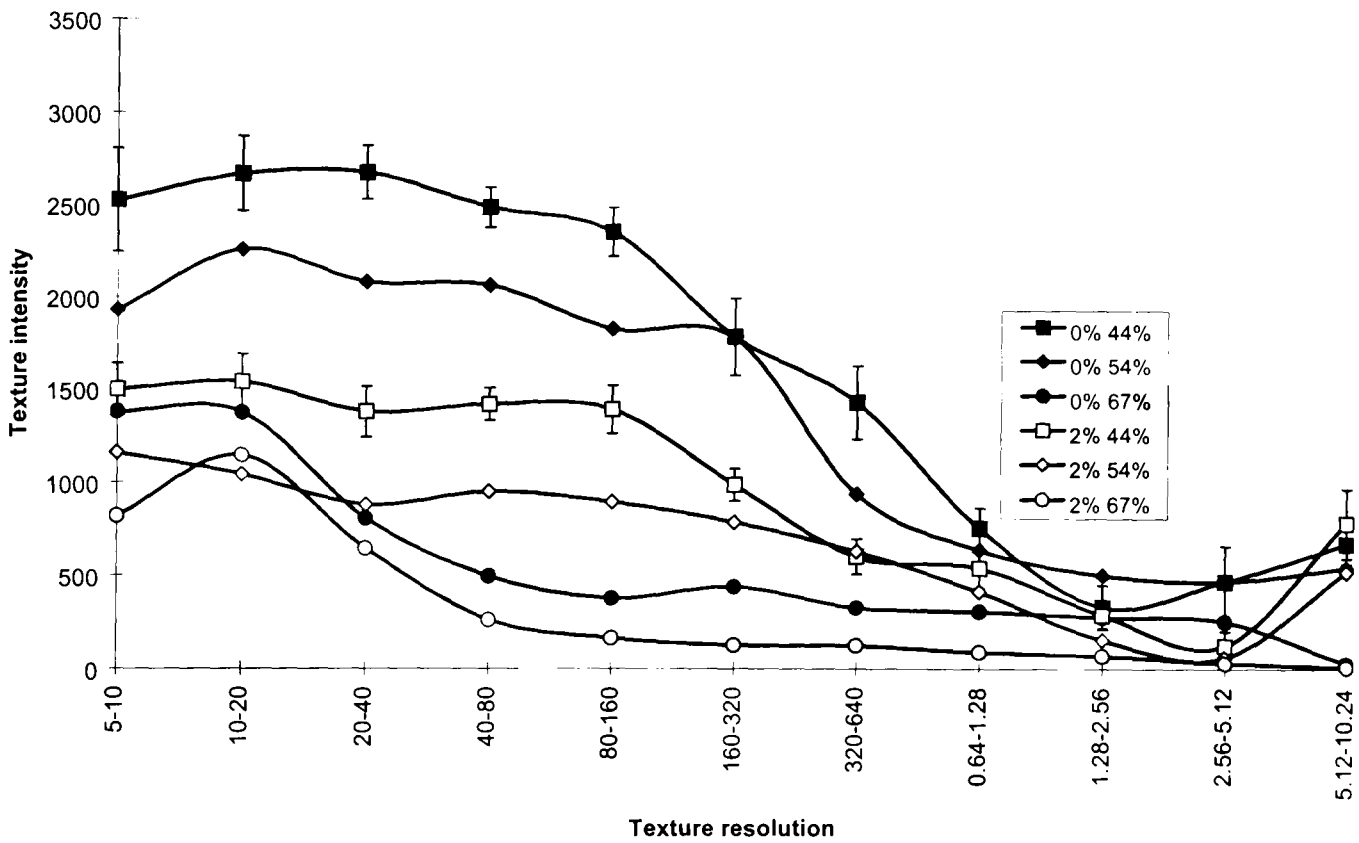

Figure 7-47 A graph of texture loss for extrudate with 0% and 2% added chitin, when exposed to 44%, 54%, and 67% relative humidities for 24 hours. For clarity, error bars are provided for the 44% data only. Note the lines are lower for extrudate containing chitin than those without chitin. See Chapter 6 for a detailed explanation of texture measurement.

Results of the secondary empirical experiment showed that the samples containing chitin absorbed water far more quickly than those without. Whereas the rice-only samples took around 20 seconds to become waterlogged, the chitin-containing samples required only 2-3 seconds to become waterlogged.

7.6.4 Conclusion

The inclusion of chitin accelerated rather than prevented the loss of texture on hydration, and also increased the susceptibility of the samples when in physical contact with water.

The most probably reason for this is that the chitin fragments promoted cell wall rupture, producing a sponge rather than a foam. Further work is required to confirm this hypothesis.

8 General discussion

8.1 Moisture Adsorption by Expanded Rice

The major objective of the work described in this thesis was to understand the different performance of conventionally puffed and extruded puffed rice within a confectionery product. It was quickly found that under controlled conditions the texture of the extruded product deteriorated far more rapidly than the texture of the conventional product. This was in agreement with observations made within Nestle. Two hypotheses were proposed for this difference. Firstly that the equilibrium moisture content at the appropriate water activity (0.55) was higher for the extruded product. Secondly that the rate of water adsorption was higher in the extruded material. It was found that the second hypothesis was the correct one. A number of possible reasons for this difference in rate of water adsorption were considered. These included differences in the degree of starch conversion, and a different and less stable packing of amylose-lipid complexes in the extruded material resulting in a conversion on storage to the more stable form with subsequent water adsorption. A third possible reason was a difference in product morphology, with an open cell sponge for the extruded material compared with a closed cell foam for the conventionally processed product. These three hypotheses will now be discussed separately.

8.1.1 Degree of Starch Conversion

The degree of starch conversion was interpreted primarily in terms of WSI. This parameter increases with increasing degree of starch conversion. When comparing a conventionally puffed rice product with extruded product it was found that the WSI was indeed higher for the extruded product, although the difference was not as dramatic as had been expected. A major part of the work described in the thesis then focussed on the relationship between the extruder process variables, the state of starch, and the water adsorption characteristics of the product. The variable normally used to define the severity of an extrusion process is the specific mechanical energy (SME). In contrast to what is often believed, a clear relationship between SME and starch conversion was not obtained. It was however found that there was a reasonably good correlation between the WSI and the rate of hydration of the sample after

subsequent drying. This correlation was obtained as a result of data from more than fifty samples, and provided convincing support for the hypothesis regarding the relationship between starch conversion and rate of water adsorption. There was little correlation between the equilibrium moisture content and degree of starch conversion. as would be expected in view of the observation that the equilibrium moisture contents of the conventionally processed and industrially extruded samples were similar.

Although WSI provides one measure of starch conversion, more information can be obtained from a microscopic examination of the samples.

The conventionally processed samples showed a clear structural feature; no birefringent granules were present, but individual unswollen granules could be identified. These granules were translucent, and described as "jellybeans." They could only be viewed under crossed polarising light with a quarter wave plate, and at high magnification. In the conventionally puffed rice samples, there appeared to be monolayers of these granules forming cell walls. It was considered that this structural feature could result in a lower water adsorption rate because the outer layers of the starch granules may shield the inner layers, thus making fewer water binding sites available to water vapour.

8.1.2 Packing of Amylose-Lipid Complexes

X-ray measurements were made of the form of the amylose-lipid complex. Conditions leading to a high level of starch conversion (low moisture contents and high temperatures) resulted in an E-type X-ray diffraction pattern. It would be expected that on hydration this converted to the more stable V-type pattern (Fan *et al.*, 1996b). Although there was some relationship between the rate of hydration and the type of pattern with E-type samples hydrating more rapidly than V-type samples, it was considered that this simply reflected a difference in the degree of starch conversion. The type of packing was considered to be a consequence of the processing conditions, and not to be the cause of the different hydration rates.

8.1.3 Product Morphology

Substantial microscopy was carried out on the extruded samples. This led to a number of conclusions. It was found that sponge-like structures were only found in samples that were extruded at very low water contents, and hence high SME's. In most cases however, closed cell foam structures were observed, thus the difference between hydration rates for the bulk of the samples could not be explained by variations in the degree of bubble interconnectivity within the samples.

It is of interest to consider how close it would be possible to get to a conventionally processed krispie using extrusion cooking. In this work, an attempt was made to produce the "jellybean" type structure by extrusion (due to thermal only gelatinisation; see Section 7.5.4). This was achieved by either reducing the screw speed at relatively low water content, or by increasing the water content at higher screw speeds. Surprisingly, it was found that this type of structure could be observed for products prepared at a specific and lower screw speed. The reasons for this were not entirely clear and further work involving the measurement of residence times would be required to confirm the hypothesis that under these conditions high residence times are encountered resulting in thermal as opposed to mechanical conversion. Although the type of starch conversion found in the conventionally processed samples can be achieved by extrusion, the degree of expansion required cannot be simultaneously obtained. The author believes that it would be possible to devise a process where continuous cooking is carried out within an extruder under very gentle conditions (low SME and high moisture). The samples would then be cut into small spheres, tempered to the appropriate moisture content, and subsequently oven-puffed. When this is compared with a conventional krispie process the downstream tempering and puffing would be similar; only the cooking conditions would be different. The advantages of this are that products can be made to any size or shape, secondly the cooking time is substantially reduced (residence times within an extruder approximately 1 minute, compared to an hour for conventional cooking) Recipe and process variable changes could be made almost instantaneously for extrusion cooking. Example – an inadequately or overcooked product could be corrected for almost immediately without having to examine a large batch of process material. Clearly, further development work would be required to achieve this. One of

the limitations of this work was the use of WSI and WAI to follow starch conversion. There have been substantial developments in the use of the rapid viscosity analyser to examine processed cereal products e.g. Guy (1997). Any subsequent development program should use this methodology to drive the process.

8.2 Texture Measurement

Although it was not the main objective, a significant achievement of this work was the development of a new approach to the mechanical measurement of texture of foamed foods. The "line length" approach described in Chapter 6 does, the author believes, have some advantages over other approaches.

9 Glossary

ε	adsorption energy.
∞	Infinity.
A	A form of crystallinity of native starch: A chain connected to a B-chain in an amylopectin molecule. Section 4.2.1; Cross-sectional area. Section 4.5.2.
amylopectin	The branched form of starch. Section 4.2.1.
amylose	The generally linear form of starch. Section 4.2.1.
A_w	Water activity. The hydrating power of a sample as compared to water. Measured from 0 to 1. Section 4.7.1.
B	A form of crystallinity of native starch; A chain connected to the C-chain in an amylopectin molecule. Section 4.2.1.
barrel	The wall of the extruder in which the screws rotate. Section 4.6.4.1.
batch process	Production process that is non-continuous (e.g. consecutive cooking of vats of rice rather than a continuous rotating drum cooker).
C	A form of crystallinity of native starch; The reducing chain in an amylopectin molecule. Section 4.2.1.
$\frac{\partial c}{\partial x}$	Concentration gradient. Section 4.5.1.
$\underline{\nabla}c$	Concentration gradient in three dimensions. Section 4.5.1.
$C_\times$	Number of Maltese Crosses in one gram of sample.
$\overline{C_\times}$	Estimated error in measuring $C_\times$.
cell	A plant cell; A bubble of gas.
chain; A,B,C	Designations given to parts of the amylopectin molecule. Section

	4.2.1.
conventionally processed	Cooked by a traditional method. See Section 4.6.1.1.
ΔC_{p1}, ΔC_{p2}, ΔC_{pn}	Change in heat capacity for samples 1, 2, and n respectively.
D	Coefficient of diffusion.
$\underline{D}$	Coefficient of diffusion in three dimensions.
dessicator	A chamber of controlled RH.
die	The exit hole of the extruder. Section 4.6.4.1.
dsb	Dry solids basis. Mass proportion of dry solids.
dwb	Dry weight basis. Mass proportion after drying.
E	A metastable starch-lipid complex. Transforms to V-type on hydration. Section 4.2.1.2.
FFT	A fast computer algorithm for performing Fourier transformations, which see.
Fourier transform	The mathematical technique of resolving a signal into a spectra of sinewaves.
G	Guggenheim constant.
glucose	A monosaccharide. The building block of starch. Section 4.2.1.2.
granule	A semi-crystalline particle of concentric spheres of starch. Section 4.2.1.2.
humidity	See Section 4.7.1.
k	Time constant for diffusion;
	Boltzmann constant.
k_o	Relaxation constant. Section 4.5.2.
krispie	A small ball of puffed rice.
M_∞	Projected value for sample mass at infinite time.
Maltese cross	Under specific conditions, starch granules appear as black Maltese crosses on white discs. Figure 4-10.
MC_{RH}	Moisture content of sample at equilibrium at relative humidity RH.

MC_t	Moisture content of sample at time t.
M_{dried}	Mass of dried sample.
$M_{equilibrium}$	Mass of sample at equilibrium.
m_{gel}	Mass of gel.
m_{sample}	Mass of sample.
$m_{solutes}$	Mass of solutes.
M_t	Mass of sample at time t.
n	Real number.
N	Number of solvent molecules absorbed at pressure p and temperature T
O	Moisture content below which expansion and collapse of foams can no longer occur. Section 4.3.3.
oven drying	See vacuum drying.
p	Pressure
P_a, P_b	Pressures inside and outside a gas cell.
q	Mean molecular partition function of adsorbed molecules.
Q	Flux of molecular diffusion. Section 4.5.1.
Q	Flux of molecular diffusion in a three dimensional system. Section 4.5.1.
RH	Relative humidity. The humidity of an atmosphere as compared to the humidity of saturated air. Measured from 0 to 100%.
sb	Solids basis.
%sb	% solids basis. The mass as a fraction of the solids in the mixture.
screw	An Archimedian screw that rotates in an extruder, mixing and conveying extrudate through the barrel. Section 4.6.4.1.
SME	Specific mechanical energy. The product of torque and screw speed in the extruder. See Section 4.2.2.1.
starch	Section 4.2.1.
t	Time variable.

T, T_3, T_4	Temperature. General and of extruder zones 3 and 4 respectively.
T_c	Critical temperature at which $P_a = P_b$.
T_g	Glass transition temperature.
T_{g1}, T_{g2}, T_{gn}	Glass transition temperature of components 1, 2, and n respectively.
V	A stable starch-lipid complex.
vacuum drying	Section 5.3.2.
w	Equilibrium moisture content.
w_m	Monolayer moisture content.
W_1, W_2, W_n	Weight fraction of components 1, 2, and n.
WAI	Water absorption index. Section 5.3.5
WAXS	Wide angle X-ray scattering. A sample is exposed to an X-ray beam. The way the X-rays are reflected from the surface of the sample is dependent upon the crystalline and/or amorphous structure of the sample.
WSI	Water solubility index. Section 5.3.5.
WVAR	Water vapour adsorption rate. Section 5.3.4.
wwb	Wet weight basis. Mass proportion before drying.

10 Bibliography

ABLETT, S., DARKE, A.H., IZZARD, M.J. and LILLFORD, P.J. (1993) Studies of the glass-transition in malto-oligomers. In *The Glassy State in Foods*. Eds. Blanshard, J.M.V. and Lillford, P.J. Nottingham University Press. 189-207.

ANDERSON, R.A., CONWAY, H.F., PFEIFER, V.F. and GRIFFIN, E.L. (1969) Gelatinisation of corn grits by roll- and extrusion cooking. *Cereal Science Today*. **14**(1), 4-11.

ANDERSSON, Y. (1983) Extrusion a short description of the process and some preliminary studies on the influence of fat. In *Fats (lipids) in Baking and Extrusion*. Ed. Marcuse, R. Contribution at a lipidforum symposium, Göteborg. **April 11-12**, 120-124.

BARRETT, A.M., NORMAND, M.D., PELEG, M. and ROSS, E. (1992) Characterization of the jagged stress-strain relationships of puffed extrudates using the Fast Fourier Transform and Fractal Analysis. *Journal of Food Science*. **57**, 227-232, 235.

BELITZ, H.D. and GROSCH, W. (1987) *Food Chemistry*. Springer-Verlag, Berlin Heidelberg.

BENCZEDI D., TOMKA, I. AND ESCHER, F. (1998a) Thermodynamics of amorphous Starch-Water Systems. 1. Volume Fluctuations. *Macromolecules*. **31**(9), 3055-3061.

BENCZEDI D., TOMKA, I. AND ESCHER, F. (1998b) Thermodynamics of amorphous Starch-Water Systems. 2. Concentration Fluctuations. *Macromolecules*. **31**(9), 3062-3074.

BENDER, A.E. (1990) *Dictionary of Nutrition and Food Technology*. 6th ed. Butterworths, London. (No specific reference but used regularly).

BIETZ, J.A. (1982) Cereal prolamin evolution and homology revealed by sequence-analysis. *Biochemical Genetics*. **20**. 1039-1053.

BLANSHARD, J.M.V., BATES, D.R., MUHR, A.H.. WORCESTER, D.L. and HIGGINS, J.S. (1984) Small angle neutron scattering studies of starch granule structure. *Carbohydrate Polymers*. **4**, 427-442.

BLANSHARD, J.M.V. (1987) Starch granule structure and function: a physicochemical approach. In *Starch: Properties and Potential*. Ed. Galliard, T. John Wiley and Sons, Chichester, UK. Ch.2.

BLANSHARD, J.M.V. (1995) The glass transition, its nature and significance in food processing. In *Physico-Chemical Aspects of Food Processing*. Ed. Beckett, S.T. Blackie Academic and Professional, UK. 17-48.

BORCH, J., SARKO, A. and MARCHESSAULT, R.H. (1972) Light Scattering analysis of starch granules. *Journal of Colloid and Interface Science*. **41**(3), 574-587.

BORGES, A. and PELEG, M. (1996) Determination of the apparent fractal dimension of the force displacement curves of brittle snacks by four different algorithms. *Journal of Texture Studies*. **27**, 243-255.

BOURNE, M.C., SANDOVAL, A.M.R., VILLALOBOS, M.C. and BUCKLE, T.S. (1975) Training a sensory texture profile panel and development of a standard rating scale in Columbia. *Journal of Texture Studies*. **6**, 43-52.

BOUSSINGAULT, J.B. (1852) *Ann. Chimie Physique*. **36**, 490.

BOUTON, P.E. and HARRIS, P.V. (1978) Factors affecting tensile and Warner Bratzeler shear values of raw and cooked meat. *Journal of Texture Studies*. **9**, 395-413.

BRAY, F. (1986) *The Rice Economies: Technology and Development in Asian Societies*. Blackwell, UK.

BROCKINGTON, S.F. (1950) Breakfast cereal technology. *Food Technology*. **4**. 396.

BROCKINGTON, S.F. and KELLY, V.J. (1972) Rice breakfast cereals and infant foods. In *Rice: Chemistry and Technology*. 1st ed. Ed Houston. Ch.16, 400-418.

CAMERON, R.E. and DONALD, A.M. (1992) Small angle X-Ray scattering of the annealing and gelatinization of starch. *Polymer*. **33**. 2628-2638.

CHANG, T.T. (1976) Rice. In *Evolution of Crop Plants*. Ed. Simmonds, N.W. Longman, London, UK. 98-104.

CHINNASWAMY, R. and BHATTACHARYA, K.R. (1986) Characteristics of gel-chromatographic fractions of starch in relation to rice and expanded rice-product qualities. *Starke*. **38**, 51-57.

COLONNA, P. and MERCIER, C. (1983) Macromolecular modifications of manioc starch components by extrusion cooking with and without lipids. *Carbohydrate Polymers*. **3**, 87-108.

COLONNA, P., TAYEB, J. and MERCIER, C. (1989) Extrusion Cooking of starch and starchy products. In *Extrusion Cooking*. Eds. Mercier, C., Linko, P. and Harper, J.M. AACC, St Paul, Minnesota. 247-320.

COUCHMAN, P.R. and KARASZ, F.E. (1978) A classical thermodynamic discussion of the effect of composition on glass transition temperatures. *Macromolecules*. **11**, 117-119.

DACREMONT, C. (1995) Spectral composition of eating sounds generated by crispy, crunchy and crackly foods. *Journal of Texture Studies*. **26**, 27-43.

DONALD, A.M., WARBURTON, S.C. and SMITH, A.C. (1993) Physical changes consequent on the extrusion of starch. In *The Glassy State in Foods*. Eds. Blanshard, J.M.V. and Lillford, P.J. Nottingham University Press. 375-393.

DONALD, A.M., WAIGH. T.A.. JENKINS, P.J.. GIDLEY. M.J., DEBET, M. and SMITH, A. (1997) Internal structure of starch granules revealed by scattering studies. In *Starch Structure and Functionality*. Eds. Frazier. P.J.. Donald, A.M. and Richmond, P. The Royal Society of Chemistry. 172-179.

FAN, J., MITCHELL, J.R. and BLANSHARD, J.M.V. (1994). A computer simulation of the dynamics of bubble growth and shrinkage during extrudate expansion. *Journal of Food Engineering.* **23**, 337-356.

FAN, J. (1994) *Bubble Growth and Starch Conversion in Extruded and Baked Cereal Systems*. PhD Thesis, University of Nottingham. UK.

FAN, J., MITCHELL, J.R. and BLANSHARD, J.M.V. (1996a) The effect of sugars on the extrusion of maize grits: I. The role of the glass transition in determining product density and shape. *International Journal of Food Science and Technology.* **31**, 55-65.

FAN, J., MITCHELL, J.R., BLANSHARD, J.M.V. (1996b.) The effect of sugars on the extrusion of maize grits: II. Starch conversion. *International Journal of Food Science and Technology.* **31**, 67-76.

F.A.O. (1989) *Food Outlook, No 3.* Food Agriculture Organization, Rome, Italy.

FARHAT, I.A. (1996) *Molecular Mobility and Interactions in Bioploymer-Sugar-Water systems.* PhD thesis, University of Nottingham.

FARHAT, I.A., BLANSHARD, J.M.V., MELVIN, J.L. and MITCHELL, J.R. (1997) The effects of water and sugars upon the retrogradation of amylopectin in the region ($T-T_g$) between 0 and 85°C. In *Starch Structure and Functionality*. Eds. Frazier, P.J., Donald, A.M. and Richmond, P. The Royal Society of Chemistry. 86-95.

FAST, R.B. and CALDWELL, E.F. (1990) *Breakfast Cereals and How they are Made*. American Association of Cereal Chemists, Inc., St Paul, Minnesota, USA.

FLORY, P.J. (1953) *Principles of Polymer Chemistry*. Cornell University Press, Ithaca, New York.

FRENCH, D. (1972) Fine structure of starch and its relationship to the organisation of starch granules. *Journal of the Japanese Society of Starch Science*. **19**(1), 8-25.

FRENCH, D. (1984) Organisation of Starch Granules. In *Starch: Chemistry and Technology*. Eds. Whistler, R.L., BeMiller, J. and Paschall, E.F. Academic Press Inc., London. 183-247.

GALLIARD, T. and BOWLER, P. (1987) Morphology and composition of starch. In *Starch: Properties and Potential*, ed. Galliard, T. John Wiley and Sons, Chichester. Ch.3, 55-78.

GIBBS, J.H. (1956) Nature of the glass transition in polymers. *Journal of Chemical Physics*. **25**, 185-186.

GIBBS, J.H. and DIMARZIO, E.A. (1958) Nature of the glass transition and the glassy state. *Journal of Chemical Physics*. **28**, 373-383.

GREENSPAN, L. (1977) Humidity fixed points of binary saturated aqueous solutions. *Journal of Research of the National Bureau of Standards (Section A: Physics and Chemistry)*. **81**, 89-96.

HIZUKURI, S., TAKEDA, Y., MARUTA, N. and JULIANO, B.O. (1989) Molecular structures of rice starch. *Carbohydrate Research*. **189**, 227-235.

HOLLINGER, G. and MARSCHESSAULT, R.H. (1975) Ultrastructure of acid- an enzyme modified cross-linked potato starch. *Biopolymers*. **14**, 265-276.

IMAI, E., HATAE, K. and SHIMADA, A. (1995) Oral perception of grittiness: Effect of particle size and concentration of the dispersed particles and the dispersion medium. *Journal of Texture Studies*. **26**, 561-576.

I.R.R.I. (1988) *IRRI Rice Facts 1988*. The International Rice Research Institute. The Phillipines.

JENKINS, P.J., CAMERON, R.E., DONALD, A.M., BRAS, W., DERBYSHIRE, G.E., MANT, G.R. and RYAN, A.J. (1994) In-situ simultaneous small and wide angle X-ray scattering: A new technique to study starch gelatinisation. *Journal of Polymer Science. Part B: Polymer Physics*. **32**, 1579-1583.

JONES, W.H. (1992) Quality and processing considerations in the production of crisp rice cereal. *Cereal Foods World*. **37**(5), 367-371.

JULIANO, B.O. (1985) Polysaccharides, proteins and lipids of rice. In *Rice Chemistry and Technology*. Ed Juliano, B.O. American Association of Cereal Chemists Inc. St Paul, Minnesota, USA. 59-174.

KALICHEVSKY, M.T. and BLANSHARD, J.M.V. (1992a) A study of the effect of water on the glass transition of 1/1 mixtures of amylopectin, casein and gluten using DSC and DMTA. *Carbohydrate Polymers*. **19**, 271-278.

KALICHEVSKY, M.T., JAROSZKIEWICZ, E.M., ABLETT, S., BLANSHARD, J.M.V. and LILLFORD, P.J. (1992b) The glass transition of amylopectin measured by DSC, DMTA, and NMR. *Carbohydrate Polymers*. **18**, 77-88.

KALICHEVSKY, M.T. and BLANSHARD, J.M.V. (1993a) The effect of fructose and water on the glass transition of amylopectin. *Carbohydrate Polymers*. **20**, 107-113.

KALICHEVSKY, M.T., BLANSHARD, J.M.V. and JAROSZKIEWICZ, E.M. (1993b) A study of the glass transitions of amlopectin-sugar mixtures. *Polymer*. **34**, 346-358.

KAREL, M. and LANGER, R. (1988) Controlled release of food additives. In *Flavour Encapsulation*. Eds. Risch, S.J. and Reineccius, G.A. American Chemical Society Symposium Series 370. Washington DC. 177-191.

KAREL, M. and SAGUY, I. (1991) Effects of water on diffusion in food systems. In *Water Relationships in Foods*. Eds Levine, H. and Slade, L. Plenum Press. USA. 157-174.

KASSENBECK, P. (1975) Electron microscope contribution to the study of the fine structure of wheat starch. *Starch*. **27**(7), 217-227.

KATZ, J.R. (1928) Gelatinisation and retrogradation of starch in relation to the problem of bread staling. In *A Comprehensive Survey of Starch Chemistry*. Ed. Walton, R.P. The Chemical Catalogue Company Inc., New York. 100-117.

KAYE, B. (1993) Infinite coastlines and other wiggly lines. In *Chaos & Complexity*, VCH Publishers, New York. Ch.8, 307-383.

KELLOGG, J.L. (1935) 5 February. Cereal Food. U.S. Patent 1,990,382.

KENDALL, M.G. and BUCKLAND, W.R. (1982) *A Dictionary of Statistical Terms*. 4th ed. Longman Group Ltd, London and New York.

KROG, N. (1971) Amylose Complexing effect of Food Grade Emulsifiers. *Die Stärke*. **23**(6), 206-210.

LARSSON, K. (1980) Inhibition of starch gelatinisation by amylose-lipid complex formation. *Starch/Stärke*. **32**(4), 125-126.

LAUNAY, B. and LISCH, J.M. (1983) Twin-screw extrusion cooking of starches: Flow behaviour of starch pastes, expansion and mechanical properties of extrudates. *Journal of Food Engineering*. **2**, 259-280.

LELIÈVRE, J. (1973) Starch gelatinization. *Journal of Applied Polymer Science*. **18**, 293-296.

LE MESTE, M., VOILLEY, A. and COLAS, B. (1991) In *Water Relationships in Foods*. Eds Levine, H. and Slade, L. Plenum Press, USA. 123-138.

LIVINGS, S.J., BREACH, C. and DONALD, A.M. (199?) Physical ageing of wheat flour based confectionery wafers. *Carbohydrate Polymers*. **34**, 347-355.

MACGREGOR, E.A. and GREENWOOD, C.T. (1980) *Polymers in Nature*. J. Wiley and Sons Ltd., Chichester, UK.

MANSFIELD, M.L. (1993) An overview of theories of the glass transition. In *The Glassy State in Foods*. Eds. Blanshard, J.M.V. and Lillford, P.J. Nottingham University Press. 103-122.

MATHEWS, C.K. and VAN HOLDE, K.E. (1990) *Biochemistry*. The Benjamin/Cummings Publishing Company Inc, Redwood City, USA.

MERCIER, C., CHARBONNIÈRE, R., GALLANT, D. and GUILBOT, A. (1979) Structural modifications of various starches by extrusion cooking with a twin-screw French extruder. In *Polysaccharides in Foods*. Eds. Blanshard, J.M.V. and Mitchell, J.R. Butterworths, London. **10**, 153-170.

MERCIER, C., CHARBONNERIE, R., GREBAUT, J. and De La GUERIVIERE, J.F. (1980) Formation of amylose-lipid complexes by twin-screw extrusion cooking of manioc starch. *Cereal Chemistry*. **57**, 4-9.

MITCHELL, J.R., FAN, J. and BLANSHARD, J.M.V. (1994) The shrinkage domain. *Extrusion Communique*. **7**, 10-12.

NICHOLLS, R.J., APPELQVIST, I.A.M., DAVIES, A.P., INGMAN, S.J. and LILLFORD, P.J. (1995) Glass transitions and the fracture-behavior of gluten and starches within the glassy state. *Journal of Cereal Science*. **21**, 25-36.

NIXON, R. and PELEG, M. (1995) Effect of sample volume on the compressive force-deformation curves of corn flakes tested in bulk. *Journal of Texture Studies*. **26**, 59-69.

NORTON, C.R.T., MITCHELL, J.R. and BLANSHARD, J.M.V. (1998) Mechanical measurement of crisp and crackly textures. *Journal of Texture Studies*. **29**, 239-253.

NUEBEL, C. and PELEG, M. (1993) Compressive stress-strain relationships of two puffed cereals in bulk. *Journal of Food Science*. **58**(6), 1356-1360, 1374.

NUEBEL, C. and PELEG, M. (1994) Compressive stress-strain relationships of agglomerated instant coffee. *Journal of Food Process Engineering*. **17**, 383-400.

ONG, M.H. (1994) *Factors Affecting the Molecular Properties of Starch and their Relation to the Texture of Cooked Rice*. PhD Thesis, University of Nottingham, UK.

ONG, M.H. and BLANSHARD, J.M.V. (1995) Texture determinants in cooked, parboiled rice. 1: Rice Starch amylose and the fine structure of amylopectin. *Journal of Cereal Science*. **21**, 251-260.

ORFORD, P.D., PARKER, R. and RING, S.G. (1990) Aspects of the glass transition behaviour of mixtures of carbohydrates of low molecular weight. *Carbohydrate Research*. **196**, 11-18.

PELEG, M. (1979) Characterization of the stress relaxation curves of solid foods. *Journal of Food Science*. **44**, 277-281.

PELEG, M. (1993) Do irregular stress-strain relationships of crunchy foods have regular periodicities? *Journal of Texture Studies*. **24**, 215-227.

PEPPAS, N.A. and BRANNON-PEPPAS, L. (1994) Water diffusion and sorption in amorphous molecular systems and foods. *Journal of Food Engineering*. **22**, 189-210.

RADHIKA REDDY, K.R., ALI, S.Z. and BHATTACHARYA, K.R. (1993) The fine structure of rice-starch amylopectin and its relation to the texture of cooked rice. *Carbohydrate Polymers*. **22**, 267-275.

RADHIKA REDDY, K.R., SUBRAMANIAN, R., ALI, S.Z. and BHATTACHARYA, K.R. (1994) Viscoelastic properties of rice-flour and their relationship to amylose content and rice quality. *Cereal Chemistry*. **71**, 548-552.

RAMESH, M., ZAKIUDDIN ALI, S. and BHATTACHARYA, K.R. (1999) Structure of rice starch and its relation to cooked-rice texture. *Carbohydrate Polymers*. **38**(4), 337-347.

RAMIREZ, R. (1985) *The FFT : Fundamentals and Concepts*. Prentice-Hall, Eaglewood Cliffs, New Jersey, USA.

ROBIN, J.P., MERCIER, C., CHARBONNIÈRE, R. and GUILBOT, A. (1974) Lintnerised starches. Gel filtration and enzymatic studies of insoluble residues after prolonged acid treatment of potato starch. *Cereal Chemistry*. **51**, 389-406.

ROHM, H. (1990) Consumer awareness of food texture in Austria. *Journal of Texture Studies*. **21**, 363-373.

RONAYNE, J. (1986) *Introduction to Digital Communications Switching*. Pitman Publishing, London.

ROONEY, L.W., FAUBION, J.M. and EARP, C.F. (1982) Scanning electron microscopy of cereal grains. In *New Frontiers in Food Microstructure*. Ed. Bechtel, D.B. AACC, USA. 201-240.

ROOZEN, M.J.G.W. and HEMMINGA, M.A. (1990) Molecular motion in sucrose-water mixtures in the liquid and glassy state as studied by spin probe ESR. *Journal of Physical Chemistry*. **94**, 7326-7329.

ROOZEN, M.J.G.W. and HEMMINGA, M.A. (1991) Molecular motion in carbohydrate and water mixtures in the liquid and glassy states as studied by spin-probe ESR. *Special Publication of the Royal Society of Chemistry*. **82**, 531-536.

ROUDAUT, G., DACREMONT, C. and LEMESTE, M. (1998) Influence of water on the crispness of cereal-based foods: Acoustic, mechanical, and sensory studies. *Journal of Texture Studies*. **29**(2), 199-213.

RUSS, J.C. (1994) *Fractal Surfaces*. Plenum Press, New York.

SANDHYA RANI, M.R. and BHATTACHARYA, K.R. (1995a) Rheology of rice-flour pastes: relationship of paste breakdown to rice quality, and a simplified Brabender viscograph test. *Journal of Texture Studies*. **26**, 587-598.

SANDHYA RANI, M.R. and BHATTACHARYA, K.R. (1995b) Microscopy of rice starch granules during cooking. *Starke*. **47**, 334-337.

SANDRECZKI, T.C. and BROWN, I.M. (1988) Motional behaviour and correlation of nitroxide spin probes above and below the glass-transition. *Macromolecules*. **21**, 504-510.

SAUVAGEOT, F. and BLOND, G. (1991) Effect of water activity on crispness of breakfast cereals. *Journal of Texture Studies*. **22**, 423-442.

SEYMOUR, S.K. and HAMANN, D.D. (1988) Crispness and crunchiness of selected low moisture foods. *Journal of Texture Studies*. **19**, 79-95.

SINGH, R.P. and HELDMAN, D.R. (1993) *Introduction to Food Engineering*. Second Edition. Academic Press, London.

SLADE, L. and LEVINE, H. (1991) Beyond water activity. In *CRC Critical Reviews in Food Science and Nutrition*. **30**, 115-360.

SLADE, L. and LEVINE, H. (1993) The glassy state phenomenon in food molecules. In *The Glassy State in Foods*. Eds. Blanshard, J.M.V. and Lillford, P.J. Nottingham University Press. 35-102.

STONE SOUP GROUP (1996) *Fractint 19.6*. Free computer software, available at http://spanky.triumph.ca/www/fractint/fractint.html or other sites.

SUGISAKI, M., SUGA, H. and SEKI, S. (1968) *Bull Chemistry Society*. Japan. **41**. 2591-2599.

SWYNGEDAU, S., NUSSINOVITCH, A., ROY, I., PELEG, M. and HUANG, V. (1991) Comparison of four nodes for the compressibilities of breads and plastic foams. *Journal of Food Science*. **50**, 750-759.

SZCZESNIAK, A.S. and SKINNER, E.Z. (1973) Meaning of texture words to the consumer. *Journal of Texture Studies*. **4**, 378-384.

TAKEDA, Y., HIZUKURI, S. and JULIANO, B.O. (1987) Structures of rice amylopectins with low and high affinities for iodine. *Carbohydrate Research*. **168**, 79-88.

TAKEDA, Y., MARUTA, N., HIZUKURI, S. and JULIANO, B.O. (1989) Structures of indica rice starches (IR 48 and IR 64) having intermediate affinities for iodine. *Carbohydrate Research*. **187**, 287-294.

TEN BRINKE, G., KARASZ, F.E. and ELLIS, T.S. (1983) Depression of glass trransition temperatures of polymer networks by diluents. *Macromolecules*. **16**, 244-299.

TESCH, R., NORMAND, M.D. and PELEG, M. (1994) Compressive stress-strain relationships of agglomerated instant coffee. *Journal of Texture Studies*. **26**, 685-694.

VOISEY, P.W. (1976) Engineering assessment and critique of instruments used for meat tenderness evaluation. *Journal of Texture Studies*. **7**, 11-48.

WANG, Y.J. and JANE, J. (1994) Correlation between glass-transition temperature and starch retrogradation in the presence of sugars and maltodextrins. *Cereal Chemistry*. **71**, 527-531.

WATT, B.K. and MERRILL, A.L. (1963) *Composition of Foods*. Agriculture Handbook No. 8, ARS, USDA, Washington, D.C., USA.

WHALEN, P.J., BASON, M.L., BOOTH, R.I., WALKER, C.E. and WILLIAMS, P.J. (1997) Measurement of extrusion effects by viscosity profile using the rapid viscoanalyser. *Cereal Foods World*. **42**, 469-475.

WOOTTON, M., WEEDEN, D. and MUNK, N. (1971) A rapid method for the estimation of starch gelatinisation in processed foods. *Food Technology in Australia*. **December**, 612-615.

ZELEZNAK, K.J. and HOSENEY, R.C. (1987) The glass transition in starch. *Cereal Chemistry*. **64**, 121-124.

ZOBEL, H.F. (1984) Gelatinization of starch and mechanical properties of starch pastes. In *Starch: Chemistry and Technology*. 2nd edition. Eds. Whistler, R.L., Benmiller, J.N. and Paschall, E.F. Academic Press Inc., Orlando, USA. 285-309.

ZOBEL, H.F. (1988) Molecules to granules – A comprehensive starch review. *Starch/Stärke*. **40**, 44-50.

11 Publication